

**DAMAGE AND REPAIR IN EXPERIMENTAL CORTICAL
DEMYELINATION**

Dissertation

for the award of the degree

“Doctor of Philosophy” (Ph.D.)

Division of Mathematics and Natural Sciences

of the Georg-August-Universität Göttingen

submitted by

Enrique Garea Rodríguez

from Minden, Germany

Göttingen 2009

Thesis Committee:

Prof. Christine Stadelmann-Nessler (Reviewer)

Department of Neuropathology, University Medical Center Göttingen

Prof. Eberhard Fuchs (Reviewer)

Clinical Neurobiology Laboratory, German Primate Center

Prof. Mikael Simons

Membrane Biology, Max-Planck-Institute for Experimental Medicine

Date of oral examination:

DEDICADO A MIS PADRES

Declaration

I hereby declare that I wrote this thesis independently and with no other sources and aids than quoted. This thesis has not been submitted elsewhere for any academic degree.

Enrique Garea Rodriguez

Date: 29.10.2009

CONTENTS

FIGURES	VII
TABLES	VII
ABBREVIATIONS	VIII
SUMMARY	1
1. INTRODUCTION	3
1.1 Multiple Sclerosis	3
1.1.1 Etiology of MS	3
1.1.2 Clinical presentation	4
1.1.3 Immunology	5
1.1.4 Histopathology	6
1.1.5 Cortical lesions	6
1.1.6 Remyelination	8
1.1.7 Mechanisms of remyelination	8
1.2 Myelin	9
1.2.1 Structure and function of myelin	9
1.2.2 Myelin proteins	10
1.3 Oligodendrogenesis	11
1.3.1 Developmental oligodendrogenesis	11
1.3.2 Proliferation and differentiation promoting factors	13
1.3.3 Adult oligodendrogenesis	13
1.4 Animal models of MS	14
1.4.1 Toxin-induced demyelination models	14
1.4.2 EAE	16
1.4.3 Targeted cortical EAE model	17
1.5 Aim	18
2. MATERIALS AND METHODS	19
2.1 Study design	19
2.2 Animals and groups	22
2.3 Solutions and reagents	23
2.4 Operations and procedures	27
2.4.1 Immunogen	27
2.4.2 Sensitization procedure	27
2.4.3 Intracerebral stereotactic injection	27
2.4.4 5-bromo-2-deoxyuridine (BrdU) injection	28
2.4.5 Blood sampling and serum preparation	29
2.5 Enzyme-linked immunosorbent assay (ELISA) for detection of anti-MOG autoantibodies	29
2.6 Histology	30

2.6.1 Tissue processing	30
2.6.1.1 Perfusion and sectioning	30
2.6.1.2 Deparaffination and dehydration of histological sections	30
2.6.2 Histochemical stainings	31
2.6.2.1 Hematoxylin and eosin (HE) staining	31
2.6.2.2 Bielschowsky silver staining (modified)	31
2.6.3 Immunohistochemistry	32
2.6.3.1 Antigen retrieval	32
2.6.3.2 GFAP immunohistochemistry	32
2.6.3.3 MBP immunohistochemistry	33
2.6.3.4 ED1 immunohistochemistry	33
2.6.3.5 MBP/NogoA double immunohistochemistry	34
2.6.3.6 Olig2/PLP double immunofluorescence	34
2.6.3.7 NogoA/BrdU double immunohistochemistry	35
2.6.3.8 Olig2/BrdU double immunohistochemistry	36
2.7 Photoimaging and morphometric analysis	36
2.8 Statistics	39
3. RESULTS	40
3.1 Detection of anti-MOG autoantibody titres	40
3.2 Gliosis	40
3.3 Topology of de- and remyelination in the focal cortical EAE model	42
3.3.1 Extent of demyelinated area	45
3.3.2 Length of subpial lesions	47
3.3.3 Fraction of myelinated axons	47
3.4 Evaluation of activated macrophages/microglia	48
3.4.1 Density of activated macrophages within center of lesion	51
3.4.2 Density of activated macrophages/microglia throughout all cortical layers	52
3.5 Axonal integrity	54
3.6 Oligodendrocyte loss and recovery	55
3.6.1 Oligodendrocyte density	56
3.6.2 Proliferation of NogoA-positive oligodendrocytes	58
3.7 Oligodendroglial progenitors	61
3.7.1 Proliferation of oligodendroglial progenitors	64
4 DISCUSSION	69
4.1 Targeted cortical demyelination shares similarities with cortical MS lesions	69
4.2 Effect of repeated demyelinating lesions on remyelination	71
4.3 Inflammation in repeated targeted cortical EAE lesions	72
4.4 Preserved axonal integrity after repetitive demyelination	73
4.5 Oligodendrocyte recruitment in the targeted cortical EAE model	74
4.6 The origin of proliferated OPCs	76
4.7 Indications of overstrained remyelination capacity	77
4.8 Role of reactive astrocytes on remyelination	77
4.9 Hormonal effects on targeted cortical EAE	78
4.10 Conclusions	79

5 REFERENCES	80
6 APPENDIX	100
6.1 Effect of targeted cortical EAE lesion on estrous cycle	100
6.2 Acknowledgements	101
6.3 Curriculum Vitae	102

FIGURES

Figure 1: Proliferation and differentiation of oligodendrocytes during development	12
Figure 2: Experimental design	21
Figure 3: Regions of interest used for histological evaluation	38
Figure 4: Anti-MOG autoantibody titres	40
Figure 5: HE-staining of local gliosis	41
Figure 6: GFAP immunohistochemistry of local gliosis	42
Figure 7: Focal cortical EAE lesion	44
Figure 8: Cortical demyelination and remyelination after repetitive lesion induction	45
Figure 9: Extent of demyelination	46
Figure 10: Fraction of myelinated axons	48
Figure 11: Inflammatory demyelination in the focal cortical EAE model	50
Figure 12: Transient activation of macrophages/microglia	51
Figure 13: Density of activated macrophages/microglia	53
Figure 14: Axonal integrity	54
Figure 15: Axonal density	55
Figure 16: Loss of oligodendrocytes during focal cortical inflammatory demyelination	56
Figure 17: Spontaneous recovery of oligodendrocytes in subpial lesions	57
Figure 18: Density of oligodendrocytes	58
Figure 19: Oligodendrocyte proliferation during remyelination	59
Figure 20: Proliferation of NogoA-positive cells after repeated demyelinating events	60
Figure 21: Early effects of lesion induction on proliferation of NogoA-positive cells	60
Figure 22: Effect of lesion induction on proliferation of mature oligodendrocytes after remyelination	61
Figure 23: Unaltered oligodendroglial progenitor population	64
Figure 24: Density of oligodendroglial progenitors	64
Figure 25: Proliferation of olig2-positive OPCs within subpial lesions	66
Figure 26: OPC proliferation after repeated demyelinating events	67
Figure 27: Early effects of lesion induction on OPC proliferation	67
Figure 28: Effects of lesion induction on OPC proliferation after remyelination	68

TABLES

Table 1: Numbers of animals, groups and time points of the repetitive lesioning approach	22
Table 2: Numbers of animals, groups and time points of the single lesioning approach	22

ABBREVIATIONS

ABH Biozzi mice	antibody high Biozzi mice
ADEM	acute disseminated encephalomyelitis
ANOVA	analysis of variance
AP	alkaline phosphatase
APAAP	alkaline phosphatase anti-alkaline phosphatase
APC	antigen presenting cell
APP	amyloid precursor protein
BBB	blood brain barrier
BCIP	5-bromo-4-chloro-3-indolyl phosphate
bFGF	basic fibroblast growth factor
BrdU	5-bromo-2-deoxyuridine
BSA	bovine serum albumin
CCR5	chemokine (C-C motif) receptor 5
CNP1	2',3'-cyclic nucleotide 3'-phosphodiesterase 1
CNS	central nervous system
CXCL1	chemokine (C-X-C motif) ligand 1
CXCR3	chemokine (C-X-C motif) receptor 3
Cy3	indocarbocyanine 3
DAB	3,3'-diaminobenzidine tetrachloride
DNA	deoxyribonucleic acid
EAE	experimental autoimmune encephalomyelitis
EDSS	expanded disability status scale
ELISA	enzyme-linked immunosorbent assay
Erb2	eukaryotic ribosome biogenesis protein 2
FCS	fetal calf serum
FGF	fibroblast growth factor
FGF-2	fibroblast growth factor-2
GABA	gamma-aminobutyric acid
GC	galactocerebroside (also known as GalC)
GFAP	glial fibrillary acidic protein

HE staining	hematoxylin and eosin staining
ICAM-1	intercellular adhesion molecule-1
IFA	incomplete Freund's adjuvant
IFN- γ	interferon- γ
IGF-1	insulin-like growth factor-1
IgG	immunoglobulin G
IL-1 β	interleukin-1 β
IL-2	interleukin-2
IP-10	interferon-inducible protein-10
LFA-1	leukocyte function-associated antigen-1
LIF	leukemia inhibitory factor
LSD-test	least significance difference test
M1	primary motor cortex
MAG	myelin-associated glycoprotein
MBP	myelin basic protein
MHC	major histocompatibility complex
MMP	matrix metalloprotease
MOG	myelin oligodendrocyte glycoprotein
MS	multiple sclerosis
Myt1	myelin transcription factor 1
NBT	4-nitro blue tetrazolium chloride
NG2	neuronal/glial 2 (proteoglycan)
Nkx2.2	Nk2 transcription factor related, locus 2
NMDA	N-methyl D-aspartate
NRG1	Neuregulin 1
NT3	neurotrophin 3
O4	anti-oligodendrocyte marker O4
Olig1	oligodendrocyte transcription factor 1
OPC	oligodendrocyte precursor cell
PBS	phosphate buffered saline
PDGF- α R	platelet-derived growth factor- α receptor

PDGF	platelet-derived growth factor
PFA	paraformaldehyde
PLP	proteolipid protein
PPMS	primary progressive MS
rMOG	recombinant myelin oligodendrocyte glycoprotein
RMS	rostral migratory pathway
RRMS	relapsing-remitting MS
S1	primary somatosensory cortex
Sox2	Sry-related HMG box
SPMS	secondary progressive MS
SVZ	subventricular zone
TBS	Tris buffered saline
TGF- β	transforming growth factor- β
Th1 cells	T helper cells
TNF- α	tumor necrosis factor- α
Tris	tris(hydroxymethyl)aminomethane
Tris-EDTA	tris-ethylenediaminetetraacetic acid
VCAM-I	vascular cell adhesion molecule-I
VLA-4	very late antigen-4 (integrin α 4 β 1)
ZTE	Zentrale Tierexperimentelle Einrichtung

SUMMARY

Remyelination represents an important self repair mechanism in demyelinating diseases such as multiple sclerosis (MS). The intrinsic regenerative potential of the cerebral cortex is considerable, however cortical MS lesions frequently fail to remyelinate, especially at later stages of the disease. Repeated demyelinating events are one assumed cause of remyelination failure and the subject of this work.

The aim of the study was to determine whether repetitive demyelinating episodes may exhaust the intrinsic cortical remyelinating capacity. Therefore, MS-like lesions were induced in the rat targeted cortical experimental autoimmune encephalomyelitis (EAE) model in a repeated manner. After subcutaneous immunization with recombinant rat myelin oligodendrocyte glycoprotein (rMOG), a cytokine cocktail composed of the proinflammatory cytokines tumor necrosis factor- α (TNF- α) and interferon- γ (IFN- γ) was stereotactically injected in the rat cerebral cortex thereby leading to focal inflammatory demyelinating lesions. Lesions were repetitively induced at intervals of three weeks, simulating the repetitive events in relapsing-remitting MS.

Histological analysis revealed widespread subpial and intracortical demyelinated lesions within the injected cortical hemisphere 3 days after lesion induction. Demyelination was accompanied by loss of mature oligodendrocytes and activation/recruitment of macrophages/microglia at this time point. However, three weeks after lesion induction extensive remyelination, restoration of oligodendrocyte population and resolution of inflammation was observed. This picture of de- and remyelination was consistently observed even after four cycles of demyelination at the same anatomical area. Although the fraction of myelinated axons was extensively restored after repetitive lesioning it did not fully recover. The initial inflammatory response measured by the density of activated macrophages/microglia was markedly stronger compared to the subsequent episodes. In contrast to NogoA-positive cells, oligodendrocyte transcription factor 2 (olig2)-positive oligodendrocyte precursor cell (OPC) density was stable and even increased at particular time points. Proliferation of olig2 and NogoA-positive cell populations was observed during demyelination. However, only few proliferated NogoA-positive cells were

identified within remyelinated lesions, in contrast to substantial proliferation of olig2-positive OPCs.

This work demonstrates the extensive intrinsic regenerative capacity of the rat cerebral cortex after repeated demyelinating insults. Four cycles of cortical demyelinating episodes did not lead to reduction of the cortical remyelinating capacity in our experimental setting. Our results suggest furthermore that oligodendroglial recruitment occurs by differentiation of existing rather than newly generated OPCs within the cerebral cortex. Findings from these studies will contribute to understanding the underlying processes of remyelination with implications for MS.

1. INTRODUCTION

MS also known as *encephalomyelitis disseminata*, is one of the most common neurological diseases in young adults. MS was first described by Jean Martin Charcot in 1868 and is currently believed to be an autoimmune disorder causing inflammatory demyelination in the central nervous system (CNS). In northern Europe the general population prevalence of MS varies in average between 20-60/100000, being more common in females (Sospedra and Martin, 2005).

As MS is a complex and heterogeneous disorder, many questions remain open despite intensive research. The main focus of this study addresses cortical pathology of MS which extent has been underestimated for a long time by the scientific community. This chapter provides an introduction to clinical and pathological features of multiple sclerosis, especially focussing on cortical grey matter pathology. In addition, remyelination, oligodendroglial recruitment and genesis will be addressed. Finally, the targeted cortical EAE model which is used for studying repetitive inflammatory demyelination will be introduced.

1.1 Multiple Sclerosis

1.1.1 Etiology of MS

Despite extensive efforts the etiology of MS remains enigmatic. MS is considered to be autoimmune in nature, but its exact cause remains still unknown. However, it occurs to be a result of genetic and environmental factors (Sospedra and Martin, 2005; Gold et al., 2006).

Genetic predisposition seems to play a role since first-degree relatives and monozygotic twins of affected individuals show a higher risk to develop MS (Sospedra and Martin, 2005). Furthermore, susceptible genes on chromosome 6p21 in the area of the major histocompatibility complex (MHC) seem to account for 10-60% of genetic risk in MS (Hillert and Olerup, 1993; Haines *et al.*, 1998; Oksenberg *et al.*, 2008).

In addition to genetic factors, epidemiological studies strongly suggest that environmental factors are involved in disease predisposition. To these factors belong e.g. sunlight exposure and ultraviolet radiation, hormonal and hygienic status, as well as the consequences of socioeconomic and industrial development (Sospedra and Martin, 2005).

Infectious agents have been furthermore postulated to cause MS. This is supported by studies showing a possible association between viral infections and exacerbations of MS symptoms (Bebbe *et al.*, 1967; Sibley *et al.*, 1985). Especially, the Epstein-Barr virus (EBV) has been related to MS but its direct implication in the disease remains unproven (Johnson, 1994; Bagert, 2009).

1.1.2 Clinical presentation

MS patients suffer from a variety of neurological symptoms, such as optic neuritis, sensory disturbances, weakness, diplopia, diminished dexterity, ataxia, fatigue and bladder dysfunction. Symptoms occur in either discrete attacks (relapsing forms) or slowly accumulating over time (progressive forms). The initial symptoms are often transient and mild, but worsen often with time ending with permanent disability. With regard to its clinical course, three main subtypes have been described (Lublin *et al.*, 1996):

Relapsing-remitting MS (RRMS):

The relapsing remitting subtype is the most frequent (85-90%) subtype of MS. It is characterized by relapses followed by remissions without any disease activity in between. Despite remission, disability may accumulate after each relapse.

Primary progressive MS (PPMS):

This subtype is characterized by progressive disability from onset of the disease, with no or occasional relapses and remissions. Approximately 10 to 15% percent of all MS patients show a primary progressive course.

Secondary progressive MS (SPMS):

The secondary progressive subtype describes patients with initial relapsing-remitting MS, who then experience progressive disability with no definite remission. The conversion from the relapsing-remitting to the secondary progressive phase on average takes place between 15 and 20 years after disease onset.

1.1.3 Immunology

MS is considered to be caused by an autoimmune response against unknown antigens of the myelin sheaths. According to this concept, myelin antigens are recognized by professional antigen presenting cells (APCs) and presented in the periphery via MHC class II molecules to T helper 1 (Th1) cells. Following activation, priming and clonal expansion, CD4-positive cells infiltrate the CNS where they re-encounter their antigen. Upon restimulation by microglia, CD4-positive cells initiate effector functions such as the secretion of the pro-inflammatory cytokines TNF- α , IFN- γ and interleukin 2 (IL-2) (Merril, 1992). Thereby, attracted macrophages and resident microglia become activated, which in turn contribute to the inflammatory milieu by the release of matrix metalloproteinases (MMPs), oxyradicals and TNF- α . In addition, the secretion of the chemoattractants interferon-inducible protein-10 (IP-10) and Rantes and the activation of their respective receptors chemokine (C-X-C motif) receptor 3 (CXCR3) and chemokine (C-C motif) receptor 5 (CCR5), promote the recruitment of leukocytes into the sites of inflammation (Simpson *et al.*, 1998; Martínez-Cáceres *et al.*, 2002). CNS migration through the blood brain barrier (BBB) is enabled by the upregulation of the intercellular adhesion molecule-I (ICAM-I) and the vascular cell adhesion molecule-I (VCAM-I) on endothelial cells and their ligands leukocyte function-associated antigen-1 (LFA-1) and very late antigen-4 (VLA-4), the last ones being expressed on the surface of activated effector cells (Yusuf-Makagiansar *et al.*, 2002).

Class I MHC-restricted CD8-positive cells are supposed to play an important role in MS. They are considered to directly target oligodendrocytes and axons, indicated by secretion of cytotoxic granules and upregulation of cytotoxic T-cell markers such as Fas, Fas-ligand and granzyme B (Lazzarini, 2004). B- and plasma-cells located in the meninges and perivascular space is suggested to contribute to the pathogenesis by mediating

myelin-specific antibody responses in a subset of MS patients (Lucchinetti *et al.*, 2000; Serafini *et al.*, 2004). Antibodies may bind to membrane bound antigens enabling Fc-receptor-mediated cytotoxicity and phagocytosis by activated macrophages. Furthermore, the complement cascade is initiated (Lazzarini, 2004).

Inflammation usually resolves after each relapse and is promoted by a transition of CD4-positive Th1 to Th2 cells. These lymphocytes secrete anti-inflammatory cytokines such as IL-4, IL5, IL-10, IL-13 and transforming growth factor- β (TGF- β), silencing the inflammatory reaction (Issazadeh *et al.*, 1995).

1.1.4 Histopathology

MS is characterized by multifocal, demyelinated plaques with glial scar formation. T-cell infiltration occurs in all active MS lesions. However, histopathological heterogeneity was observed in MS lesions. Accordingly, four histopathological patterns were proposed (Lucchinetti *et al.*, 2000). Pattern I describes a macrophage-associated demyelination promoted by toxic products such as TNF- α or reactive oxygen species (Probert *et al.*, 2000; Griot *et al.*, 1990). In addition to macrophage activation, antibody and complement-mediated demyelination takes place in pattern II. Distal oligodendrogliopathy (pattern III) and primary oligodendrocyte degeneration (Pattern IV) was observed in a subgroup of patients (Lucchinetti *et al.*, 2000).

Importantly, these patterns describe the acute phase of disease in which inflammation and demyelination is still ongoing, and therefore termed “active” lesions. In contrast, chronic or inactive lesions, lacking signs of active demyelination, are characterized by demyelination, astrogliosis, axonal damage, and loss and can not be arranged to one of the four aforementioned patterns (Lazzarini, 2004).

1.1.5 Cortical lesions

Grey matter involvement in MS has already been observed in early disease history (Taylor, 1892; Sander, 1898; Brownel and Hughes, 1962). Later however, cortical lesions have been overseen for decades. Due to significant improvement in staining techniques,

they were finally rediscovered by the end of the century (Kidd *et al.*, 1999; Peterson *et al.*, 2001; Bo *et al.*, 2003). Since the use of sensitive in vivo imaging techniques, the importance of cortical involvement becomes more apparent (Filippi *et al.*, 1996; Geurts *et al.*, 2005; Kangarlu *et al.*, 2007).

Cortical demyelination is a frequent phenomenon occurring in 90% of MS patients with long disease duration (Albert *et al.*, 2007). On average, between 10-25% of cortical grey matter is demyelinated (Albert *et al.*, 2007; Bo *et al.*, 2003; Kutzelnigg *et al.*, 2005; Gilmore *et al.*, 2009). In the progressive stage of the disease CNS grey matter is even more affected compared to white matter (Gilmore *et al.*, 2009). Three main types of cortical lesions have been described, namely leukocortical lesions, which extend through white and grey matter, pure intracortical lesions and subpial lesions. Last mentioned lesion type is the most frequent and extensive one (Peterson *et al.*, 2001; Bo *et al.*, 2003).

Compared to white matter lesions, cortical demyelination is less inflammatory, presenting with reduced lymphocyte infiltration and reduced microglia activation (Peterson *et al.*, 2001; Bo *et al.*, 2003). Furthermore, complement deposition, limited astrogliosis and relative axonal preservation was reported (Schwab and McGeer, 2002; Peterson *et al.*, 2001; Wegner *et al.*, 2006; Vercellino *et al.*, 2005). Despite weak lymphocyte-mediated inflammation, follicle-like structures harbouring B-cells were observed in the sulcal meninges of SPMS patients. These structures are associated with enhanced axonal damage and disability (Serafini *et al.*, 2004; Magliozzi *et al.*, 2007). In addition to moderate axonal damage, neuronal loss and cortical atrophy was reported (Wegner *et al.*, 2006). On the contrary, reduction of synaptic densities does not necessarily occur (Vercellino *et al.*, 2005; Kutzelnigg *et al.*, 2007). However, reduced expression of amino acid transporters and gamma-aminobutyric acid (GABA) related transcripts, and enhanced excitotoxicity underline the functional consequences of cortical MS lesions (Vercellino *et al.*, 2007; Dutta *et al.*, 2006).

Classically, MS patients present with sensory and motor symptoms. In case of cortical involvement patients may additionally suffer from cognitive and neuropsychiatric symptoms, thus contributing to disease severity already in early stages of the disease (Skegg *et al.*, 1993; Haase *et al.*, 2003; Zarei *et al.*, 2006).

1.1.6 Remyelination

Remyelination is an important repair mechanism and is accompanied by functional recovery such as the reestablishment of salutatory conduction and the resolution of clinical symptoms (Smith *et al.*, 1979; Jeffery *et al.*, 1997; Merkler and Liebetanz, 2006). Remyelinated axons have thinner and shorter internodes and usually do not attain original dimensions (Blakemore, 1974; Ludwin and Maitland, 1984). In histological sections of MS patients, remyelinated areas are characterized by pale and less dense myelin, so called “shadow plaques” (Itoyama *et al.*, 1980). Furthermore, remyelinated lesions can be detected by magnetic resonance imaging (Barkhof *et al.*, 2003; Merkler *et al.*, 2005).

Remyelination is a frequent phenomenon, occurring in more than 50% of MS plaques (Lucchinetti *et al.*, 1999; Patrikios *et al.*, 2006, Patani *et al.*, 2007). However, the grade of remyelination depends on anatomical location and disease stage (Stadelmann and Brück, 2008; Goldschmidt *et al.*, 2009). As an example, regions close to the ventricle walls remyelinate less, opposed to those in the deep white matter (Patrikios *et al.*, 2006). In turn, cortical grey matter remyelination is more frequent and extensive compared to white matter lesions (Albert *et al.*, 2007). Despite long disease duration extensive remyelination can occur, but fails in the majority of cases at later stages of the disease (Patani *et al.*, 2007; Goldschmidt *et al.*, 2009).

Remyelination is neuroprotective, preventing secondary axonal damage (Kornek *et al.*, 2000; Irvine and Blakemore, 2008; Trapp and Nave, 2008). Furthermore, the presence of myelin proteins such as proteolipid protein (PLP) and 2',3'-cyclic nucleotide 3'-phosphodiesterase 1 (CNP1), plays an important role in axon stability (Lappe-Siefke *et al.*, 2003; Griffiths *et al.*, 1998; Edgar and Garbern, 2004).

1.1.7 Mechanisms of remyelination

Loss of remyelination capacity is considered to play an important role in MS pathology, however, the mechanisms causing impaired remyelination are not fully understood. To date there are three main hypotheses which describe the different possible causes of remyelination failure (Franklin and French-Constant 2008). The first is known as the

failure of recruitment hypothesis, in which inadequate provision of OPCs might be the cause of incomplete or total lack of myelin restoration. The second hypothesis describes how OPCs, after being recruited into the sites of demyelination fail to differentiate to remyelinating oligodendrocytes. Lastly, the dysregulation hypothesis suggests that remyelination might fail due to disturbances of the precise coordination of regenerative cellular events (Franklin and Kotter, 2008). Furthermore, disturbed axon-glia interactions may hinder remyelination (Franklin, 2002). Age is an aggravating factor for the efficacy of endogenous remyelination as shown in animal studies (Sim *et al.*, 2002; Shen *et al.*, 2008).

Treatments improving remyelination are not available yet. However, basic research in animal models proposes new approaches for future remyelination strategies. These include the enhancement of endogenous repair mechanisms such as the proliferation and differentiation of endogenous OPCs (Franklin and Kotter, 2008). Furthermore, successful transplantation of myelinating cells has been proven in several animal studies, but its therapeutic potential in humans remains open (Stangel und Trebst, 2006). The current standard therapy for MS consists of treatment with immunomodulatory drugs. These therapeutic approaches may indirectly influence remyelination by preventing further myelin damage (Lazzarini, 2004).

1.2 Myelin

1.2.1 Structure and function of myelin

Neurons communicate by depolarizing the electrical potentials of their membranes, a process called action potential. This occurs by exchange of sodium and potassium along closely distributed channels on the axon. The majority of axons are wrapped by lipid-rich, lamellar structures named myelin sheaths. Due to the myelin-sheaths insulating properties, action potentials jump between myelin free spaces, a process called salutatory conduction. This provides fast and energy-efficient signaling over longer distances, allowing cross linking of remote brain areas. In the CNS myelin sheaths are built by specialized cells called oligodendrocytes. The complex radial geometry allows these cells

to build multiple internodes on axons within their reaching area. Axons are accompanied by many oligodendrocytes, each of one myelinating a particular segment along the axonal route. In contrary, dendrites are never myelinated. Myelin sheaths are compact spiraled cellular processes that contain two plasma membranes and no cytoplasm. Opposed to other cell membranes, myelin is composed of up to 75% of lipids. Furthermore, a variety of membrane proteins and cytoskeletal components are involved in formation and maintenance of this complex cell organelle. Briefly, the most abundant ones are PLP, the myelin basic protein (MBP), and the myelin associated glycoprotein (MAG).

1.2.2 Myelin proteins

PLP is the major integral membrane protein of myelin consisting of four transmembrane domains. It is distributed in compact myelin, and is important for structural stability of myelin, keeping normal spacing between single sheaths. Lack of PLP and its splice variant DM20 does not impair myelination but leads to structural disturbances followed by axonal damage in adulthood (Trapp and Nave, 2008).

MBP is an extrinsic membrane protein located in the cytoplasmic leaflets of compact myelin. The MBP deficient shiverer mouse shows hypo- and dysmyelination, indicating an important role of this protein in myelin formation and preservation (Lazzarini, 2004).

MAG is located in the periaxosomal and mesoaxonal membranes of compact myelin. This protein has been shown to participate in the control of compact myelin distribution and is essential for myelination and axonal integrity (Quarles, 2007).

Myelin oligodendrocyte glycoprotein (MOG) is an integral membrane protein consisting of an immunoglobulin G (IgG)-like extracellular domain, a transmembrane domain, a membrane associated domain and two cytoplasmic domains. Quantitatively, it comprises of 0.05-0.1% of total myelin protein. However, it is of high immunological importance since it is an autoantigen frequently used to induce EAE. MOG is suggested to be a cellular adhesive molecule, regulating oligodendrocyte microtubule stability. Further, MOG might mediate interactions between myelin and the immune system, in particular the complement cascade (Lazzarini, 2004).

1.3 Oligodendrogenesis

1.3.1 Developmental oligodendrogenesis

Neurons, astrocytes and oligodendrocytes are the most common cell types in the vertebrate CNS. Oligodendrocytes arise from the neuroepithelial cells of discrete neural tube regions (Ono *et al.*, 1995). They first appear as so called oligodendrocyte precursor cells (OPCs) along the rostro-caudal extent at the ventral part of the spinal cord. In more rostral parts of the CNS the earliest oligodendroglial precursors are located in the ventricular and subventricular zone (Ono *et al.*, 1997). Later, new sources of proliferation are available, such as the medial and lateral ganglionic eminence, from where new OPCs migrate into the developing cerebral cortex (reviewed in Miller, 2002).

Proliferation, migration and maturation of oligodendrocytes are orchestrated by a variety of signaling molecules, but also by gene and protein expression. At the beginning both neuronal and oligodendroglial lineages respond to the signaling molecule sonic hedgehog and express the transcription factor Olig2 (Zhou *et al.*, 2001). Later, combinatorial expression of olig1, olig2 and Nk2 transcription factor related locus 2 (Nkx2.2) provides the generation of OPCs. At this stage OPCs can be detected with the monoclonal antibody A2B5, which is directed against a specific ganglioside epitope (Zhou *et al.*, 2001). Further, migrating early progenitors express the sulfated proteoglycan neuronal/glial 2 (NG2) and the platelet derived growth factor receptor α (PDGF- α R), by which they can be distinguished from neuronal precursors. Motoneurons also express Olig2, but they follow the neuronal lineage by additional expression of Ngn1 and Ngn2 (Lu *et al.*, 2002). Once departed from the neuronal lineage, precursors differentiate to astrocytes and oligodendrocytes and are therefore termed oligodendrocyte-type-2 astrocyte (O-2A) progenitor cells (Raff *et al.*, 1984). OPCs continue their maturation and express galactosulfatide, which is detectable using the monoclonal anti-oligodendrocyte marker O4 (Warrington and Pfeiffer, 1992). O4-positive OPCs, also termed late OPCs are postmigratory but still proliferative (Pfeiffer *et al.*, 1993).

After migration from the germinal zones, OPCs evenly distribute in gray and white matter followed by a wave of differentiation spreading from the corpus callosum towards the pial surface (Nishiyama *et al.*, 1996; Pringle *et al.*, 1992; Reynolds and Hardy, 1997).

Differentiation is mediated by down regulation of NG2 and PDGF- α R. In addition, myelin proteins are expressed such as MAG, CNP, MBP but not PLP and MOG. Finally, myelinating oligodendrocytes express PLP and MOG. Premyelinating oligodendrocytes which do not differentiate to myelinating oligodendrocytes undergo apoptosis, occurring in approximately 50% of these cells. However, a small population of proliferative late OPCs remains in the adult CNS after development.

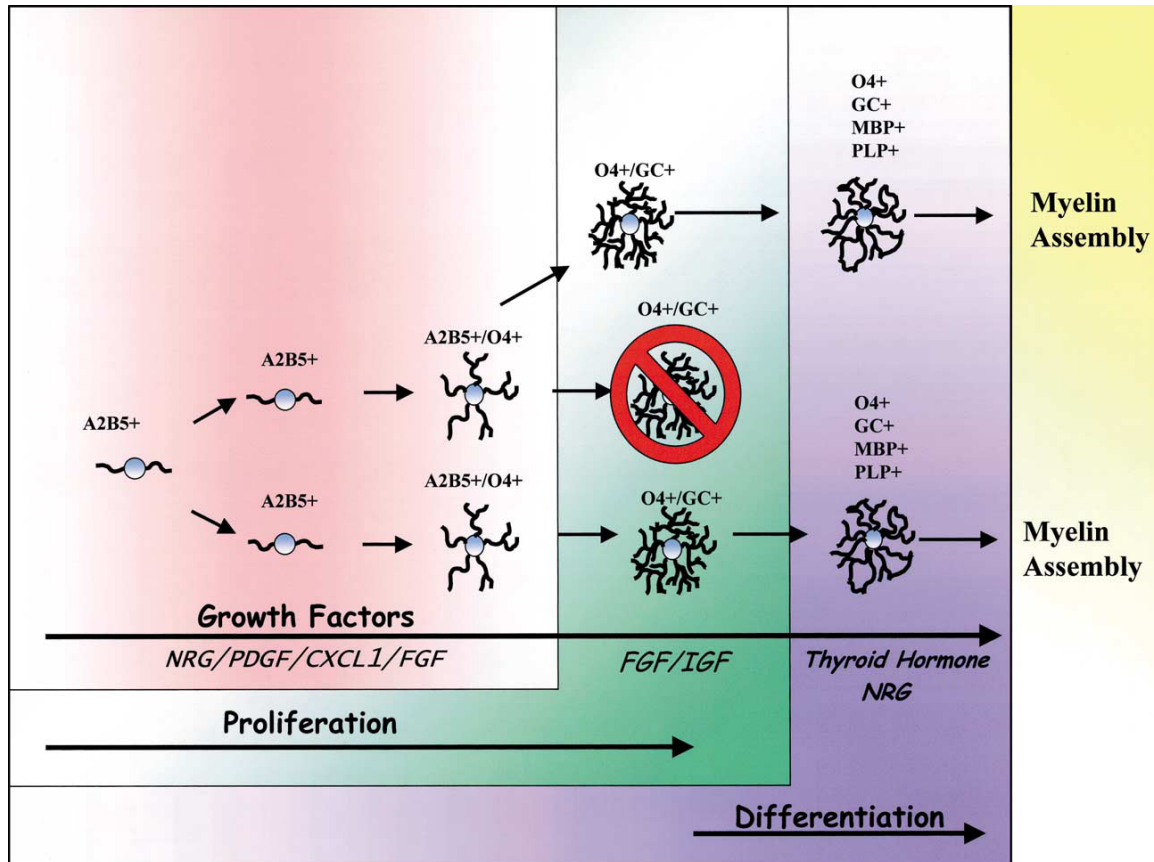


(Figure obtained from Miller, 2002)

Figure 1: Proliferation and differentiation of oligodendrocytes during development

Developmental oligodendroglial precursor cells (OPCs) derive from the subventricular zone (SVZ) of the neural tube. Upon the proliferative and migratory effects of hormonal factors such as platelet-derived growth factor (PDGF) and fibroblast growth factor (FGF), early OPCs can be detected using the monoclonal antibody A2B5. During the transition from proliferation to differentiation of oligodendroglial cells, the expression of surface antigens such as galactocerebroside (GC) and galactosulfatide (which can be recognized by the monoclonal antibody O4) increases. Myelin proteins such as myelin basic protein (MBP) and proteolipid protein (PLP) are expressed at late stages of differentiation and are required for myelin assembly. OPCs which do not complete the maturation process undergo apoptosis.

1.3.2 Proliferation and differentiation promoting factors

A variety of trophic factors promote proliferation. As an example, platelet derived growth factor (PDGF) which is released by astrocytes and neurons, increases proliferation of OPCs by acting on its receptor PDGF α R (Noble *et al.*, 1988; Pringle *et al.*, 1992; Yeh *et al.*, 1991). PDGF is not only a potential mitogen, it is also required for oligodendroglial survival (Fruttiger *et al.*, 1999). The beneficial effects of PDGF are enhanced by the presence of the chemokine (C-X-C motif) ligand 1 (CXCL1) (Robinson *et al.*, 1998). Moreover, CXCL1 regulates the migration of immature progenitors (Tsai *et al.*, 2002). The basic fibroblast growth factor (FGFb) also supports proliferation by enhancing the expression of PDGF- α R on OPCs (McKinnon *et al.*, 1991). Further promoters of proliferation are neurotrophin-3 (NT3), fibroblast growth factor 2 (FGF2), neuregulin-1 (NRG1) and its receptor eukaryotic ribosome biogenesis protein 2 (Erb2) (Barres *et al.*, 1994, Qian *et al.*, 1997; Vartanian *et al.*, 1999; Park *et al.*, 2001).

Differentiation is accompanied by upregulation of TGF- β . Additionally, the numbers of precursors can be controlled by altering the availability of survival factors such as PDGF. Proliferation and differentiation mechanisms mesh, as factors which promote differentiation on the one hand, in turn inhibit proliferation (Lazzarini, 2004).

1.3.3 Adult oligodendrogenesis

After development, a quiescent population of NG2 and PDGF α R expressing OPCs remains in the adult CNS. In contrast to developmental OPCs, adult OPCs show a more mature phenotype as they also express O4 (Dawson *et al.*, 2000). Adult OPCs derive from developmental ones or from type B cells of the subventricular zone (Wren *et al.*, 1992; Lazzarini, 2004). Adult OPCs are abundant in the CNS and account for between 3 to 9% of all cells. Further, spinal cord OPC:oligodendrocyte ratio is 1:4, whereas 1:1 ratio was found in gray matter (Dawson *et al.*, 2003). The reason why adult OPCs do not differentiate to oligodendrocytes and why they remain as a quiescent abundant population is still unknown. Likely, gray matter environment arrests oligodendrocyte differentiation in an immature state, by the relative down regulation of humoral factors to a sub-threshold level during adulthood (Dawson *et al.*, 2000; Levine *et al.*, 2001; Lazzarini,

2004). However, adult OPCs are considered to differentiate to myelinating oligodendrocytes and replace lost ones, providing a potential source of remyelination in the diseased CNS, as occurring in MS and experimental demyelination. The higher ratio of OPC:oligodendrocyte in cerebral cortex compared to spinal cord provides a potent source of remyelinating cells that could explain the relatively effective cortical remyelination in MS patients (Lazzarini, 2004). Other studies indicate that OPCs may be involved in synaptic function (Bergles *et al.*, 2000; Jabs *et al.*, 2005; Karadottir *et al.*, 2008).

As in developmental myelination, remyelination is associated with the upregulation of the transcription factors Olig2, Nkx2.2, myelin transcription factor 1 (Myt1) and Sry-related HMG box (Sox2) (Fancy *et al.*, 2004; Watanabe *et al.*, 2004; Talbott *et al.*, 2005; Vana *et al.*, 2007). Furthermore, adult OPC proliferation and differentiation is promoted by humoral factors. The most potent mitogen is PDGF acting via its receptor PDGF α R, which is uniquely expressed on OPCs (Noble *et al.*, 1988; Wolswijk *et al.*, 1991). FGF stimulates proliferation, partly by enhancing PDGF α R expression, and inhibits differentiation on the other hand (Besnard *et al.*, 1989; Bansal and Pfeifer *et al.*, 1994; McKinnon *et al.*, 1990). The role of NT3 in adult oligodendrogenesis is not clear so far. However, studies indicate both, proliferative and differentiative effects of NT3, acting in combination with PDGF and basic fibroblast growth factor (bFGF) (Ibarrola *et al.*, 1996; McTigue *et al.*, 1998). Insulin-like growth factor-1 (IGF-1) increases proliferation and survival, enhances differentiation, and modulates expression of MBP in both OPCs and oligodendrocytes (Barres *et al.*, 1992; McMorris and Dubois-Dalcq, 1988; Saneto *et al.*, 1988).

1.4 Animal models of MS

1.4.1 Toxin-induced demyelination models

A number of animal models are available to study MS pathology and demyelination. One of the most used approaches is the injection of gliotoxic agents into locations of the CNS, producing focal demyelinating lesions. Due to the fact that spontaneous remyelination

takes place in almost all of these lesions, toxin induced demyelination provides a potent tool to study endogenous remyelination and oligodendrocyte recruitment, but also the engraftment of transplanted cells.

Lysolecithin (lysophosphatidyl choline) is a membrane solubilizing agent and was first used in experimental demyelination by Hall (Hall, 1972). Injection into the rat dorsal funiculus produces ellipsoid shaped demyelination which extends longitudinally over 3 to 8mm. Lysolecithin has a particular toxicity for myelin and oligodendrocytes. However, marginal loss of axons and astrocytes occurs in the point of injection. Following demyelination, oligodendrocyte and Schwann cell remyelination takes place.

Injection of ethidium bromide into the rat spinal cord results in much larger areas of demyelination than in the lysolecithin model (Yajima and Suzuki, 1979; Blakemore *et al.*, 1982). This deoxyribonucleic acid (DNA) intercalating agent kills oligodendrocytes, oligodendrocyte precursors and astrocytes. Both oligodendrocyte and Schwann cell remyelination takes place, depending on location and species (Woodruff and Franklin, 1999; Jeffery and Blakemore, 1997). As mentioned above, spontaneous remyelination occurs in all toxin-induced demyelination models. Therefore, the contribution of engrafted cells is difficult to evaluate. For this reason, X-radiation prior to gliotoxin injection is used to deplete the local OPC population and inhibit endogenous remyelination (Hinks *et al.*, 2001). Exogenous remyelination via cell transplantation can then be investigated in this model.

The cuprizone mouse model is a widely used non-invasive model to investigate effects directly related to demyelination and remyelination within the CNS (Blakemore, 1973; Matsushima and Morell, 2001). Feeding young adult mice with the cuprizone (bis-cyclohexanone-oxalhidrazone) for 5 weeks results in synchronous and consistent demyelination of the corpus callosum. Furthermore, strong spontaneous remyelination occurs rapidly after cuprizone removal from the diet.

In addition to aforementioned models demyelination can be induced by the injection of anti-galactocerebroside antibodies and complement (Keirstead and Blakemore, 1997). Compared to gliotoxins, lesions involve a greater area of the dorsal funiculus, but in turn are shorter in length. Furthermore, less axonal loss takes place.

1.4.2 EAE

Experimental autoimmune encephalomyelitis (EAE) is an inflammatory demyelinating disease of the CNS. EAE was first described by Rivers and colleagues in 1933 who observed that vaccination with rabbit CNS homogenate resulted in brain inflammation in rhesus monkeys (Rivers *et al.*, 1933). Today EAE is the most used animal model of MS and acute disseminated encephalomyelitis (ADEM). EAE is nowadays induced by active immunization with a single injection of defined myelin peptides/proteins such as MBP, PLP and MOG (Kabat *et al.*, 1951; Gold *et al.*, 2006). The disease can be reliably induced in many different species, such as in the marmoset monkey, guinea pig, mouse and rat. Depending on the genetic background of the species or strain and the antigen used for vaccination, EAE reproduces many clinical and immunopathological aspects of MS (Hohlfeld and Wekerle, 2001; Gold *et al.*, 2006).

The autoimmune response against myelin sheath components is driven by encephalitogenic CD4-positive T cells (Ben-Nun *et al.*, 1981). This is enabled by professional APCs which present antigen to fully reactive T cells (Dustin and Cooper, 2000). In addition, B cell derived autoantibodies play an important role in rat and marmoset leading to extensive demyelination, but not in mice (Schluesener *et al.*, 1987; Linington *et al.*, 1988; Genain *et al.*, 1995; von Budingen *et al.*, 2004). Furthermore, components of the innate immune system like macrophages and Toll-like receptors are involved in disease pathogenesis (Takeda *et al.*, 2003; Munz *et al.*, 2005).

Clinically, EAE disease is evaluated by a standardized EAE clinical score, the equivalent to the expanded disability status scale (EDSS) used in humans (Kurtzke, 1983). The clinical course of EAE can be either monophasic as in rats immunized with MBP, relapsing-remitting like in PLP/MOG peptide-immunized SJL mice, or secondary progressive such as observed in antibody high (ABH) Biozzi mice (Pender, 1987; Fritz *et al.*, 1983; McRae *et al.*, 1992; Hampton *et al.*, 2008, Gold *et al.*, 2006).

To date, MOG is the only antigen that induces a significant demyelinating antibody-mediated immune response.

1.4.3 Targeted cortical EAE model

Studying cortical MS pathology is hampered by the lack of adequate animal models, as conventional EAE predominantly affects the spinal cord, but rarely the brain. Indeed, toxin-induced demyelination approaches are available, however, they do not reflect the autoimmune nature of MS. To overcome this limitation the targeted cortical EAE model was established by Merkler and colleagues (Merkler *et al.*, 2006). Lewis rats are subcutaneously immunized with a subthreshold dose of MOG which leads to production of anti-MOG autoantibodies, but not to overt neurological symptoms. Following peripheral immune priming, lesions are induced by injection of pro-inflammatory cytokines into the cerebral cortex.

The underlying concept of this model is that application of TNF- α /IFN- γ locally attracts blood born monocytes and lymphocytes into the target area, going inline with transient BBB leakage. This allows vaccination derived anti-MOG autoantibodies to penetrate into the CNS parenchyma and to bind to their epitopes on the myelin surface. Finally, demyelination is mediated by a combination of complement and antibody-dependent cellular cytotoxicity mechanisms (Linington *et al.*, 1988; Gold *et al.*, 2006).

Histopathologically, the targeted cortical EAE model is characterized by extensive subpial and intracortical demyelination and oligodendroglial loss. The subpial lesions are reminiscent to cortical type III lesions observed in MS patients (Merkler *et al.*, 2006; Peterson *et al.*, 2001). In addition, demyelination is accompanied by microglia/macrophage activation, CD4- and CD8-positive T cell infiltration, and complement deposition. Furthermore, an acute axonal damage but no substantial neuronal loss was observed. In contrast to targeted white matter lesions, extensive cortical remyelination takes place and inflammation resolves within two weeks post lesion induction (Kerschensteiner *et al.*, 2004; Merkler *et al.*, 2006). For mentioned reasons, focal cortical EAE model is very suitable for demyelination and remyelination studies.

1.5 Aim

The failure to achieve remyelination is considered to play an important role in MS, however the mechanisms causing this failure are not fully understood. Inadequate provision of OPCs is a proposed cause of impaired or total lack of myelin restoration. A further hypothesis describes how OPCs, after being recruited into the sites of demyelination fail to differentiate to remyelinating oligodendrocytes. Irrespective of the aforementioned theories and age-dependent effects, frequency of demyelinating events may also play a role in MS. The reason for focussing on the cerebral cortex is based upon its ability to remyelinate during early stages of the disease, even after indications of repetitive demyelinating events. However, limited or impaired myelin restoration in patients with long disease duration indicates an exhaustion of the remyelination capacity.

My thesis addressed whether chronic demyelinated lesions within the cerebral cortex in MS patients are the result of repetitive demyelinating episodes.

The aims were:

1. to induce repetitive inflammatory demyelinated lesions within the same cortical area in the targeted cortical rat EAE model of MS
2. to characterize de- and re-myelination after repeated lesion inductions
3. to characterize oligodendroglial recruitment in targeted cortical EAE lesions
4. to investigate the effects of repeated targeted cortical EAE lesions on inflammation and axonal density

2. MATERIALS AND METHODS

The study was carried out at the laboratories of the Department of Neuropathology and the animal house (Zentrale Tierexperimentelle Einrichtung, ZTE) of the University Medical Center, Göttingen, according to the approval of the Bezirksregierung Braunschweig.

2.1 Study design

Our objective in the present study was to determine whether repetitive demyelinating cortical episodes may exhaust the intrinsic cortical remyelinating capacity. For this purpose, we induced repeated lesions (each of which simulates a “demyelinating episode”) at fixed intervals and a defined location in the rat cortex followed by histological assessment at different time points.

In the classical rodent EAE model, lesions are mostly confined to the spinal cord but only rarely affected the cerebral cortex. Therefore, a new model of MS was established that allows for EAE lesions to be targeted in the cerebral cortex with high accuracy in terms of the time point and location of lesion evolvment as well as lesion recovery (Merkler et al., 2006). In this animal model, rats are immunized with a subclinical dose of recombinant myelin oligodendrocyte glycoprotein (rMOG). Subclinical MOG immunization induces anti-MOG antibodies without overt clinical symptoms *per se*. In a second step, pro-inflammatory mediators are stereotactically injected into the rat cerebral cortex 1 mm caudal to bregma and 2 mm lateral to the sagittal suture, which finally induce focal extensive subpial and intracortical lesions (Figure 2). According to Paxinos stereotactic brain atlas, the affected area includes the motor (M1) and sensory cortex (S1) and allows for future behavioural analysis with regard to putative motor and sensory implications (Paxinos, 1998). The time points chosen for histological evaluation include the maximum extent of demyelination, which occurs at day 3 post lesion induction and remyelination at day 21. Lesioning was then repeated at the same particular area a total of four times at 21-day intervals, thus providing the necessary time for recovery between each demyelinating event. Animals were sacrificed at previously mentioned time points

after the first, second and fourth lesioning episodes. Histological analysis was performed with respect to demyelination, remyelination, recruitment of oligodendrocytes, inflammatory infiltrates and axonal integrity. By computer-aided and manual analysis, the following parameters were analyzed and quantified: demyelinated area, fraction of myelinated fibres and cell densities.

In order to investigate oligodendrocyte recruitment in more detail, the proliferative kinetics of oligodendroglial populations in response to demyelination was analysed. Therefore, animals were labelled with the proliferation marker 5-bromo-2-deoxyuridine (BrdU), which is incorporated in dividing cells.

High and stable serum levels of anti-MOG autoantibodies are an important prerequisite for induction of demyelinating episodes. Therefore, serum levels of MOG autoantibodies were monitored by ELISA beginning from the initial lesion (day 18 post immunization) until the last lesion induction (day 82 post immunization).

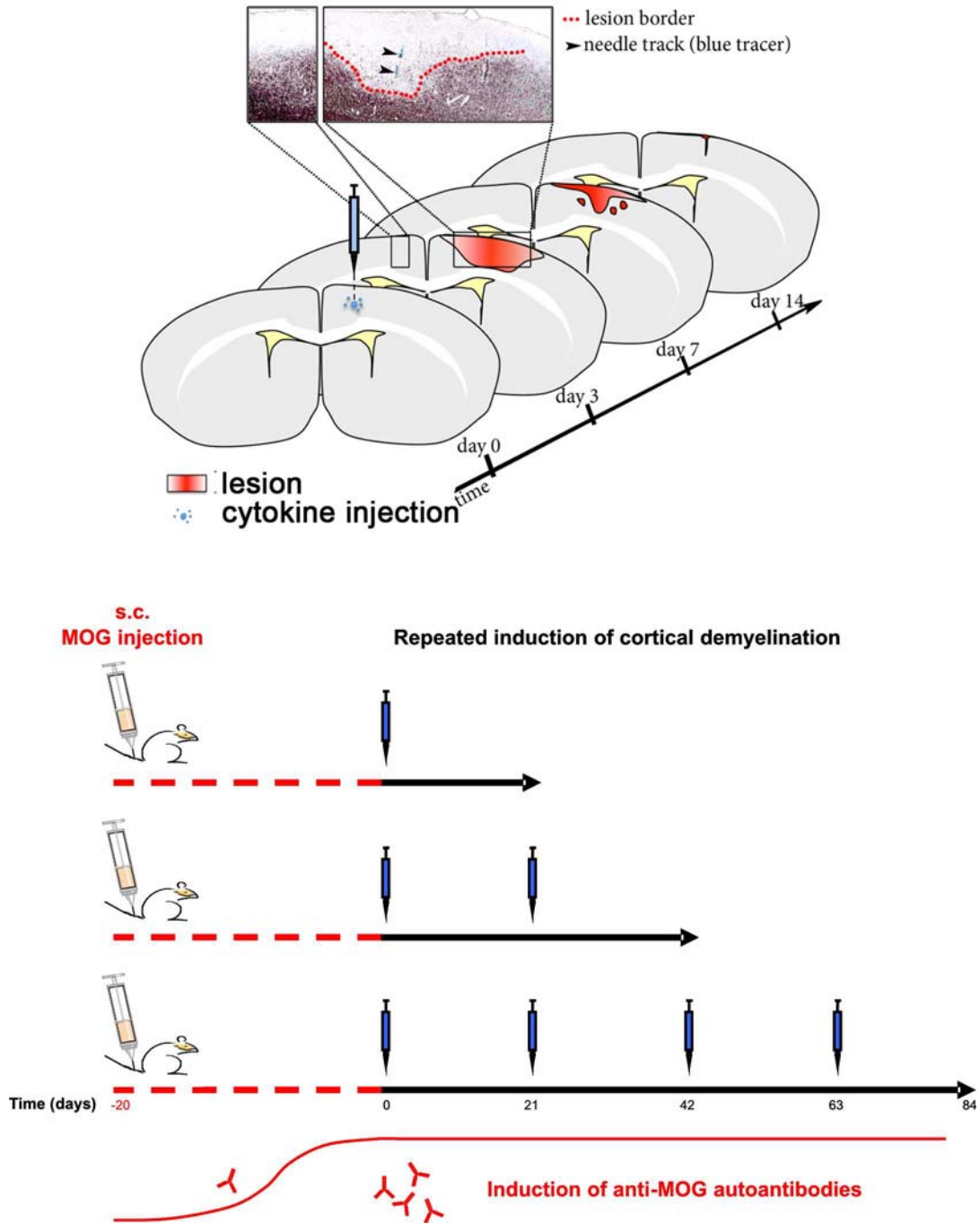


Figure 2: Experimental design

2.2 Animals and groups

A total number of n=101 adult female Lewis rats (195g ± 15, Harlan, Horst, Netherlands) were included in this study. The animals were kept in groups (max. 8 animals per cage) on a 12:12 h light/dark cycle with food and water provided ad libitum. All experiments were approved by the Bezirksregierung Braunschweig, Germany.

This study consisted of 5 independent experiments from which 4 were pooled for the repetitive lesioning approach (Table 1), as interexperimental variations were negligible. In an additional experiment, proliferation of oligodendroglial cells were analysed in more detail (Table 2). The following tables show the total numbers of animals used:

immunization	1 st injection		2 nd injection		4 th injection	
	days post injection*		days post injection*		days post injection*	
	3	21	3	21	3	21
s.c. MOG	9	11	7	5	8	18
s.c. IFA	6	-	-	-	4	-
no	6 [†]	-	-	-	-	-

* sacrifice of animals; [†] 3 of 6 animals were killed immediately after injection

Table 1: Numbers of animals, groups and time points of the repetitive lesioning approach

immunization	1 st injection		
	days post injection*		
	3	21	21 [‡]
s.c. MOG	4	6	-
s.c. IFA	5	6	6 ⁺

* sacrifice of animals; [‡] intracerebral PBS injection instead of cytokines

⁺ the contralateral side was used as a control and termed “non-injected”

Table 2: Numbers of animals, groups and time points of the single lesioning approach

2.3 Solutions and reagents

Phosphate buffered saline (PBS):

PBS (Dulbecco, Biochrom AG)	9.55g
distilled water	1000ml

1M sulfuric acid:

96% sulfuric acid (Merck)	51.1ml
distilled water	448.9ml

4% paraformaldehyde (PFA):

PFA (Merck, Germany)	40g
1.0 M sodium hydroxide	1 drop
10-fold PBS	100ml
distilled water	9000ml
adjust to pH 7.3	

0.05% Triton containing phosphate buffered saline (PBST):

PBS	1000ml
Triton X-100 (MP Biomedicals)	500 μ l

Bielschowsky silver staining:

20% silver nitrate solution:

silver nitrate (Roth)	10g
distilled water	50ml

Developer stock solution:

37% formalin (Merck)	20ml
----------------------	------

citric acid (Merck)	0.5g
65% nitric acid (Merck)	2 drops
distilled water	100ml

2% sodium thiosulfate solution:

sodium thiosulfate pentahydrate (Merck)	10g
distilled water	500ml

H & E staining:

1% acid rinse:

30% hydrochloric acid	2ml
100% Isopropyl alcohol (Merck)	198ml

1% eosin solution:

Eosin-G Certistain© (Merck)	2ml
70% isopropyl alcohol (filter before use)	198ml

Immunohistochemistry:

10mM citric acid buffer:

citric acid (Merck))	2.1g
distilled water	1000ml
adjust to pH 6	

Tris-ethylenediaminetetraacetic acid (Tris-EDTA) buffered saline:

Trizma base (Sigma)	1.21g
---------------------	-------

1.0M EDTA	1ml
distilled water	1000ml
adjust to pH 9	

0.2% casein block:

Tropix (Applied Biosystems)	2g
PBS	1000ml
Tween 20 (Merck)	1ml
heat Tropix/PBS to 50°C until it dissolves	

1.0M Tris/HCl stock solution:

trizma base (Sigma)	121g
30% hydrochloric acid	400ml
sodium chloride (Merck)	170g
distilled water	fill up to 1000ml
adjust to pH 7.5	

TBS working solution (washing buffer for immunohistochemistry):

sodium chloride (Merck)	9g
1.0M Tris/HCl	50ml
adjust to pH 7.5	

Fast Red working solution:

0.1M TBS (pH 8.2)	49ml
naphtol-ASMX-phosphate (Sigma)	10mg
dimethylformamide (Sigma)	1ml
1.0M levimasole (Sigma)	50µl
Fast Red TR salt (Sigma)	0.05g
filter before use	

3,3'-diaminobenzidine tetrachloride (DAB) working solution:

DAB (Sigma)	25mg
PBS	50ml
30% hydrogen peroxidase (Merck)	30 μ l

1% nickel ammonium sulfate solution:

nickel ammonium sulfate (Merck)	0.1g
distilled water	10ml

4-nitro blue tetrazolium chloride (NBT) stock solution:

70% N,N-dimethylformamide (Sigma)	1ml
NBT (Roche)	100mg

5-bromo-4-chloro-3-indolyl phosphate (BCIP) stock solution:

70% N,N-dimethylformamide (Sigma)	1ml
BCIP (Roche)	50mg

NBT/BCIP buffer:

1.0M Tris (Sigma-Aldrich)	100ml
5.0M NaCl (Merck)	20ml
1.0M MgCl (Merck)	50ml
distilled water	100ml

NBT/BCIP working solution:

NBT stock solution	225 μ l
--------------------	-------------

BCIP stock solution	175µl
NBT/BCIP buffer	50ml

2.4 Operations and procedures

2.4.1 Immunogen

Recombinant MOG (rMOG) was produced as described by Adelman and colleagues (Adelman *et al.*, 1995). Briefly, rMOG corresponding to the N-terminal sequence of rat MOG (amino acids 1-125) was expressed in *Escherichia coli* and purified to homogeneity. The purified protein was dissolved in 6 mol/l of urea and dialysed against 20 mmol/l of sodium acetate buffer (pH 3.0). Finally, the sample was stored at -70°C.

2.4.2 Sensitization procedure

Rats (n = 68) were anaesthetized by inhalation anaesthesia with isoflurane (Abbot, Germany) and injected subcutaneously at the base of tail with a total volume of 100µl of rMOG (50µg MOG diluted in saline) emulsified in incomplete Freund's adjuvant (IFA; Sigma-Aldrich Chemie GmbH, Steinheim, Germany). For control experiments, rats (n = 27) were injected subcutaneously at the base of the tail with a total volume of 100µl of saline emulsified in IFA. A subset of animals (n=6) received no s.c. injection (native controls). For induction of a targeted EAE lesion, MOG-sensitized rats were kept for 19-21 days and then given a stereotactic injection of cytokines into a predetermined location of the cerebral cortex.

2.4.3 Intracerebral stereotactic injection

Animals were anaesthetized by intraperitoneal (i.p.) injection of ketamine 60mg/kg bodyweight (Inresa, Freiburg, Germany) and xylazine 8mg/kg bodyweight (Riemser, Greifswald, Germany). One ml of warmed sterile saline was administered subcutaneously to maintain normal hydration during the surgical procedure and recovery. Following loss

of consciousness, the rats were mounted on a stereotactic device (Stoelting Co, IL, USA). A fine hole was then drilled through the skull 1 mm caudal to bregma and 2 mm lateral to the sagittal suture. To minimize the risk of brain damage, the drilling head was removed before penetrating the skull. The remaining thin skull was then opened by a fine scalpel, giving access to the surface of the brain. A finely calibrated glass capillary (Braun, Germany) was then stereotactically inserted, targeting the cortex at approximately 1.7 mm depth. The rats were then injected with 1 μ l of a cytokine mixture composed of 250 ng of recombinant rat tumour necrosis factor- α (TNF- α ; R&D Systems, Abingdon, UK) and 150 U of recombinant rat interferon- γ (IFN- γ ; PeproTech, London, UK) dissolved in phosphate-buffered saline (PBS, Dulbecco instamed, Biochrom AG, Germany) over a 3-min period. A trace of monastral blue (Fluka, Germany) was added as a marker dye for better visibility. Unsensitized (native) control animals (Table 1) and a subgroup of s.c. MOG immunized animals (Table 2) received PBS and monastral blue alone. After injection, the capillary was carefully withdrawn and the operation site was sealed by suture. To provide analgesia, Temgesic[©] (Essex Pharma GnbH, Germany) was administered at 0.03mg/kg during surgery and 6 hours later. Stereotactic cytokine injection was performed up to four times at intervals of 21 days, always targeting the same area (Tables 1 and 2).

2.4.4 5-bromo-2-deoxyuridine (BrdU) injection

To determine proliferation of oligodendroglial cells after lesion induction, BrdU labelling was performed. A subset of s.c. MOG (n=44) and s.c. IFA (n=17) immunized animals were injected intraperitoneally twice daily with 1.5ml 0.9% NaCl solution (Braun, Germany) containing 100mg/kg (animal weight) 5-bromo-2-deoxyuridine (BrdU, Sigma). In a subgroup of animals, BrdU administration was started immediately after a single lesion induction and continued until the animals were sacrificed at day three post lesion induction. In animals which were kept for 21 days after lesion induction, BrdU was administered for 5 days starting at day 2 after each final intracerebral cytokine/PBS injection.

2.4.5 Blood sampling and serum preparation

In a randomly selected group of animals, blood samples were taken 1-3 days before and 18-21 days after each intracerebral cytokine injection. Therefore, the rats were shortly anaesthetized by gas inhalation with isoflurane (Abbot, Germany). Following loss of consciousness, a blood sample (approx. 1ml) was immediately taken from the sublingual vein. Bleeding was then stopped by pressing a piece of cotton soaked in iron (III) chloride on the tongue. Collected blood samples were centrifuged (Centrifuge 5415 R, Eppendorf, Germany) at 13000rpm for 10min. The supernatant was then taken off and stored at -20°C for further measurements.

2.5 Enzyme-linked immunosorbent assay (ELISA) for detection of anti-MOG autoantibodies

To monitor the immune response, anti-MOG autoantibody serum levels were determined by ELISA. As a first step, 96-well maxisorp microtiter plates (Nunc, Langensfeld, Germany) were coated with rMOG at 0.4µg/50µl/well dissolved in PBST (phosphate buffered saline + 0.05% Triton). The plates were then wrapped in damp towels and stored at room temperature for 4 hours. Afterwards, the content was discarded by inverting the plates and tapping the bottom on paper towels. Plates were then blocked with 5% bovine serum albumin (BSA, Serva) dissolved in PBS (200µl/well) for 1h at room temperature and washed subsequently 5 times with water. As a last step, wells were filled with 200µl each and incubated for 15min at room temperature. Before storing at -20°C the plates were tapped on paper towels as described earlier.

Rat sera were prepared by diluting 1:100 in PBST. In addition, 1:3 serial dilutions of each sample were added on a MOG coated plate starting with the upper row. The plates were then kept humid for 2h at room temperature. To remove unbound antibodies, plates were washed 6 times with PBST. Afterwards, 50µl of IgG-specific horseradish peroxidase-conjugated goat anti-rat antibody (1:10000 in PBST; Pierce, Rockford, IL, USA) was added to each well and kept humid for 2 hours at room temperature. Following proper washing with PBST (6 times) 50µl of 3,3'-5,5'-tetramethylbenzidine (BM-Blue, POD; Roche, Basel, Switzerland) was added as a substrate. After the first row of wells

developed a blue colour, reaction was stopped immediately by adding 50µl of 1M H₂SO₄ (Merck) to all wells. Finally, optical density (OD) was measured at 450nm (Model 680, Bio-Rad, Hercules, CA, USA). Antibody titres were defined as the serum dilutions at half maximum OD.

2.6 Histology

2.6.1 Tissue processing

2.6.1.1 Perfusion and sectioning

Animals were anaesthetized by injecting a lethal dose of 14% chloral hydrate (Merck). After loss of consciousness, transcardial perfusion was performed through the left cardiac ventricle with PBS followed by 4% paraformaldehyde. Brains were then dissected and stored for 24h in 4% paraformaldehyde at 4°C. After fixation, the brain was cut in 4mm thick slices and washed in water. In addition, slices were gradually dehydrated by performing alcohol/xylol/paraffin series overnight using an automated tissue processor (Thermo Scientific, Germany). The next day, slices were embedded in paraffin. Tissue blocks were then cut in 1-2µm thin coronal sections. Serial sections adjacent to the injection site were used for further histology (injection site was recognized/identified by traces of monastral blue).

2.6.1.2 Deparaffination and dehydration of histological sections

Prior to histological stainings, sections were deparaffinized by performing graded xylol (Merck) and isopropyl alcohol (Merck) series as follows: 4 x 100% xylol (8min), 1 x xylol/alcohol (1:1, 1min), 2 x 100% alcohol (4min), 1 x 90% alcohol (4min), 1x 70% alcohol (4min), 1x 50% alcohol (4min), 1x distilled water.

Dehydration was achieved by performing the above described series in reversed order.

2.6.2 Histochemical stainings

2.6.2.1 Hematoxylin and eosin (HE) staining

HE staining was performed to obtain a general overview with regard to inflammation and astrocytosis. Sections were deparaffinized as described above, washed 3 times with distilled water and placed into Mayers Hämalaun (Merck, Germany) for 5 min. Afterwards, sections were washed with distilled water and differentiated by dipping slides once into 1% acid rinse. Subsequently, bluing was performed by bathing slides in flowing tap water for 10min. Slides were then washed in distilled water and placed into eosin solution for 5min. In addition, slides were washed (once again) in distilled water and dehydrated as described earlier. Alcohol series were performed quickly to avoid excessive elution of eosin. Finally, slides were mounted using DePex mounting medium (VWR International, Germany) and coverslipped.

2.6.2.2 Bielschowsky silver staining (modified)

To assess axonal integrity Bielschowsky silver staining was performed. Sections were deparaffinized as described earlier and washed 3 times with distilled water. Afterwards, sections were placed in 10% silver nitrate solution for 20min. Concentrated (32%) ammonium hydroxide (Merck, Germany) was added drop by drop to the nitrate solution until the formed precipitate cleared. Following washing in distilled water, the slides were placed into the silver nitrate/ammonium hydroxide solution for 15min and kept dark. While washing the slides in distilled water (containing few drops of ammonium hydroxide), 10 drops of developer stock solution was added to silver nitrate/ammonium hydroxide solution using a stirrer. Subsequently, the slides were placed into this solution for about 1 minute until color of the tissue turned to ochery. In addition, excessive silver nitrate was washed out using 2% sodium thiosulfate solution. After a final wash with distilled water, slides were dehydrated as described earlier and mounted using DePex mounting medium (VWR International, Germany) and coverslipped.

2.6.3 Immunohistochemistry

2.6.3.1 Antigen retrieval

Loss of immunoreactivity caused by paraformaldehyde fixation can be reversed if tissue is exposed to heat and acid:

Hydrated and washed slides were placed in closed polystyrene cuvettes filled to the top with 10mM citric acid (pH=6) or 1mM Tris-EDTA (pH=9) buffered saline. Slides were heated 5 times for 3 min using a microwave oven (800watt, Bosch). Between each incubation cycle (step), cuvettes were filled up alternately with buffer and distilled water. Before continuing further staining procedure, slides were left to cool down for 30min and then washed with distilled water.

2.6.3.2 GFAP immunohistochemistry

Reactive astrogliosis was assessed by immunohistochemistry using glial fibrillary acidic protein (GFAP) as a marker for astrocytes. Slides were washed 5 times in PBS between each step. Following deparaffination, endogenous peroxidases were blocked by placing slides in 3% hydrogen peroxide (dissolved in PBS) for 20min at 4°C. Unspecific antibody binding was performed by applying 100µl 10% fetal calf serum (FCS, Biochrom) for 30 min. Afterwards, excessive FCS was removed with a cleaning wipe without washing with PBS. The primary antibody mouse anti-human GFAP (1:50, clone 6F2, Dako) was added overnight at 4°C. Biotinylated sheep anti-mouse (1:200, Amersham) and ExtrAvidin (1:1000, Sigma) were applied consecutively for 1h at room temperature. Color development with DAB was performed for approximately 5min followed by counterstaining with Mayers Hämalaun (Merck, Germany). Finally, slides were dehydrated and mounted using DePex mounting medium (VWR International, Germany) and coverslipped.

2.6.3.3 MBP immunohistochemistry

Demyelination and remyelination was assessed by immunohistochemistry using MBP as a marker for myelin sheaths. Slides were washed 5 times in PBS between each step, blocking of unspecific antibody binding being an exception. Following deparaffination, endogenous peroxidases were blocked by placing slides in 3% hydrogen peroxide (dissolved in PBS) for 20min at 4°C. Unspecific antibody binding was performed by incubation with 100µl 10% fetal calf serum (FCS, Biochrom) for 30 min. The primary antibody, rabbit anti-human MBP (1:1500, A0623, Dako), was added overnight at 4°C. Biotinylated donkey anti-Rabbit (1:200, Amersham) and ExtrAvidin (1:1000, Sigma) were applied consecutively for 1h at room temperature. Color development with DAB was performed for approximately 5min followed by counterstaining with Mayers Hämalaun (Merck, Germany). In a subset of animals, color reaction was enhanced by adding 2.5ml of 1% nickel ammonium sulfate to the substrate solution (adjusted to pH 7.2). Finally, slides were dehydrated and mounted using DePex mounting medium (VWR International, Germany) and coverslipped.

2.6.3.4 ED1 immunohistochemistry

Inflammation was assessed by immunohistochemistry using ED1 as a marker for macrophages and activated microglia, respectively. Slides were washed 5 times in PBS between each step. Following deparaffination, antigen retrieval (10mM citric acid and microwave irradiation) was performed as described above. Afterwards, endogenous peroxidases were blocked by placing slides in 3% hydrogen peroxide (dissolved in PBS) for 20min at 4°C. Blocking of unspecific antibody binding was achieved by incubation with 100µl 10% FCS for 30min. Afterwards, excessive FCS was removed with a cleaning wipe without washing with PBS. The primary antibody, rabbit anti-human ED1 (clone ED1; Serotec, Oxford, UK), was applied overnight at 4°C. Biotinylated donkey anti-rabbit (1:200, Amersham) and ExtrAvidin (1:1000, Sigma) were added consecutively for 1h at room temperature. Color development with DAB was performed for approximately 5min followed by counterstaining with Mayers Hämalaun (Merck). Finally, slides were

dehydrated and mounted using DePex mounting medium (VWR International, Germany) and coverslipped.

2.6.3.5 MBP/NogoA double immunohistochemistry

To determine the oligodendrocyte density within the lesion, double immunohistochemistry was performed using MBP as a marker for myelin sheaths and NogoA (clone 11C7) as a marker for mature oligodendrocytes. Antigen retrieval (10mM citric acid and microwave irradiation) was performed followed by blocking of endogenous peroxidases and unspecific antibody binding as described above (see 2.5.3.4). The primary antibody, mouse anti-mAb11C7 (1:20000, kindly provided by M. E. Schwab, ETH Zurich), was added overnight at 4°C. Biotinylated sheep anti-mouse (1:200, Amersham) and ExtrAvidin (1:1000, Sigma) were applied consecutively for 1h at room temperature. Color development with DAB was performed for approximately 5min. To saturate open binding sites on the first primary antibody, 100µl of Fab antibody (mouse, Dako) was added followed by blocking of unspecific antibody binding sites using 100µl 10%FCS (containing 0.05% Triton-X-100, MP Biomedicals). The second primary antibody, rabbit anti-human MBP (1:1500, A0623, Dako), was applied for 2h at room temperature. Henceforth, 0.5M Tris buffered saline (TBS) was used for washing and incubation steps. Mouse anti-rabbit antibody bridge (1:50, Dako), goat anti-mouse-alkaline phosphatase (AP) (1:50, Dako) and alkaline phosphatase anti-alkaline phosphatase (APAAP) mouse (1:50, Dako) were added consecutively for 1 hour at room temperature. Color reaction was performed using NBT/BCIP (Roche) as substrate. For representative photographs, some sections were stained using Fast Red as a substrate. Finally, slides were mounted with Immu-Mount (ThermoScientific) and coverslipped.

2.6.3.6 Olig2/PLP double immunofluorescence

To determine the oligodendroglial precursor density within the lesion, double immunofluorescence staining was performed using PLP as marker for myelin sheaths and olig2 as a marker for oligodendroglial precursors/early oligodendrocytes. Antigen

retrieval (1mM Tris-EDTA, pH=9, microwave heating) was followed by blocking with 0.2% casein (Tropix, I-Block, Applied Biosystems) in PBS for 30min. The first primary antibody, rabbit anti-human olig2 (1:300 in 0.2% casein, IBL, Germany), was added overnight at 4°C. The indocarbocyanine 3 (Cy3) conjugated donkey anti-rabbit IgG (H+L) secondary antibody (1:300 in 0.2% casein, Dianova GmbH, Hamburg, Germany) was applied for 1h at room temperature. The second primary antibody, mouse anti-PLP (1:2500 in 10% FCS, clone Plpc1, Biozol), was added overnight at 4°C followed by indocarbocyanine 2 (Cy2) conjugated donkey anti-mouse IgG (H+L) secondary antibody (1:200 in 10% FCS, Dianova GmbH, Hamburg, Germany) for 1h at room temperature. Cell nuclei were stained with DAPI (1:10000 in 10%FCS, Molecular Probes) for 10min at room temperature. Finally, slides were mounted using Fluoromount (Dako) and coverslipped.

2.6.3.7 NogoA/BrdU double immunohistochemistry

To determine the mature oligodendrocyte population derived by cell division after lesion induction, double immunohistochemistry was performed. NogoA was used as a marker for mature oligodendrocytes. BrdU was used as a marker for previous cell division. Antigen retrieval (10mM citric acid and microwave irradiation) was performed followed by blocking of endogenous peroxidases and unspecific antibody binding as described above (2.5.3.4). The primary antibody, rabbit anti-NogoA (1:100 in 10% FCS, clone H300, Santa Cruz), was added overnight at 4°C. Henceforth, 0.5M Tris buffered saline (TBS) was used for washing and incubation steps till finishing the first staining. Goat anti-rabbit alkaline peroxidase (AP) conjugated antibody (1:50, D0487, Dako) was added for 45min at room temperature. Color reaction was performed using Fast Red (Sigma) as a substrate. The second primary antibody, mouse anti-BrdU (1:400 in 10% FCS, Chemicon), was applied overnight at 4°C. Biotinylated sheep anti-mouse (1:200 in 10% FCS, GE Healthcare) and ExtrAvidin (1:1000, Sigma) were added consecutively for 1h at room temperature. Color development with DAB was performed for approximately 5min followed by counterstaining with Mayers Hämalaun (Merck). Finally, slides were mounted using Immu-Mount (ThermoScientific) and coverslipped.

2.6.3.8 Olig2/BrdU double immunohistochemistry

To determine the oligodendroglial precursor density derived by cell division after lesion induction, double immunofluorescence staining was performed using olig2 as a marker for oligodendroglial precursors/early oligodendrocytes and BrdU as a marker for proliferation. Antigen retrieval (Tris-EDTA and microwave heating) was performed followed by blocking with 0.2% casein in PBS for 30min. The first primary antibody, rabbit anti-human olig2 (1:300 in 0.2% casein, IBL, Germany), was added overnight at 4°C. The Cy3-conjugated donkey anti-rabbit IgG (H+L) secondary antibody (1:300 in 0.2% casein, Dianova GmbH, Hamburg, Germany) was applied for 1h at room temperature. As a second primary antibody, mouse anti-BrdU (1:400 in 10% FCS, Chemicon) was added overnight at 4°C followed by Cy2-conjugated donkey anti-mouse IgG (H+L) secondary antibody (1:200 in 10% FCS, Dianova GmbH, Hamburg, Germany) for 1h at room temperature. Cell nuclei were stained with DAPI (1:10000 in 10%FCS, Molecular Probes) for 10min at room temperature. Finally, slides were mounted using Fluoromount (Dako) and coverslipped.

2.7 Photoimaging and morphometric analysis

Histological photographs were captured through light and fluorescent microscopes (BX 40 and BX 50, Olympus, Germany) at 20-, 40-, 200-, 400- and 1000-fold magnification, respectively. Images for computer-aided analysis were recorded with digital cameras mounted on mentioned microscopes (Color View II and DP71, Olympus, Germany).

Histological stainings were analysed as followed:

Digital images of MBP-stained sections were recorded through a light microscope (BX 40, Olympus, Germany) with a CCD camera (Color View II, Olympus, Germany) at 200-fold magnification. The size of demyelinated lesion was measured using Analysis software (Analysis, Soft Imaging System, Germany). The extent of demyelination was defined as the MBP-negative area (mm²). The length of subpial lesion was given in µm.

The fraction of myelinated axons was determined in cortical layer III within 4 fields of sight using a counting grid (10x10 squares) at 1000-fold magnification (see Figure 3, A).

The numbers of MBP-positive myelin sheaths which overlapped the crosses of the counting grid were determined on MBP-stained sections. In addition, the numbers of axons were analysed in the same way on adjacent Bielschowsky-stained sections. Afterwards, MBP-positive fibre counts were normalized to axon counts, second been set to 100% as a reference.

The macrophage/microglia reaction was determined on ED1-stained sections within two defined cortical areas. First, ED1-positive cells were counted in cortical layer III within the center of lesion within four fields of sight at 1000-fold magnification (Figure 3, A). To capture a broad area of inflammation, a further region of interest (ROI) was chosen. This ROI was defined as the cortical area lying within the upper quadrant of a standardized fictive rectangular cross, which was placed in the middle of the analyzed section orientated in the medial-lateral and dorsal-ventral direction, respectively (Figure 3, C). For both ROIs, the mean number of ED1-positive cells per square millimetre was given.

Axonal integrity was assessed on Bielschowsky silver-stained sections at 1000-fold magnification. Axons were determined in the center of lesion of cortical layer III within 4 fields of sight using a 10x10 counting grid (Figure 3, A). Axonal density was given in percent using untreated control animals as a reference (set to 100%).

NogoA-positive cell population was determined on NogoA/MBP double positive-stained sections at 400x-fold magnification. Proliferated NogoA-positive cells were determined on NogoA/BrdU double stained sections. The density of both cell populations were assessed in cortical layers I and II within 11 fields of sight of a 10x10 counting grid, covering the typically affected areas of subpial demyeliantion (Figure 3, B). Cell density was given as cells per square millimetre.

Olig2-positive and olig2/BrdU-double positive cell populations were determined on olig2/BrdU double fluorescent stained sections using a light/fluorescent microscope (BX 51, Olympus, Germany) at 200-fold magnification. Cells were counted in cortical layers I and II within three fields, which is similar to ROI used for evaluation of above mentioned NogoA-positive cell populations (Figure 3, B). Cell densities were given as cells per square millimetre.

A cell was considered “positive” or “double-positive” when the following two conditions were met:

First, the specific signal must overlap with the cell soma (NogoA, olig2, BrdU, ED1) or its dendritic processes (ED1). Second, a cell must contain a nucleus.

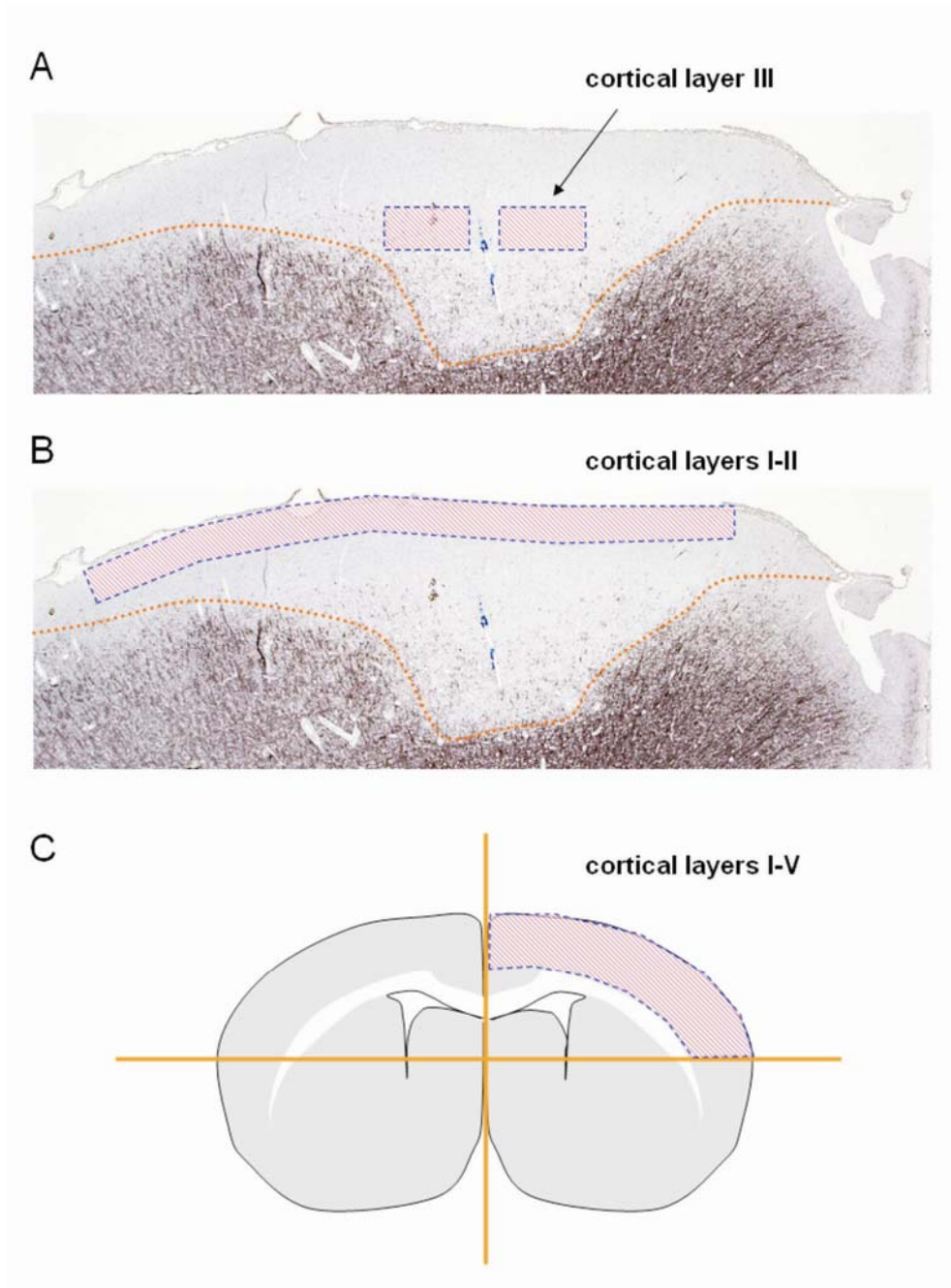


Figure 3: Regions of interest used for histological evaluation

2.8 Statistics

Statistical analysis was performed using a statistical software package (SPSS Version 12 for Windows, SPSS Inc., Chicago, IL, USA). Graphs were visualized with GraphPad version 5 for windows (GraphPad Software, San Diego, CA, USA). Normality of distribution was verified by Kolmogorow-Smirnov-test. Statistical calculations included one-way analysis of variance (ANOVA) if three or more groups were compared, followed by *post-hoc* least significance difference (LSD)-test. For comparisons between two groups, unpaired t-tests were performed. A probability value of less than 0.05 was considered significant. All data are given as mean + SEM.

3. RESULTS

3.1 Detection of anti-MOG autoantibody titres

High and stable serum levels of anti-MOG autoantibodies are an important prerequisite for induction of targeted EAE lesions. Therefore, serum levels of MOG autoantibodies were monitored by ELISA at regular intervals. High and consistent anti-MOG autoantibody titres were detected in s.c. MOG immunized animals at all time points analysed (Figure 4). As expected, s.c. IFA immunized control animals did not reveal a significant antibody response against MOG.

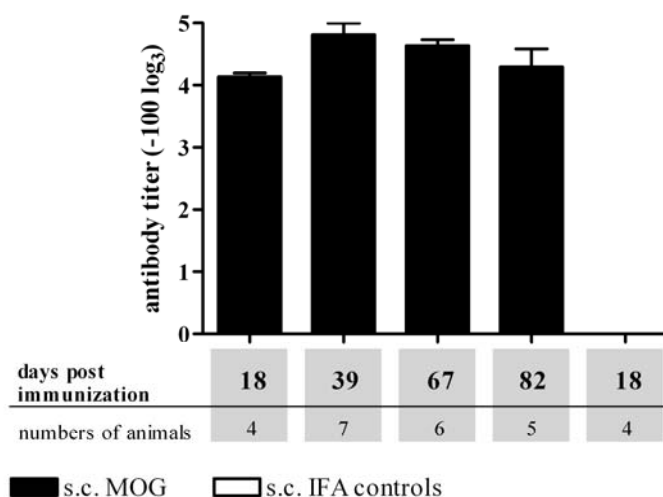


Figure 4: Anti-MOG autoantibody titres

Titres of anti-MOG autoantibodies. Time-course analysis revealed high and consistent anti-MOG antibody titres in s.c. MOG immunized animals. S.c. IFA control animals did not reveal a detectable antibody response against MOG. Data are expressed as mean + SEM. For statistical evaluation, one-way ANOVA was performed.

* antibody titres refer to the serum dilution needed to achieve half maximum OD

3.2 Gliosis

To analyse possible traumatic effects caused by surgical intervention, HE-staining and GFAP immunohistochemistry were performed. HE-staining revealed moderate gliosis and edema restricted to the close proximity of the injection site (Figure 5, A, D and E). This observation was supported by GFAP-staining showing intense GFAP-

immunoreactivity at similar areas to the HE-staining (Figure 6, A, C, F). In addition, 21 days post lesion induction, a few s.c. MOG immunized animals presented with increased subpial GFAP-immunoreactivity in remyelinated cortical areas. Aside from these aforementioned cases, adjacent areas showed no pathological abnormalities (Figure 5, B and C; Figure 6, B/D/E).

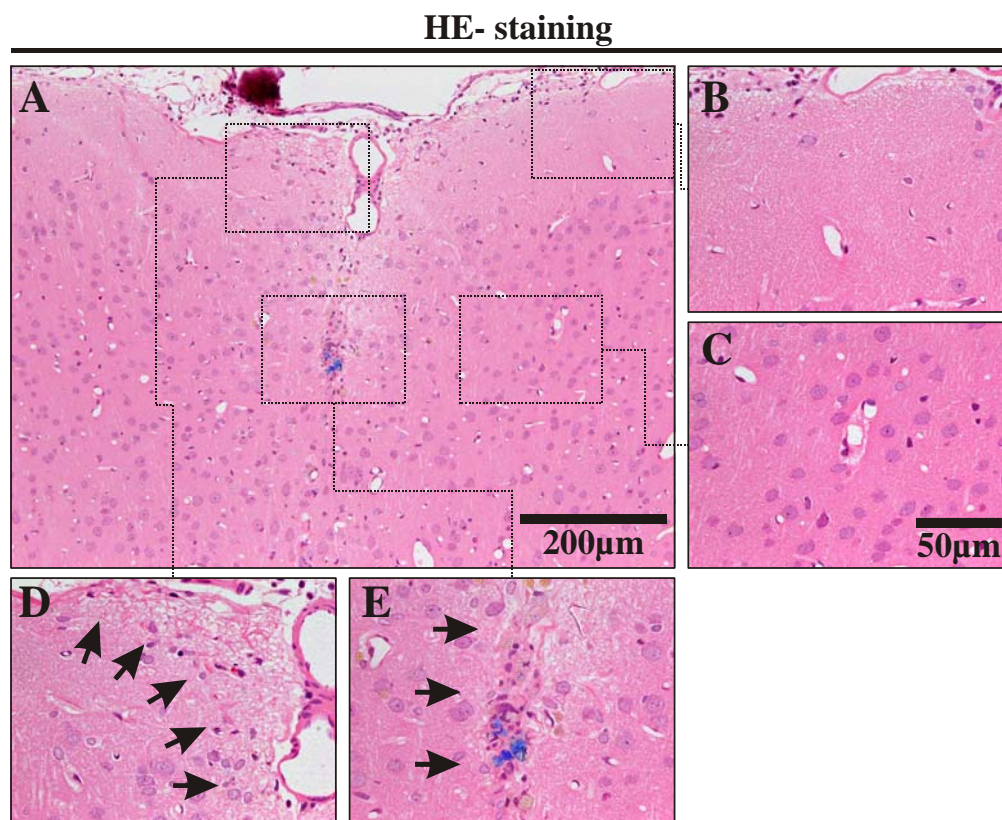


Figure 5: HE-staining of local gliosis

Representative photographs of HE-stained section of a cortical lesion (A-E). Moderate gliosis was observed at close proximity of the needle track (A/D/E). Edema and glial scar formation (D and E, indicated by arrows) were restricted to the immediate vicinity of the injection. No pathological abnormalities were observed in adjacent areas within cortical lesion (B/C).

Scale bars: A = 200µm, B-E = 50µm

GFAP- immunohistochemistry

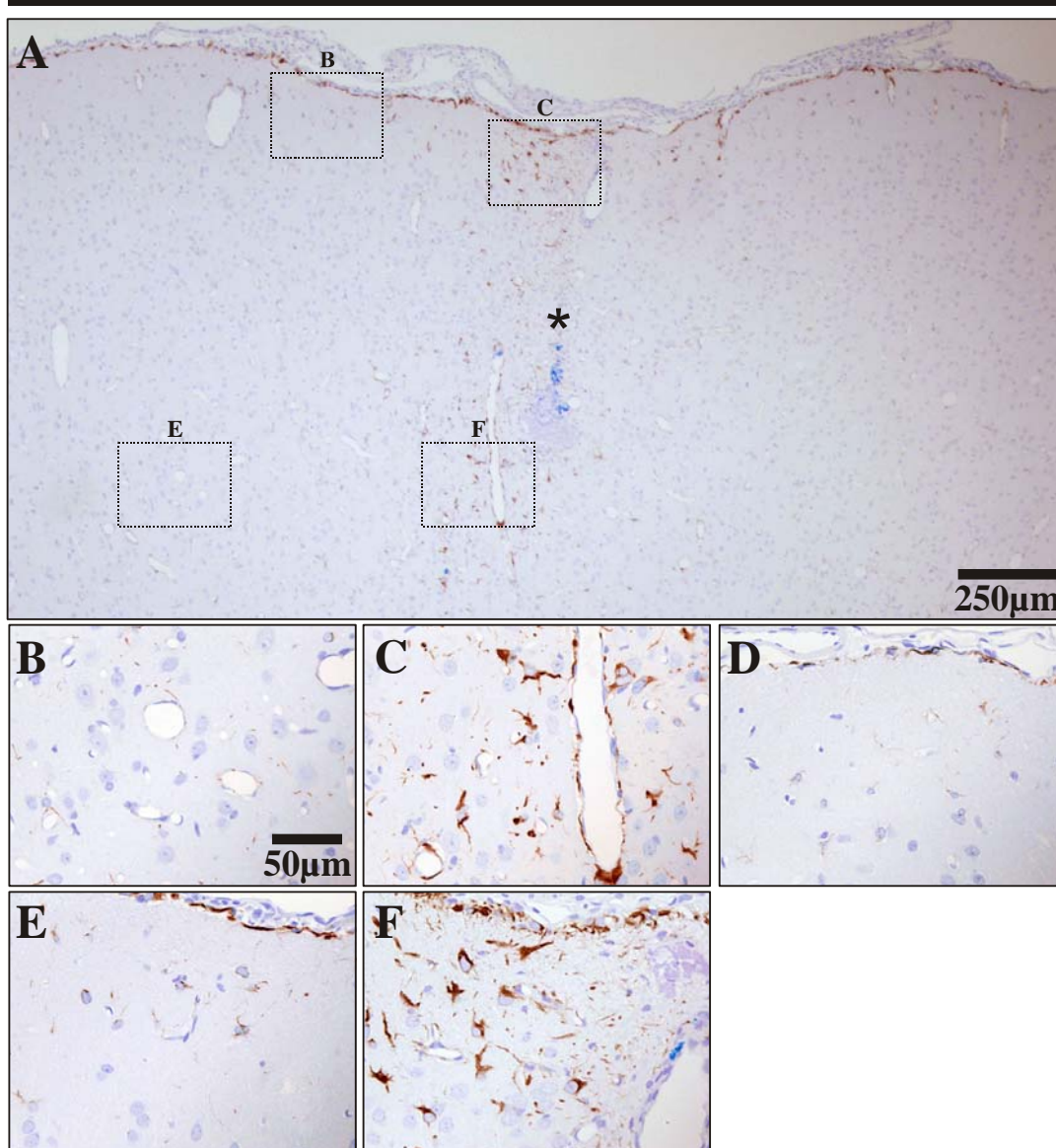


Figure 6: GFAP immunohistochemistry of local gliosis

Representative photographs of GFAP-immunostained section of a cortical lesion (A-F). GFAP immunoreactivity was observed in close proximity to the injection site (A/C/F). No pathological abnormalities were observed in adjacent areas within the cortical lesion (B//D/E).

Scale bars: A = 250µm, B-F = 50µm

3.3 Topology of de- and remyelination in the focal cortical EAE model

MBP immunohistochemistry was performed to assess demyelination and remyelination, respectively. At day three post intracerebral cytokine injection, extensive cortical

demyelination was observed in MOG primed animals (Figure 7, A-C). With regard to topology, a pronounced widespread subpial lesions was located at the site of injection (Figure 7, A-C), which often extended into deep cortical layers (layers 4-6). In the medial-lateral direction, demyelination extended more superficially (layers 1-3). The topography of these lesions was highly reminiscent of cortical type III lesions found in multiple sclerosis (Peterson *et al.*, 2001). In addition, spots of perivascular lesions were distributed along the ipsilateral cerebral cortex (Figure 7, A and B). Similar lesion pattern and similar extent of demyelination was observed in animals which received two or four intracerebral cytokine injections (Figure 8). The contralateral non-injected hemisphere showed no signs of demyelination (Figure 7, D, E and F). Cytokine injection did not show substantial tissue damage in s.c. IFA immunized control animals, even after repetitive injections (Figure 8). Cortical demyelination is a transient phenomenon; 21 days after lesion induction, extensive remyelination took place (Figure 8) and only few and small areas within the center of the lesion remained demyelinated. Even animals suffering from 2 or 4 demyelinating events showed extensive remyelination and did not differ morphologically from singly induced ones.

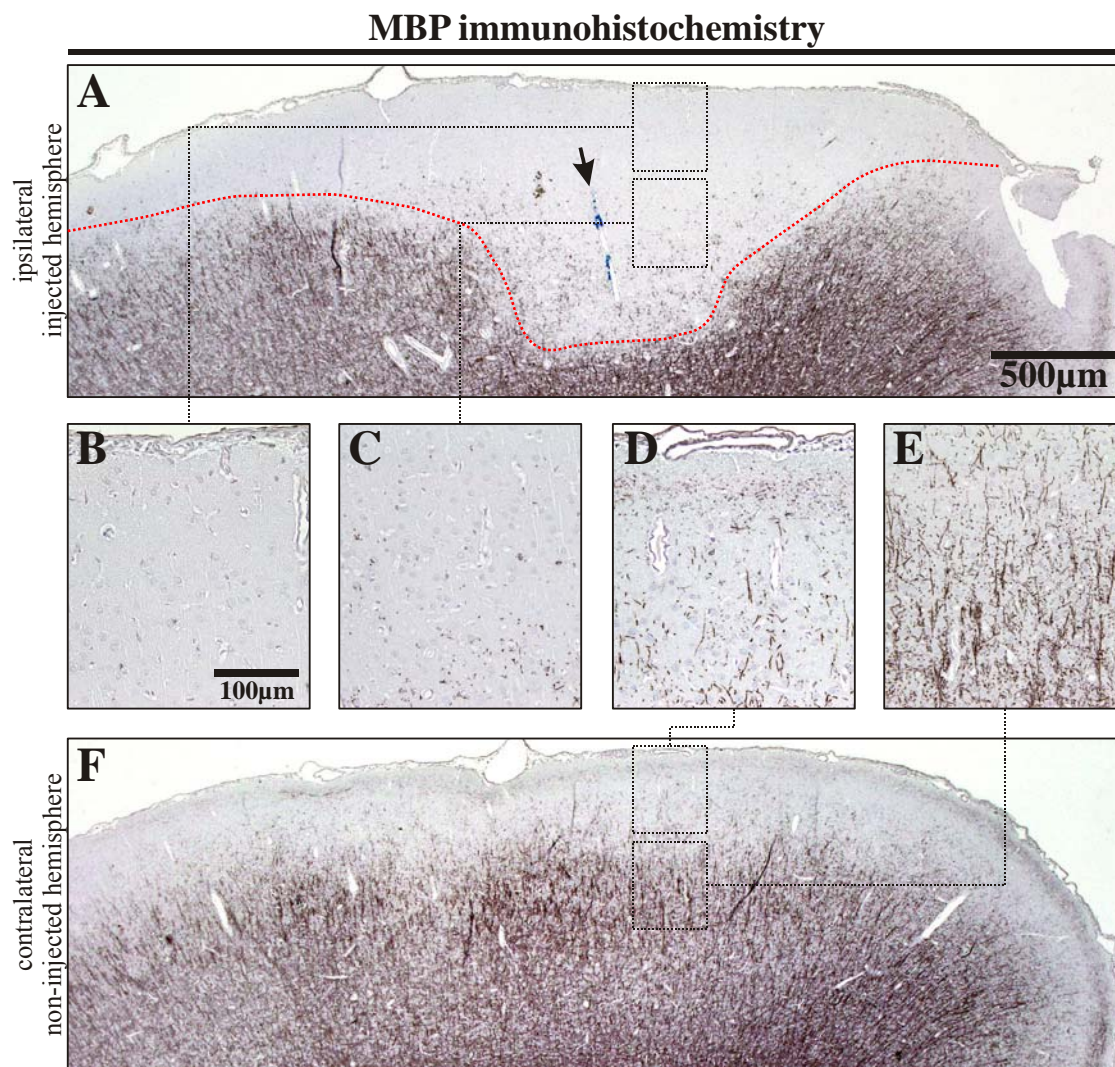


Figure 7: Focal cortical EAE lesion

Representative photographs of MBP immunostained cerebral cortex of s.c. MOG primed Lewis rats at day 3 post lesion induction (A-F). Proinflammatory cytokines such as TNF- α and IFN- γ were targeted to the cerebral cortex (indicated by arrow with a blue traced needle track underneath), leading to extensive focal demyelination (lesion border indicated by dotted line) within the ipsilateral hemisphere (A-C). The contralateral non-injected hemisphere was not affected (D-F).

Scale bars: A and F = 500 μ m, B-E = 100 μ m

MBP immunohistochemistry

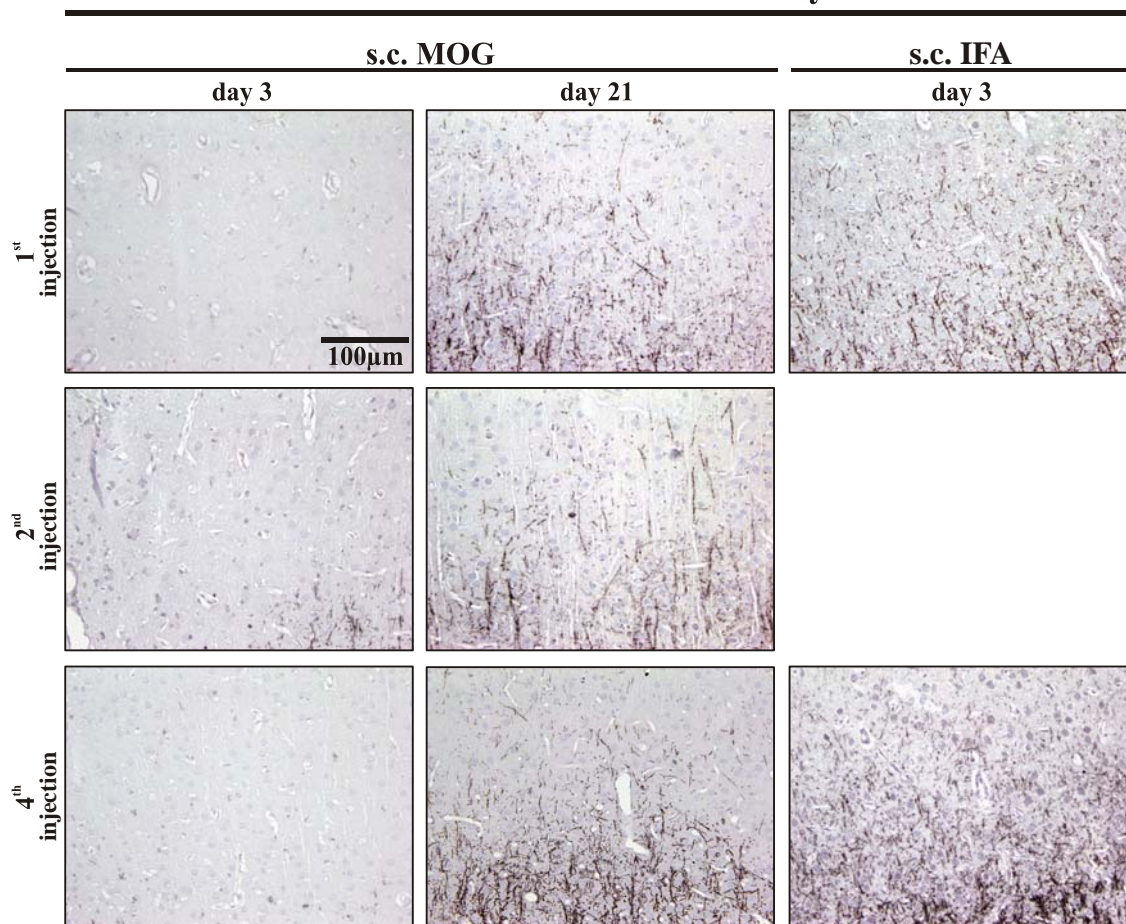


Figure 8: Cortical demyelination and remyelination after repetitive lesion induction

Representative photographs of MBP stained sections of cortical layer 3 (center of lesion). The different time points (days 3 and 21) and immunization protocols (s.c. MOG versus s.c. IFA) are arranged in columns. The numbers of lesion inductions (1st, 2nd and 4th) are arranged in rows. Repeated cortical demyelination (MBP-negative) was observed in s.c. MOG immunized animals 3 days after cytokine injection (left column). At 21 days after lesion induction, extensive remyelination (MBP-positive: dark stained fibres) took place, even after repetitive demyelinating events (middle column). S.c. MOG immunized control animals showed no signs of demyelination (right column).

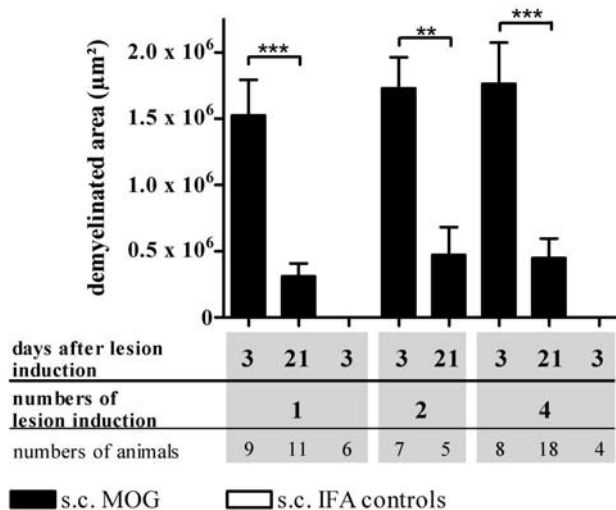
Scale bars: 100µm

3.3.1 Extent of demyelinated area

The extent of demyelination was quantified using computerbased analysis performed on photographs of MBP-stained sections. Intracerebral cytokine injection led to focal cortical demyelination in all s.c. MOG primed animals (Figure 9, A). Demyelinated area did not differ significantly between animals with singular induced lesions ($1.53 \times 10^6 \pm 2.67 \times 10^5 \mu\text{m}^2$) compared to those animals with two ($1.73 \times 10^6 \pm 2.34 \times 10^5 \mu\text{m}^2$) and four

($1.76 \times 10^6 \pm 3.12 \times 10^5 \mu\text{m}^2$) demyelinating episodes. Demyelinated area decreased significantly (one-way ANOVA $F_{5,52} = 11,013$, $p < 0,001$) twenty-one days after each previous demyelinating episode (*post-hoc* LSD-test: 1st inj. $p < 0,001$, 2nd inj. $p = 0,002$, 4th inj. $p < 0,001$). No significant difference was observed comparing groups at day 21 post lesion induction after single or repetitive lesioning. S.c. IFA immunized and cytokine injected control animals did not show any sign of demyelination.

A



B

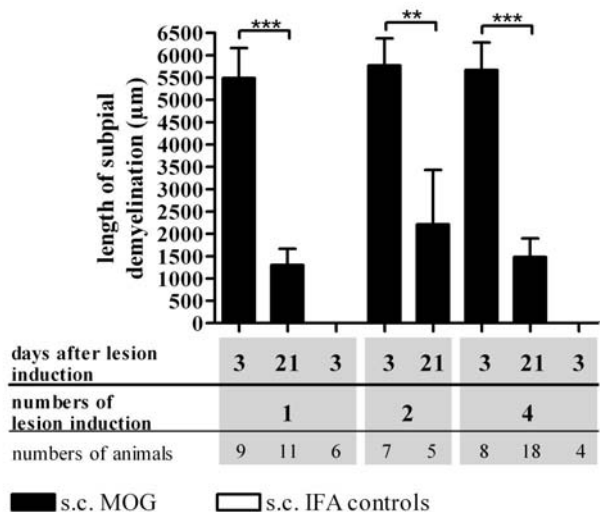


Figure 9: Extent of demyelination

(A) Extent of demyelination was determined on MBP-stained sections. Intracerebral cytokine injection following immunization with MOG led to extensive demyelination following each cytokine injection. Demyelinated area decreased significantly even after repetitive lesioning. S.c. IFA immunized control animals showed no signs of demyelination. (B) Analysis of subpial lesion length

revealed similar outcome. Data are expressed as mean + SEM. For statistical evaluation, one-way ANOVA followed by *post-hoc* LSD-test was performed (** = $p < 0.01$, *** = $p < 0.001$).

3.3.2 Length of subpial lesions

As an additional parameter, length of subpial lesion was measured. At day three post lesion induction, average subpial lesion length did not differ between singly induced lesions ($5490 \pm 670.3 \mu\text{m}$) compared to those animals with two ($5769 \pm 606.9 \mu\text{m}$) and four ($5666 \pm 621 \mu\text{m}$) demyelinating episodes (Figure 9, B). Twenty-one days after each previous lesion induction, length of subpial lesion decreased significantly (ANOVA $F_{5,52} = 14,936$, $p < 0,001$) compared to those lesions measured at day 3 (*post-hoc* LSD-test: 1st inj. $p < 0,001$, 2nd inj. $p = 0,001$, 4th inj. $p < 0,001$). No significant difference was observed comparing groups at day 21 post lesion induction. As expected, s.c. IFA immunized control groups showed no signs of demyelination.

3.3.3 Fraction of myelinated axons

To determine the ratio of myelin density to axons, the fraction of myelinated axons was measured in de- and remyelinated areas of cortical layer III. Fraction of myelinated axons is defined as the ratio of MBP-positive fibres to axons (determined on Bielschowsky silver-stained sections). In untreated age matched control animals, a considerably high fraction of myelinated axons (mean $40.58 \pm 2.67\%$) was determined. At day 3 post lesion induction, almost no myelin was detected in s.c. MOG immunized animals (Figure 10, 1st inj.: $1.27 \pm 0.58\%$, 2nd inj.: $2.67 \pm 1.12\%$, 4th inj.: $0.52 \pm 0.34\%$). Twenty-one days after lesion induction, the fraction of myelinated axons (1st inj.: $16.22 \pm 3.02\%$, 2nd inj.: 21.95 ± 3.84 , 4th inj.: $16.64 \pm 2.99\%$) increased significantly (one-way ANOVA $F_{8,61}=10,727$ $p < 0,001$) in all s.c. MOG immunized groups (*post-hoc* LSD-test: 1st inj.: $p = 0.012$, 2nd inj.: $p = 0.02$, 4th inj.: $p = 0.011$). Comparisons between s.c. MOG immunized groups at day 21 revealed no significant statistical differences. Albeit a substantial fraction of axon remyelinated at day 21, the obtained values were still significantly lower as compared to the control groups (*post-hoc* LSD-test: 1st inj.: $p < 0.001$, 2nd inj.: $p = 0.013$, 4th inj.: $p < 0.001$). At day 3 post lesion induction, fraction of myelinated axons was significantly reduced compared to control groups (*post-hoc* LSD-test: 1st, 2nd and 4th inj.: $p < 0.001$).

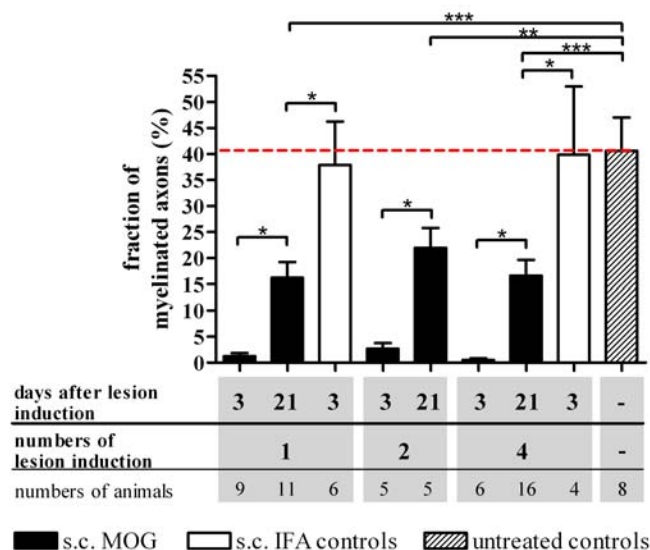


Figure 10: Fraction of myelinated axons

Fraction of myelinated axons was expressed as the percentage of myelin density normalized to axonal density. After each lesion induction, almost complete loss of myelin content was determined within the center of lesion of s.c. MOG immunized animals. Twenty-one days after lesion induction, the fraction of myelinated axons recovered significantly. However, remyelinated lesions showed significantly reduced fraction of myelinated axons compared to normally myelinated cerebral cortex (untreated controls). In contrast, IFA immunized controls showed similar fraction of myelin as untreated controls. Data are expressed as mean + SEM. For statistical evaluation, one-way ANOVA followed by *post-hoc* LSD-test was performed (* = $p < 0.05$, ** = $p < 0.01$, *** = $p < 0.001$).

3.4 Evaluation of activated macrophages/microglia

To assess inflammatory activity during de- and remyelination, immunohistochemistry was performed using ED1 as a marker for activated macrophages/microglia.

Demyelination was accompanied by inflammation (Figure 11). At day 3 after lesion induction, ED1-positive cells were detected within and near demyelinated areas (Figure 11, H). With regard to morphology, two different ED1-positive cell types were observed:

- 1) Ramified macrophages/microglia were the predominant population in s.c. IFA immunized control animals (Figure 11, G) but were also abundant within lesions of s.c. MOG primed animals.
- 2) Foamy macrophages were mainly found at day 3 post lesion induction in s.c. MOG immunized animals, indicating demyelination (Figure 11, F).

Extensive and dense parenchymal infiltrates were predominantly located in the center of subpial lesions (Figure 11, E and H). In contrast, perivascular infiltrates (Figure 11, D) were also observed in nearby non-demyelinated cortical areas (Figure 11, H). Inflammation was more pronounced after single lesioning in both density and extent of activated macrophages/microglia. ED1-positive cells were also detected in repetitively injected animals, but macrophage/microglia activation seemed to be less pronounced compared to singly injected ones (Figure 12). Inflammation resolved 21 days after lesion induction. Just few ED1-positive cells were observed in close vicinity to the needle track, similar to s.c. IFA immunized control animals. The contralateral non injected side appeared normal and rarely few ED1-positive cells were detected in the subpial region of the sulcus centralis.

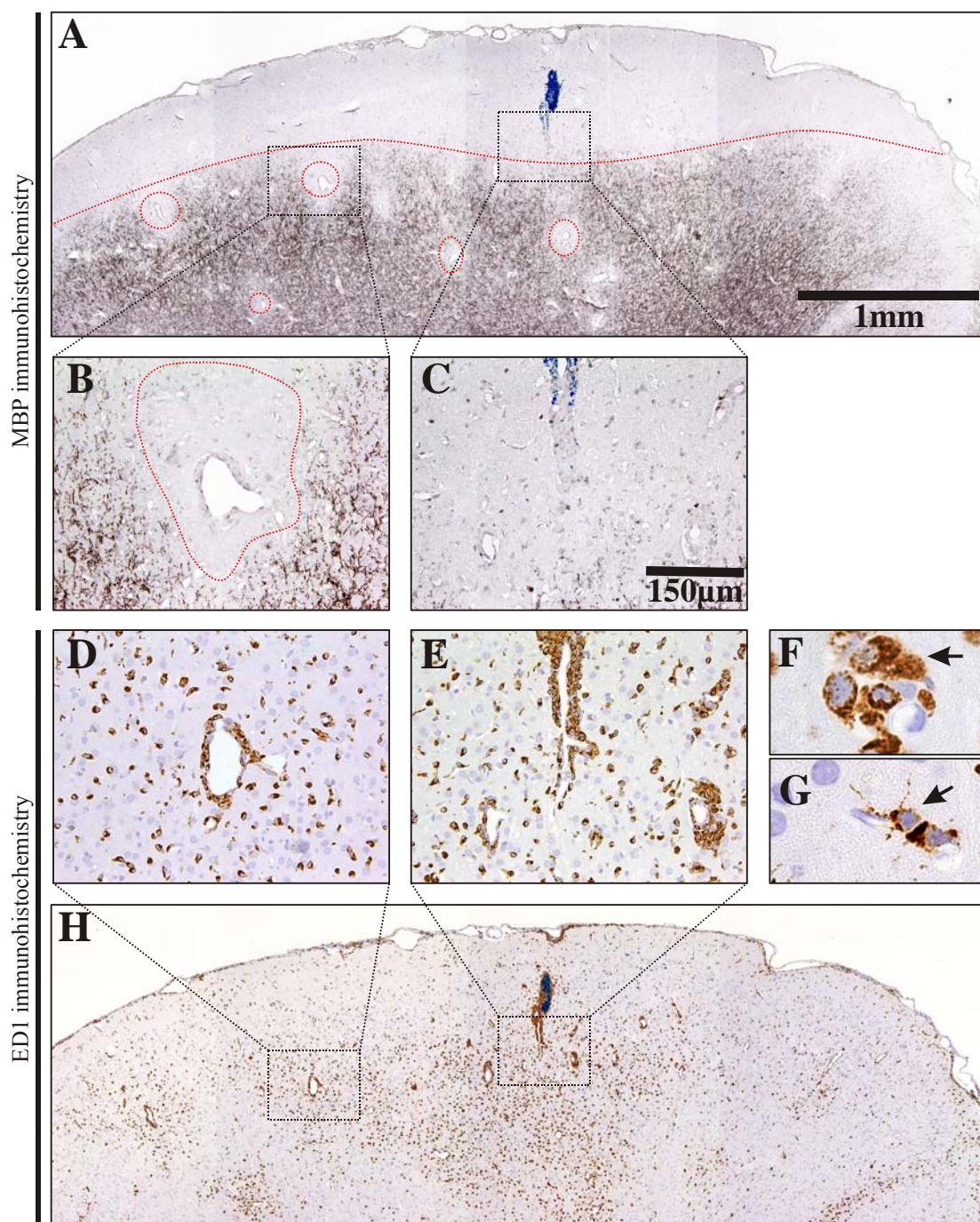


Figure 11: Inflammatory demyelination in the focal cortical EAE model

Representative photographs of the cerebral cortex of s.c. MOG primed Lewis rats at day 3 post lesion induction. Subpially demyelinated lesions (A and C, lesion border is indicated by dotted line) and perivascular lesions (A and B, lesions are surrounded by dotted circles) were identified by MBP immunohistochemistry (lesions are MBP-negative). Demyelination was accompanied by activation of microglia/macrophages visualized by ED1 immunohistochemistry (D-H). Perivascular (D) and parenchymal (E) spots of ED1-positive cells were distributed within and near demyelinated areas (H, see also A-C). Foamy macrophages indicating demyelination, were predominantly found at day 3 after lesion induction (F, indicated by arrow). Ramified ED1-positive cells (G, indicated by arrow) were observed in s.c. MOG primed demyelinated/remyelinated animals and s.c. IFA controls, respectively.

Scale bars: A and H = 1mm, B-E = 150 μ m

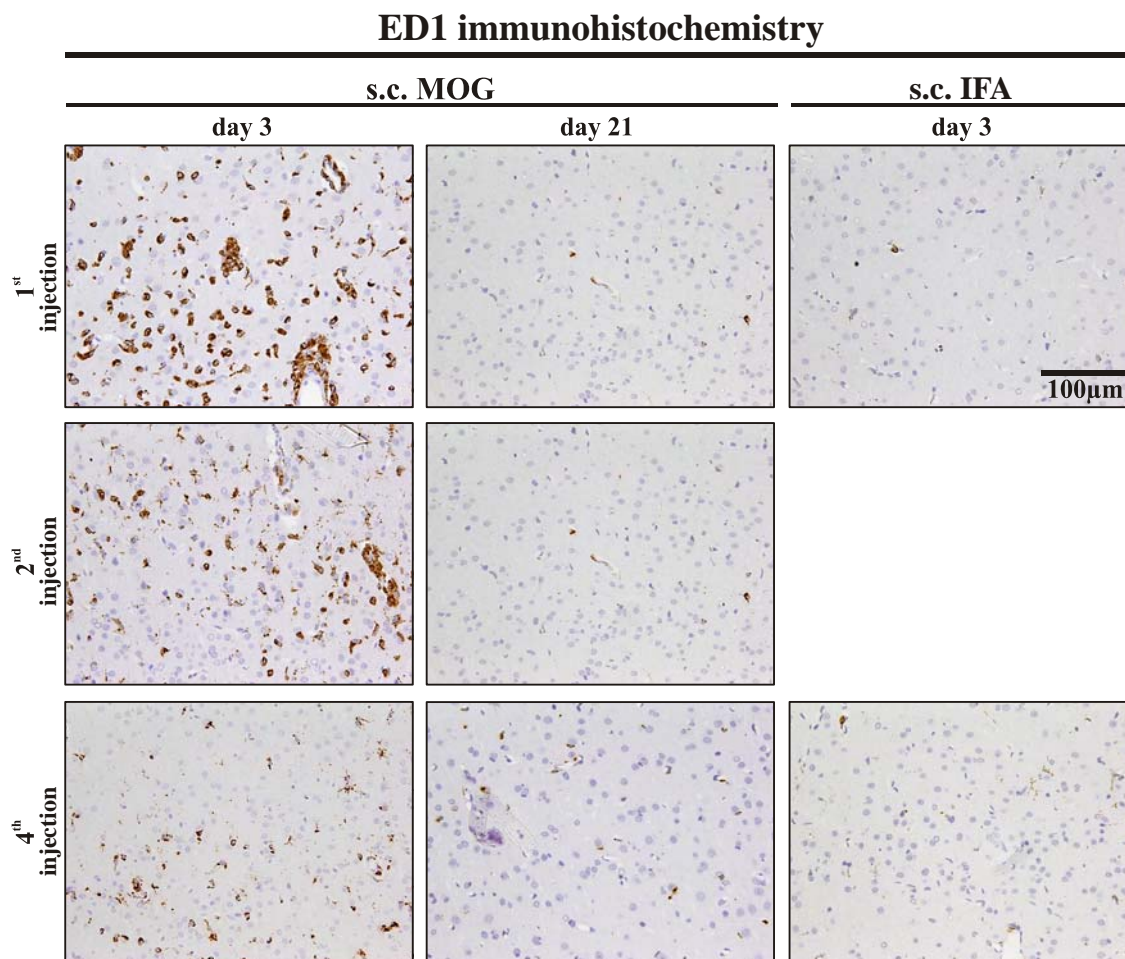


Figure 12: Transient activation of macrophages/microglia

Representative photographs of ED1 stained sections of the lesioned cerebral cortex. The time points of histological evaluation (days 3 and 21) and immunization protocols (s.c. MOG versus s.c. IFA) are arranged in columns. The numbers of lesion inductions (1st, 2nd and 4th) are arranged in rows. Strong activation of microglia/macrophages was observed in s.c. MOG immunized animals at day 3 post lesion induction (left column). Inflammation resolved within 21 days post lesion induction (middle column). In s.c. IFA immunized control animals, no substantial activation of microglia/macrophages was observed (right column).

Scale bar: 100µm

3.4.1 Density of activated macrophages within center of lesion

Density of activated macrophages/microglia was analysed on ED1 stained sections in cortical layer 3 within the center of lesion:

At day 3 post lesion induction, high densities of ED1-positive cells were detected after each demyelinating episode in s.c. MOG immunized animals (Figure 13 A, 1st inj.: 537.1

± 56.64 cells/mm², 2nd inj.: 485.3 ± 52.81 cells/mm², 4th inj.: 360.0 ± 66.32 cells/mm²). After four demyelinating episodes, values decreased significantly (one-way ANOVA $F_{7,59} = 41,874$, $p < 0,001$) compared to animals with a single (*post-hoc* LSD-test: $p = 0.01$) or two demyelinating episodes (*post-hoc* LSD-test: $p = 0.022$). Twenty-one days after each demyelinating episode, density of ED1-positive cells (1st inj.: 67.64 ± 13.05 cells/mm², 2nd inj.: 70.4 ± 17.23 cells/mm², 4th inj.: 57.33 ± 5.83 cells/mm²) decreased significantly compared to day 3 animals (*post-hoc* LSD-test: 1st, 2nd and 4th inj.: $p < 0.001$) and were similar to s.c. IFA immunized control groups (1st inj.: 56.00 ± 10.73 cells/mm², 4th inj.: 72.00 ± 4.62 cells/mm²). S.c. MOG immunized animals analysed at day 3 post lesion induction showed significantly increased values when compared to their corresponding s.c. IFA immunized control group (*post-hoc* LSD-test: 1st and 4th inj.: $p < 0.001$).

3.4.2 Density of activated macrophages/microglia throughout all cortical layers

As mentioned above, activated macrophages/microglia were also distributed beyond the border of demyelinated lesions. Therefore, quantification of activated macrophages/microglia was performed in a broad area including all cortical layers (Figure 3, B). Density of ED1-positive cells reached highest values at day 3 of singly injected s.c. MOG immunized animals (58.48 ± 10.75 cells/mm², Figure 13, B). Although a substantial accumulation of ED1-positive cells were observed after two and four demyelinating episodes (2nd inj.: 28.80 ± 4.84 cells/mm², 4th inj.: 25.11 ± 3.99 cells/mm²), their numbers were decreased (one-way ANOVA $F_{7,59} = 19,031$, $p < 0,001$) when compared to single injected animals (*post-hoc* LSD-test: 2nd and 4th inj.: $p < 0.001$). Twenty-one days after each demyelinating episode, density of ED1-positive cell counts (1st inj.: 4.77 ± 1.88 cells/mm², 2nd inj.: 6.04 ± 1.29 cells/mm², 4th inj.: 4.33 ± 0.67 cells/mm²) dropped sharply and significantly compared to day 3 animals (*post-hoc* LSD-test: 1st inj.: $p < 0.001$, 2nd inj.: $p = 0.007$, 4th inj.: $p = 0.001$), reaching similar values as s.c. IFA immunized control groups (1st inj.: 3.113 ± 0.19 cells/mm², 4th inj.: 4.88 ± 0.58 cells/mm²). S.c. MOG immunized animals analyzed at day 3 post lesion induction showed significantly increased values when compared to their corresponding s.c. IFA immunized control group (*post-hoc* LSD-test: 1st inj.: $p < 0.001$, 4th inj.: $p < 0.016$).

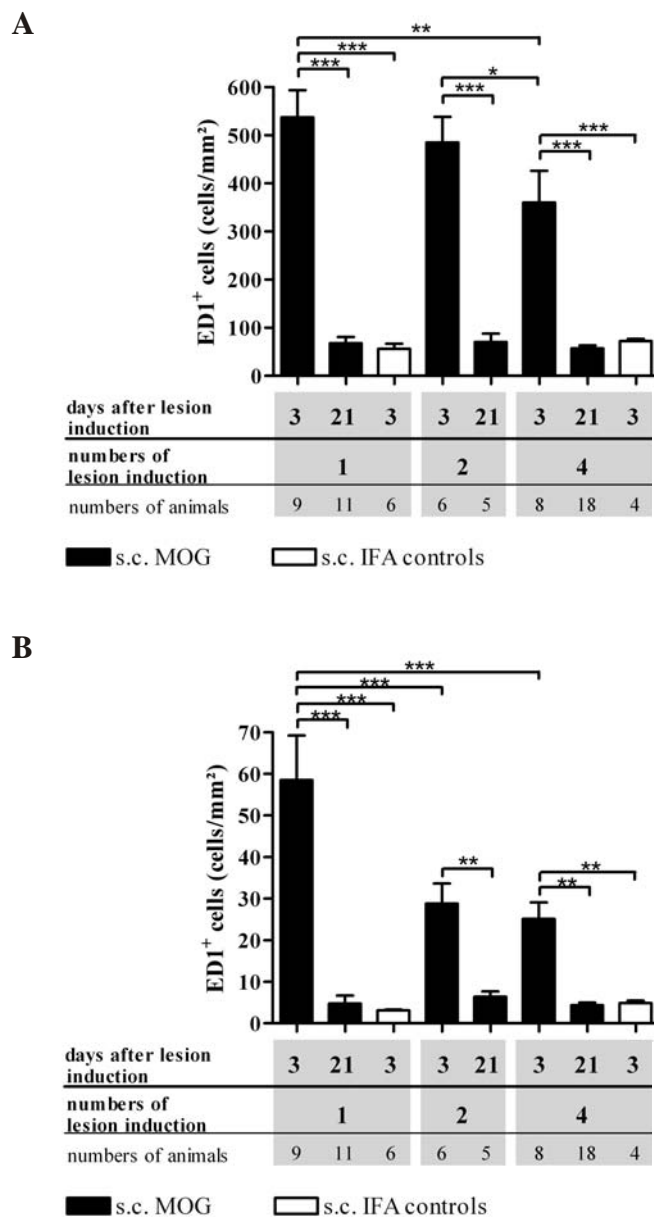


Figure 13: Density of activated macrophages/microglia

Density of activated macrophages was determined on ED1-stained sections. Strong and extensive activation of macrophages/microglia was observed in s.c. MOG immunized animals 3 days post lesion induction. (A) Within the center of lesion in cortical layer III, density of ED1-positive cells decreased significantly after four lesion inductions compared to previous ones. (B) Quantification of ED1-positive cells performed in a wider cortical lesional area (ranging from layer I-V) revealed significantly decreased cell counts already after two lesion inductions. Twenty-one days after each lesion induction, inflammation resolved as only few ED1-positive cells were detected (A and B). S.c. IFA immunized controls showed negligible numbers of ED1-positive cells (A and B). Data are expressed as mean + SEM. For statistical evaluation, one-way ANOVA followed by *post-hoc* LSD-test was performed (* = $p < 0.05$, ** = $p < 0.01$, *** = $p < 0.001$).

3.5 Axonal integrity

To analyse putative degenerative effects on axons, Bielschowsky silver stained sections were analysed in cortical layer III at the center of lesion. Bielschowsky silver staining showed no substantial alterations of axonal morphology, except in areas immediately adjacent to the injection site due to surgical minitrauma (Figure 14). Quantitative analysis revealed constant levels in axonal density in s.c. MOG immunized animals (Figure 15, 1st inj.: $92.16 \pm 9.48\%$, 2nd inj.: $112.0 \pm 14.27\%$, 4th inj.: $90.33 \pm 12.91\%$) and s.c. IFA immunized control animals (1st inj.: $96.68 \pm 7.95\%$, 4th inj.: $116.0 \pm 19.27\%$) at day 3 after lesion induction. No significant differences were detected. These results show that neither cortical demyelination nor surgical intervention causes substantial loss of axonal structures.

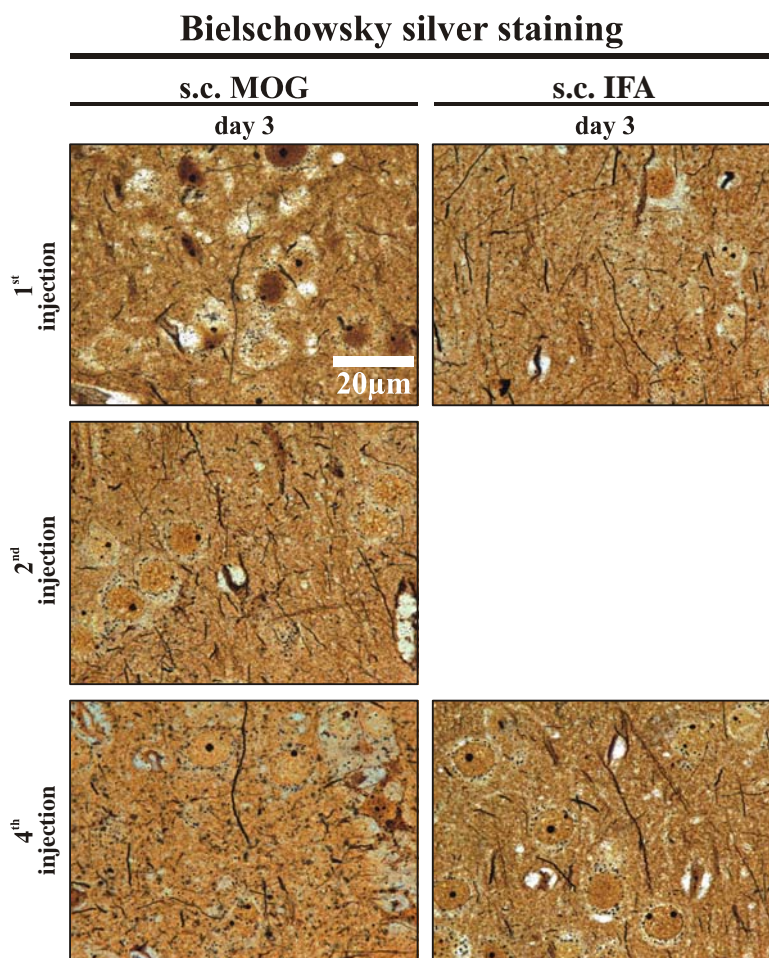


Figure 14: Axonal integrity

Representative photographs of Bielschowsky silver-stained sections of cortical layer 3 (center of lesion). The different immunization protocols (s.c. MOG and s.c. IFA) are arranged in columns. The different numbers of lesion inductions (1st, 2nd and 4th) are arranged in rows. Axonal distribution appeared normal in s.c. MOG and s.c. IFA immunized control animals.

Scale bars: 20µm

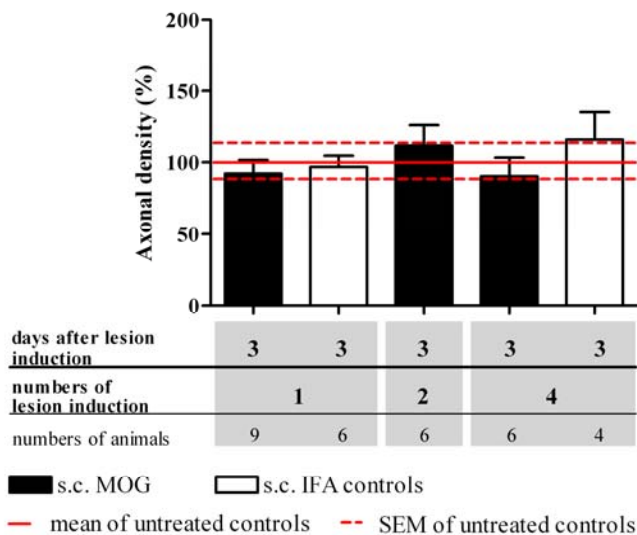


Figure 15: Axonal density

Axonal density was determined on Bielschowsky silver-stained sections. No alterations in axonal density were detected within center of lesion in cortical layer III. Data are expressed as mean + SEM.

3.6 Oligodendrocyte loss and recovery

To determine an effect of demyelination and subsequent remyelination on oligodendrocyte population, immunohistochemistry was performed using NogoA as a marker for mature oligodendrocytes.

Three days after intracerebral cytokine injection, substantial loss of oligodendrocytes was observed within demyelinated cortical lesions of s.c. MOG immunized animals. Oligodendroglial loss was most obvious within the center of intracortical lesions of several animals (Figure 16). Furthermore, a reduction of oligodendrocyte densities was also evident in demyelinated subpial areas after single and repeated lesioning (Figure 17). Following remyelination at 21 after lesion induction, the oligodendrocyte population was again recovered. No loss of oligodendrocytes was observed in s.c. IFA immunized animals.

NogoA/MBP double immunohistochemistry

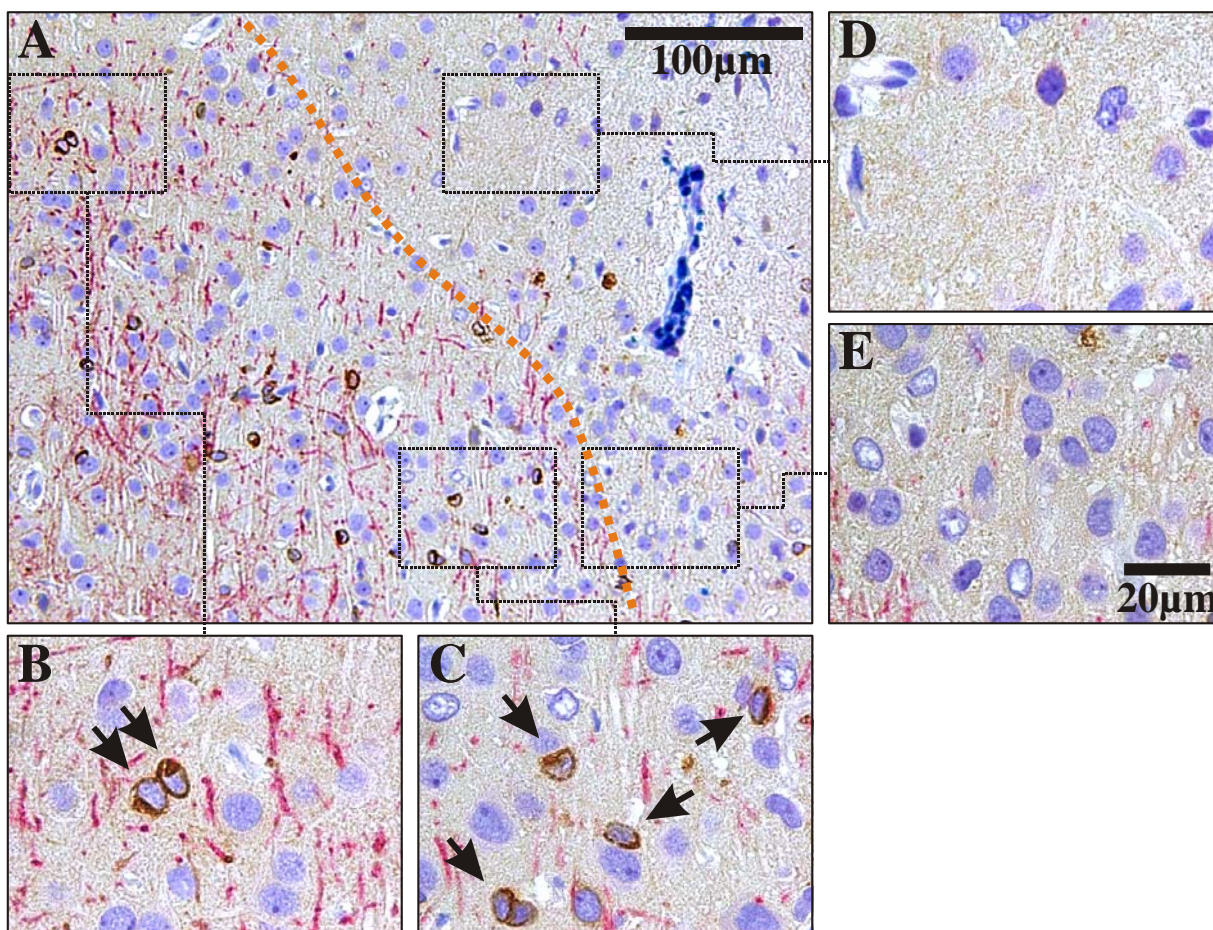


Figure 16: Loss of oligodendrocytes during focal cortical inflammatory demyelination

Representative photographs of a NogoA/MBP double-immunostained section of a cortical lesion. In normal appearing gray matter (MBP-positive myelin sheaths = red) numerous oligodendrocytes (indicated by arrows) were observed (A, B and C). Demyelination (lesion border is indicated by dotted line) was accompanied by loss of oligodendrocytes (A, D and E).

Scale bars: A= 100µm, B-E = 20µm

3.6.1 Oligodendrocyte density

Quantitative analysis of oligodendrocyte density in subpial lesions revealed significant differences between analysed groups (Figure 18, one-way ANOVA $F_{8,51} = 4,041$, $p = 0.001$). At day 3 after singly induced lesion in s.c. MOG immunized animals, *post-hoc* LSD-test revealed decreased oligodendrocyte density (4.91 ± 1.54 cells/mm²) compared to remyelinated animals (16.27 ± 3.59 cells/mm², $p = 0.004$), s.c. IFA controls (1st inj.: 20.77 ± 2.63 cells/mm², $p = 0.001$) and untreated controls (17.89 ± 2.64 cells/mm², $p = 0.002$). After a second demyelinating episode, s.c. MOG immunized animals showed a decrease

in oligodendrocyte density at day 3 (11.14 ± 3.04 cells/mm²) compared to remyelinated animals at day 21 (23.52 ± 3.88 cells/mm², *post-hoc* LSD-test: $p = 0.011$). After a fourth demyelinating episode, oligodendrocyte density was not significantly decreased in day 3 animals (6.75 ± 2.84 cells/mm²) compared to the corresponding remyelinated s.c. MOG immunized group at day 21 (11.57 ± 3.0 cells/mm²) and the corresponding s.c. IFA control group (4th inj.: 16.07 ± 0.8 cells/mm²), but was significantly decreased when compared to untreated controls (*post-hoc* LSD-test: $p = 0.014$).

NogoA/MBP double immunohistochemistry

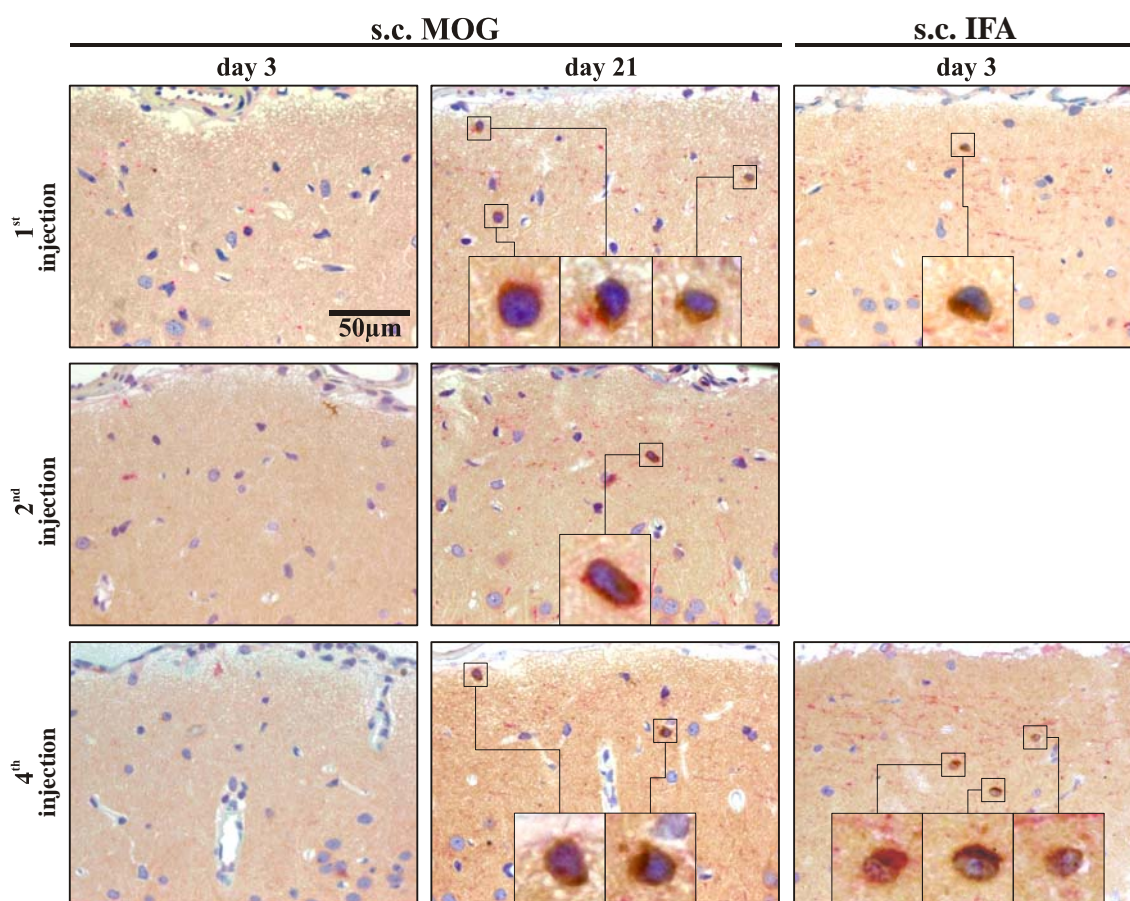


Figure 17: Spontaneous recovery of oligodendrocytes in subpial lesions

Representative photographs of NogoA/MBP double immunostained sections of lesioned subpial cortical area. The different time points (days 3 and 21) and immunization protocols (s.c. MOG and s.c. IFA) are arranged in columns. The different numbers of lesion inductions (1st, 2nd and 4th) are arranged in rows. Loss of oligodendrocytes (brown shaped cells) was observed within subpial lesions at day 3 post lesion induction (left column). Twenty-one days after lesion induction, NogoA-positive cell population recovered (middle column). NogoA-positive cell population was not affected in s.c. IFA primed controls (right column).

Scale bars: 50µm, length of enlarged image = 14µm

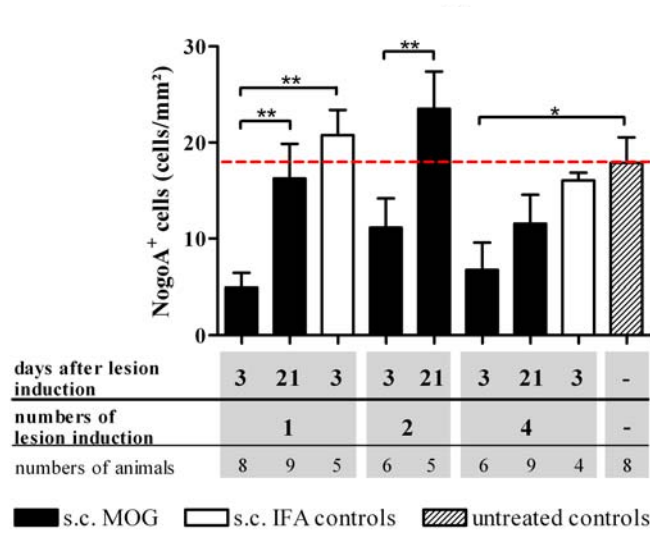


Figure 18: Density of oligodendrocytes

Oligodendrocyte density was determined within lesioned subpial cerebral cortex of NogoA/MBP double stained sections. At 3 days post lesion induction, NogoA-positive cell density decreased significantly followed by recovery (at day 21) after single and two demyelinating events. At day 3 post fourth lesion induction, loss of oligodendrocytes was only significant when compared to untreated controls. Data are expressed as mean + SEM. The mean of the untreated controls is indicated by dotted line. For statistical evaluation, one-way ANOVA followed by *post-hoc* LSD-test was performed (* = $p < 0.05$, ** = $p < 0.01$).

3.6.2 Proliferation of NogoA-positive oligodendrocytes

To assess the effect of repeated lesion induction on the proliferation of oligodendrocytes, NogoA-positive cells were labelled with the proliferation marker BrdU. Oligodendrocytes which underwent cell division during BrdU administration were detected by NogoA/BrdU double immunohistochemistry (Figure 19).

At day 21 after single lesioning, few cells double-positive for NogoA and BrdU were detected within remyelinated subpial areas of s.c. MOG immunized animals (Figure 20, 3.87 ± 1.14 cells/mm²). NogoA/BrdU-double positive cell density did not differ significantly in repetitively injected animals (2nd inj.: 0.57 ± 0.51 cells/mm², 4th inj.: 2.34 ± 0.73 cells/mm²).

The proliferation of oligodendrocytes was analysed in more detail in a further experiment. Three days post lesion induction (Figure 21), few NogoA/BrdU double-positive cells were detected in s.c. MOG immunized (4.66 ± 2.15 cells/mm²) and IFA

immunized controls animals (2.87 ± 1.98 cells/mm²). At 21 days post lesion induction (Figure 22), comparably low densities of NogoA/BrdU double-positive cells were detected in s.c. MOG immunized animals (2.30 ± 2.30 cells/mm²) and s.c. IFA immunized control animals (cytokine injection: 1.16 ± 0.804 ; PBS injection: 0.78 ± 0.49 cells/mm²; no injection: 0.35 ± 0.35 cells/mm²). No significant differences were detected between the groups at day three or day 21 post lesion induction.

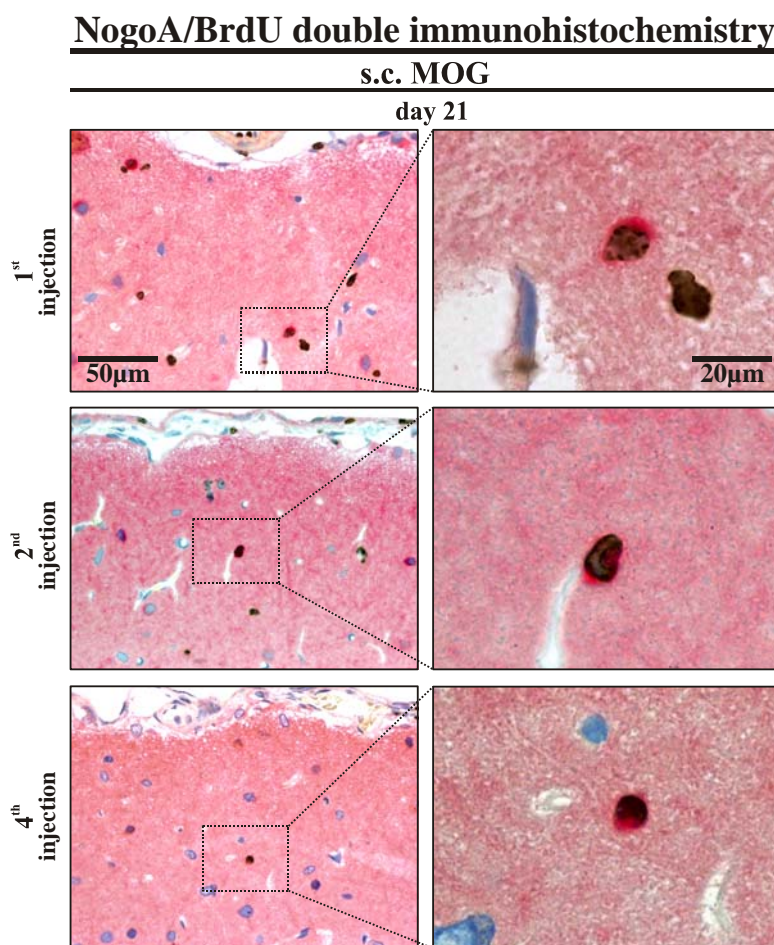


Figure 19: Oligodendrocyte proliferation during remyelination

Representative photographs of NogoA/BrdU double immunostained sections of subpial lesions. The different numbers of lesion inductions (1st, 2nd and 4th) are arranged in rows. Few mature NogoA-labelled oligodendrocytes cells (red) incorporated the proliferation marker BrdU (brown), which was administrated at days 2 to 7 post lesion induction.

Scale bars: left column = 50µm, right column = 20µm

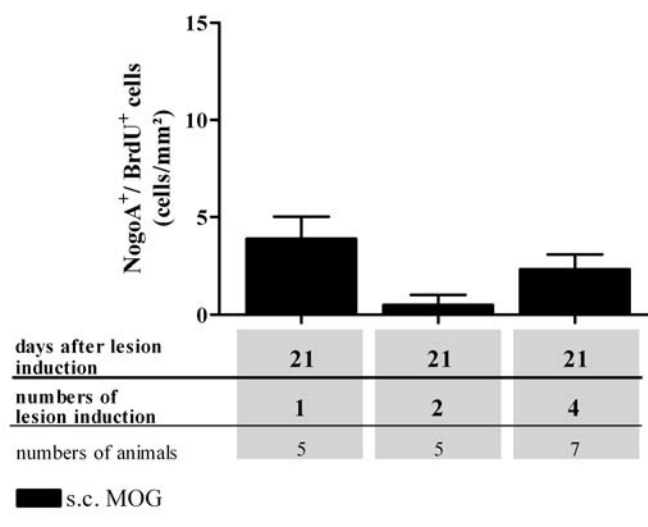


Figure 20: Proliferation of NogoA-positive cells after repeated demyelinating events

Density of proliferated oligodendrocytes within lesioned subpial cerebral cortex was determined on NogoA/BrdU double positive stained sections. Twenty-one days post lesion induction, few NogoA/BrdU double positive cells were detected. No statistical differences were observed between singly and repetitively lesioned animals. Data are expressed as mean + SEM.

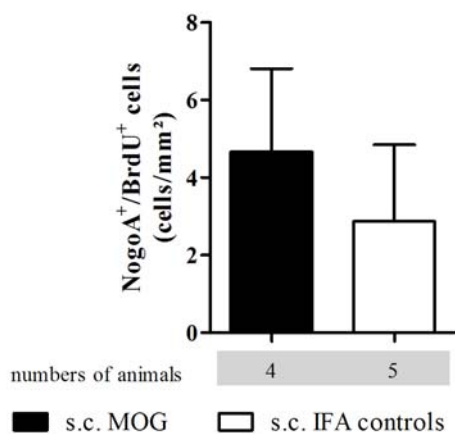


Figure 21: Early effects of lesion induction on proliferation of NogoA-positive cells

Proliferation of mature oligodendrocytes was determined within lesioned subpial cerebral cortex on NogoA/BrdU double immunostained sections. Three days post lesion induction, proliferating NogoA-positive cells were observed in both s.c. MOG and s.c. IFA immunized animals. Values did not differ significantly between groups. Data are expressed as mean + SEM.

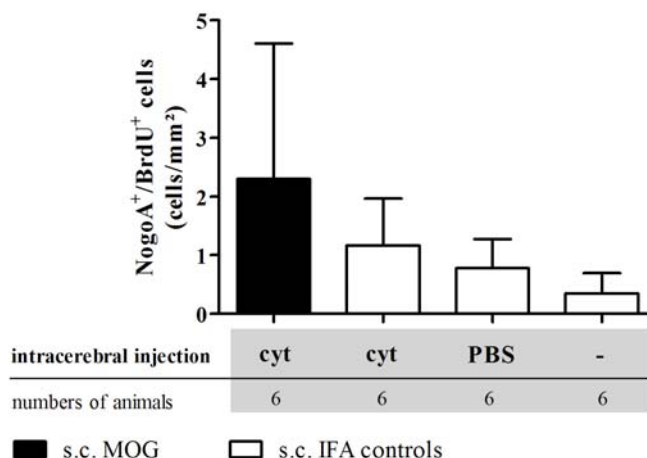


Figure 22: Effect of lesion induction on proliferation of mature oligodendrocytes after remyelination

Proliferation of mature oligodendrocytes was determined within lesioned subpial cerebral cortex on NogoA/BrdU double immunohistochemical sections. Twenty-one days post lesion induction, few proliferated oligodendrocytes were detected. S.c. MOG immunized animals did not differ significantly from PBS-injected and non-injected controls. Abbreviations: cyt = cytokines. Data are expressed as mean + SEM.

3.7 Oligodendroglial progenitors

To investigate the effect of inflammatory demyelination on oligodendroglial progenitor population, we performed immunohistochemical staining for olig2 (Figure 23).

At the peak of demyelination at day three after lesion induction, density of olig2-positive cells did not alter in s.c. MOG immunized animals (45.75 ± 2.9 cells/mm²). However, at day 21 after lesion induction, olig2-positive cell density (60.05 ± 6.21 cells/mm²) increased significantly (one-way ANOVA $F_{8,48} = 3,045$ $p=0.007$) compared to day 3 animals (*post-hoc* LSD-test: $p = 0.005$), s.c. IFA controls (1st inj.: 40.8 ± 0.97 cells/mm², *post-hoc* LSD-test: $p = 0.001$) and untreated controls (45.69 ± 2.53 cells/mm², *post-hoc* LSD-test: $p = 0.005$). After two demyelinating episodes, cell density was increased in both day 3 group (54.14 ± 3.08 cells/mm², *post-hoc* LSD-test: $p = 0.041$) and day 21 group (57.69 ± 4.27 cells/mm², *post-hoc* LSD-test: $p = 0.014$) compared to repetitively injected s.c. IFA immunized controls (46.1 ± 5.54 cells/mm²). Three days after four repetitively induced lesions, olig2-positive cell density (59.9 ± 5.2 cells/mm²) was increased compared to repetitively injected s.c. IFA immunized controls (46.1 ± 5.34 cells/mm², *post-hoc* LSD-test: $p = 0.02$) and untreated controls (45.69 ± 2.53 cells/mm², *post-hoc* LSD-test: $p = 0.013$). Twenty-one days after the last

intracerebral cytokine injection, cell density (49.44 ± 6.24 cells/mm²) did not differ compared to control groups.

Olig2/PLP double immunofluorescence

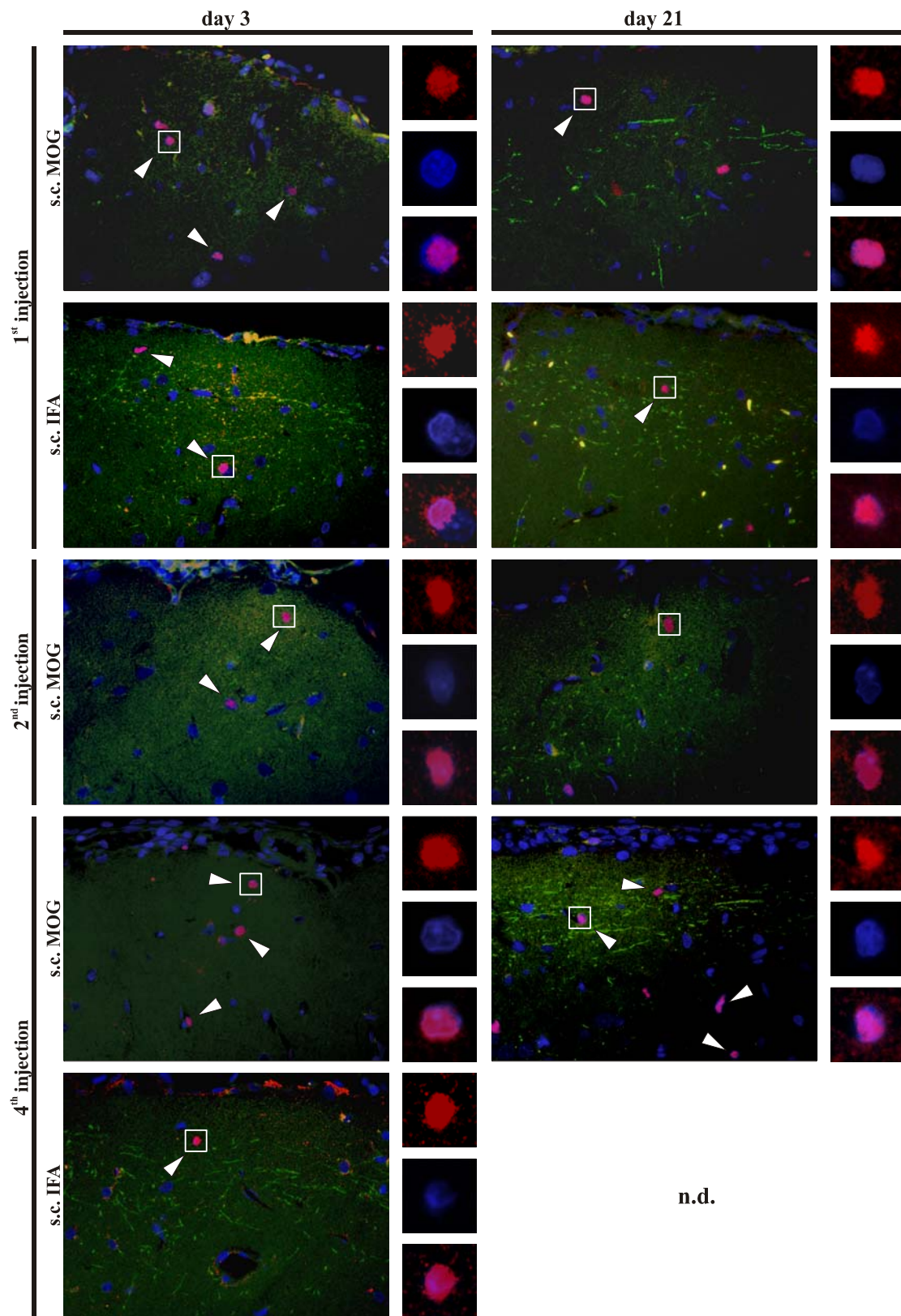


Figure 23: Unaltered oligodendroglial progenitor population

Representative photographs of olig2/PLP double fluorescent sections of the lesioned subpial cerebral cortex. The different time points (days 3 and 21) are arranged in columns. Lesion inductions (1st, 2nd and 4th) and immunization protocols (s.c. MOG and s.c. IFA) are arranged in rows. Merged overview photographs consist of olig2 (red), PLP (green) and DAPI (blue). Magnifications of single cells show olig2 (red, upper inset), DAPI (blue, middle inset) and merged signals (lower inset). Numbers of olig2-positive cell population remained unaltered even after repetitive lesion inductions. Abbreviation: .n.d. = not determined.

Scale bar = 50µm, length of enlarged image = 16µm

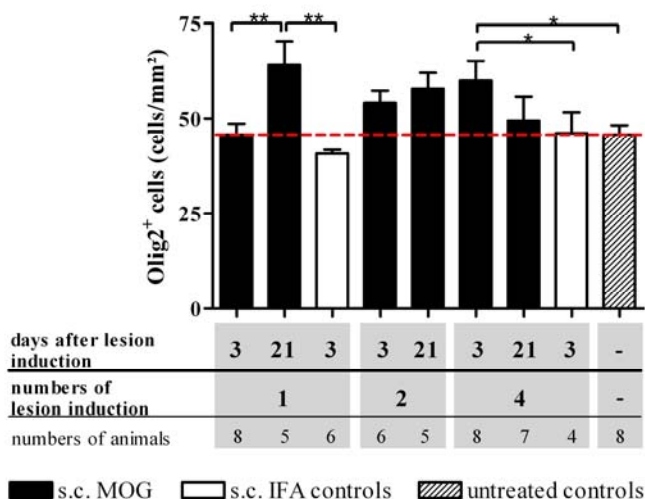


Figure 24: Density of oligodendroglial progenitors

Oligodendroglial progenitor density was determined within lesioned subpial cerebral cortex of olig2-stained sections. Olig2-positive cell density did not decrease at any examined time point, even after repetitive lesioning. Twenty-one days after single lesioning and 3 days after four demyelinating events, olig2-positive cell density increased significantly. Data are expressed as mean + SEM. Mean of untreated controls is indicated by dotted line. For statistical evaluation, one-way ANOVA followed by *post-hoc* LSD-test was performed (* = $p < 0.05$, ** = $p < 0.01$).

3.7.1 Proliferation of oligodendroglial progenitors

To assess the effect of repeated lesion induction on the proliferation of oligodendrocytes, NogoA-positive cells were labelled with the proliferation marker BrdU. Oligodendrocytes which underwent cell division during BrdU administration were detected by NogoA/BrdU double immunohistochemistry (Figure 19). Cells double positive for olig2/BrdU were quantified in subpial lesions of s.c. MOG immunized animals at day 21 after lesion induction.

Olig2/BrdU double-positive cells were detected within the subpial cortical lesions (Figure 25). Constant values were measured after one (12.32 ± 2.65 cells/mm²), two (8.78 ± 2.08 cells/mm²) and four (8.57 ± 1.84 cells/mm²) demyelinating events (Figure 26).

In a further experiment, the proliferation of oligodendroglial cells was analysed in more detail. Three days post lesion induction (Figure 27), relatively high numbers of olig2/BrdU double-positive cells were detected in s.c. MOG immunized (23.34 ± 6.69 cells/mm²) and IFA immunized control animals (12.29 ± 2.88). No significant differences were detected between both groups. Twenty-one days post lesion induction (Figure 28), high numbers of olig2/BrdU double-positive cells were detected in s.c. MOG immunized animals (15.83 ± 2.06), which were significantly increased (one-way ANOVA $F_{3,2} = 6,594$, $p = 0.003$) compared to all s.c. IFA immunized control groups (cytokine injection: 9.94 ± 1.23 cells/mm², $p = 0.048$; PBS injection: 7.70 ± 2.63 cells/mm², $p = 0.007$; no injection: 4.34 ± 1.12 cells/mm², $p < 0.001$). Within the control groups, no statistical differences were observed, but there was a trend for increase between non-injected animals and those which received an intracebral cytokine injection ($p = 0.06$). These experiments showed an increased proliferation of OPCs upon demyelinating insult within the cerebral cortex.

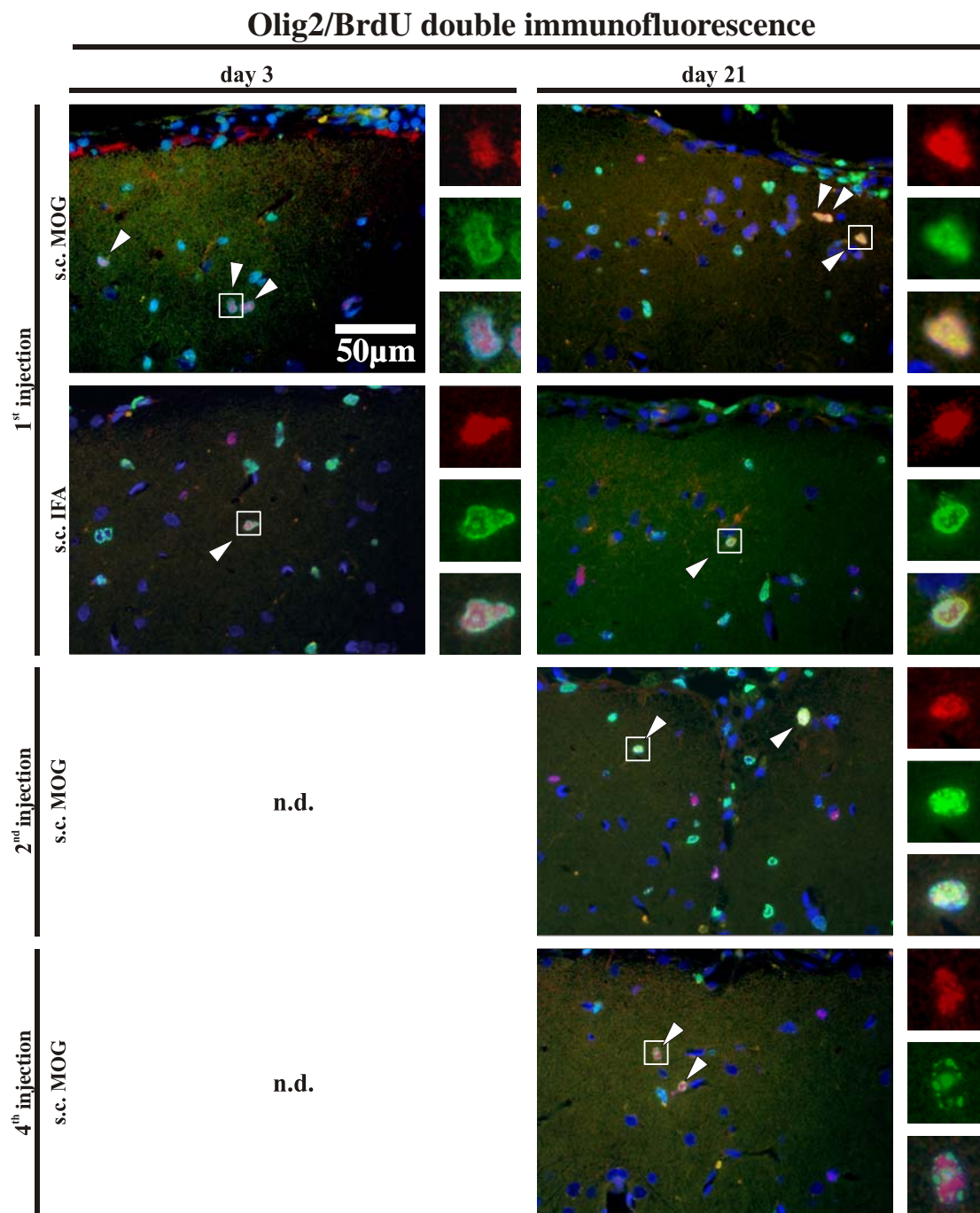


Figure 25: Proliferation of olig2-positive OPCs within subpial lesions

Representative photographs of olig2/BrdU double fluorescent sections of the lesioned subpial cerebral cortex. The different time points (days 3 and 21) are arranged in columns. Lesion inductions (1st, 2nd and 4th) and immunization protocols (s.c. MOG and s.c. IFA) are arranged in rows. Merged overview photographs consist of olig2 (red), BrdU (green) and DAPI (blue). Magnifications of

single cells show olig2 (red, upper inset), BrdU (green, middle inset) and merged signals (incl. DAPI, lower inset). Substantial proliferation of olig2-positive cells was observed at days 3 and 21 after lesion induction. Abbreviation: .n.d. = not determined.

Scale bar = 50 μ m, length of enlarged image = 16 μ m

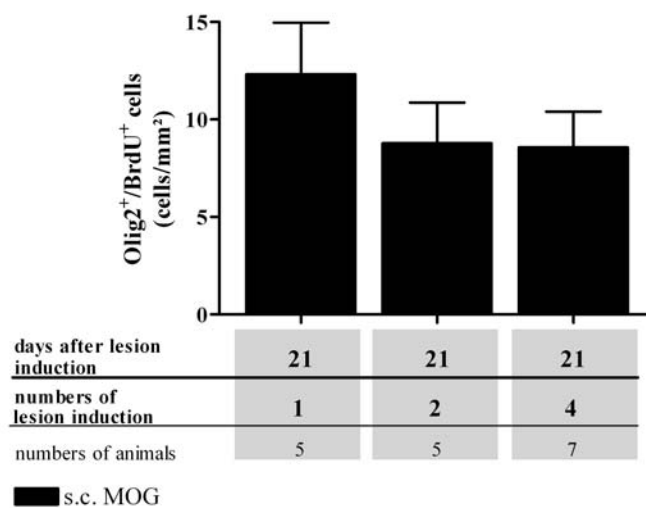


Figure 26: OPC proliferation after repeated demyelinating events

Proliferated oligodendroglial progenitor population was determined within lesioned subpial cerebral cortex by olig2/BrdU double immunofluorescence. Twenty-one days post lesion induction, moderate density of Olig2/BrdU double-positive cells was detected. Values did not differ significantly after repetitive lesion induction. Data are expressed as mean + SEM.

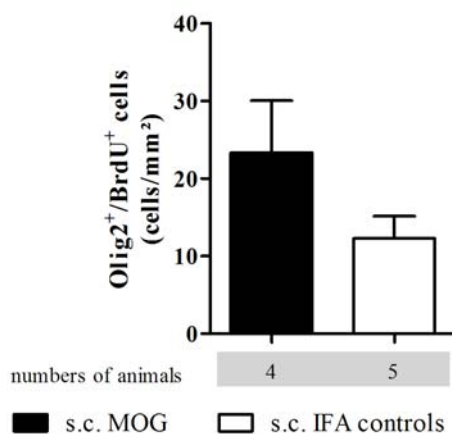


Figure 27: Early effects of lesion induction on OPC proliferation

Proliferation of the oligodendroglial progenitor population was determined within lesioned subpial cerebral cortex by olig2/BrdU double immunofluorescence. At 3 days post lesion induction, substantial proliferation of olig2-positive cells was observed in both s.c. MOG and s.c. IFA immunized animals. Values did not differ significantly between groups. Data are expressed as mean + SEM.

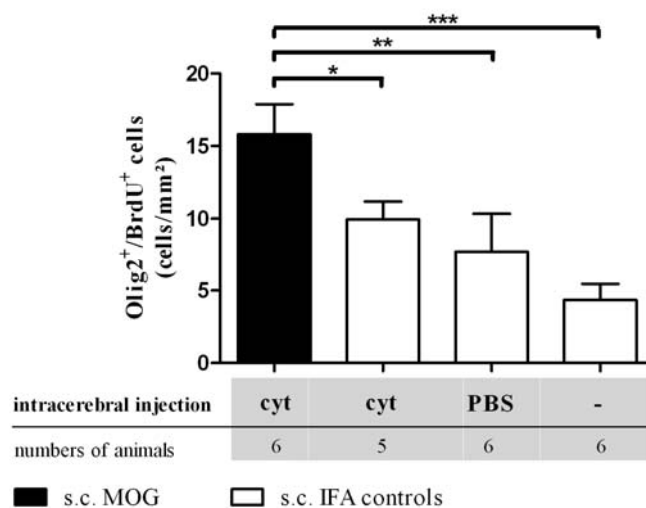


Figure 28: Effects of lesion induction on OPC proliferation after remyelination

Proliferation of the oligodendroglial progenitor population was determined within lesioned subpial cerebral cortex by olig2/BrdU double immunofluorescence. Twenty-one days post lesion induction, Olig2/brdU double-positive cell density was significantly increased compared to the s.c. IFA control groups. Abbreviations: cyt = cytokines. Data are expressed as mean + SEM. For statistical evaluation, one-way ANOVA followed by *post-hoc* LSD-test was performed (* = $p < 0.05$, ** = $p < 0.01$, *** = $p < 0.001$)

4 DISCUSSION

In the presented study I investigated the impact of repeated cortical demyelination on the intrinsic remyelination capacity.

Histological analysis revealed widespread subpial and intracortical demyelinated lesions within the injected cortical hemisphere. Demyelination was accompanied by loss of oligodendrocytes and activation of macrophages/microglia but without apparent axonal loss. Although the fraction of myelinated axons did not fully recover, an extensive remyelination, restored oligodendrocyte population and resolution of inflammation was observed even after repeated lesioning. This was accompanied by a proliferative response of olig2 and NogoA-positive cell populations that was already observed during demyelination.

4.1 Targeted cortical demyelination shares similarities with cortical MS lesions

The study of cortical pathology in MS and its clinical manifestations, as well as underlying mechanisms has been hampered by the lack of suitable animal models. The cerebral cortex shows frequent involvement in MS patients. In contrast, in the classical rodent EAE model, lesions are mostly confined to the spinal cord but only rarely affected the cerebral cortex. Alternatively, injection of gliotoxins e.g. lysolecithin or ethidium bromide were used to induce lesions within the brain of rodents (Yajima and Suzuki, 1979; Hall, 1972). However, these models do not reflect the immunopathological nature of MS lesions in the cerebral cortex. Interestingly, the evolvement of cortical EAE lesions was observed in the marmoset EAE model. These lesions occurred spontaneously during the disease course and highly resemble cortical MS lesion pathology (von Budingen *et al.*, 2004; Pomeroy *et al.*, 2005; Merkler *et al.*, 2006; Merkler *et al.*, 2006b). However, experiments with outbred primates show high requirements for infrastructure and animal husbandry, that can only be accomplished in highly specialized centers. A further limitation in using outbred primates is the unpredictable disease course, making it difficult to reproduce cortical lesions in a standardized manner.

To gain insight into the important aspects of cortical MS, a novel animal model was recently developed in our laboratory that allows for the targeted induction of cortical demyelinating lesions (Merkler *et al.*, 2006). Sensitization of rats against MOG resulted in a subclinical immune response. In a second step, stereotactic injection of pro-inflammatory cytokines into a defined area of the animal's cortex led to cortical demyelination that shows considerable similarities to human cortical MS pathology (Merkler *et al.*, 2006). Importantly, neither subclinical MOG sensitization nor cytokine injection alone can cause demyelination or important cellular inflammation in the CNS.

As described in the previous study, we could detect predominantly subpial but also intracortical lesions in the targeted EAE model that were reminiscent of cortical lesion type II and III described in MS patients (Peterson *et al.* 2001). This lesion topology remained consistent over repeated cycles of de- and re-myelination. Furthermore, cellular composition of inflammatory infiltrates matched the observation of cortical MS lesions. It is possible that the observed topology may be caused by the distribution of injected cytokines in our model. After having been targeted to the deeper cortical layers, the injected cytokines are likely to partially drain back to the subpial surface. Thereby, the BBB may predominantly be affected in these areas resulting in transient BBB breakdown and/or upregulation of adhesion molecules on endothelial cells (Yusuf-Makagiansar *et al.*, 2002). In a setting of previous priming against MOG, it is conceivable that demyelinating anti-MOG autoantibodies cross the altered BBB as a consequence of cytokine injection and subsequently trigger a localized inflammatory response within the affected areas. An alternative hypothesis for the observed lesion distribution would be that macrophages accumulate preferentially at the meningeal area of cytokine injection and thereby secrete demyelinating inflammatory cytokines into the subpial cortical area (Serafini *et al.*, 2007). However, this latter scenario is rather unlikely in our model, since IFA immunized animals did not reveal signs of demyelination despite the fact that these animals showed a certain accumulation of macrophages in the meningeal areas following cytokine injection (data not shown). Furthermore, recent findings in MS showed that meningeal inflammation seems not to be associated with cortical demyelination (Geurts *et al.*, 2009).

4.2 Effect of repeated demyelinating lesions on remyelination

Cortical remyelination is a frequent and important repair mechanism in MS (Patani *et al.*, 2007; Patrikios *et al.*, 2006). The cerebral cortex showed a more extensive remyelinating capacity as compared to white matter MS lesions (Albert *et al.*, 2007). Nevertheless, the number of chronic demyelinated plaques in the cerebral cortex increases with ongoing disease progression (Peterson *et al.*, 2001; Bo *et al.*, 2003; Patani *et al.*, 2007; Goldschmidt *et al.*, 2009; Gilmore *et al.*, 2009; Bo, 2009). Therefore, the objective of this study was to investigate the effect of repetitive inflammatory demyelination on the endogenous cortical remyelination capacity.

Although cortical lesions were repeatedly induced in our study, animals revealed extensive and in some cases nearly complete remyelination, even after four demyelinating episodes. Our results are in line with a previous study which proved successful myelin restoration after repeated cycles of ethidium bromide-induced demyelination (Penderis *et al.*, 2003). Together, these results suggest at first glance that remyelination failure - as can be observed in chronic MS cases - might not solely be the result of repetitive demyelinating episodes and further suggest that there are still other unknown mediators that may contribute to this phenomenon. Clearly, our study can nevertheless not exclude that four cycles of de- and re-myelination may just not be enough to exhaust the intrinsic remyelinating capacity of the cerebral cortex, and that remyelination failure in MS may reflect the final consequence of a multitude of such events that was not sufficiently recreated by our repeated lesioning approach. One may therefore speculate that the targeted cortical EAE lesions reflect the early relapsing-remitting disease course of MS, in which chronic cortical demyelination is less pronounced (Stadelmann *et al.*, 2008). Furthermore, possible differences in the intrinsic properties of remyelinating oligodendrocytes in humans and rodents may account for these observations.

As a further parameter of remyelination, we determined the fraction of myelinated fibres in the remyelinated cortex. This analysis revealed a reduced fraction of remyelinated fibres three weeks after lesioning. To exclude that this change might be explained by still incomplete remyelination at this time point, we performed in a subset of animals similar

analysis five weeks after demyelination (data not shown). However, the fraction of remyelinating fibres remained reduced even at this later time point as compared to age-matched controls. Thus, this data indicates that the process of remyelination was almost already complete three weeks after lesion induction. These results indicate that although remyelination is extensive, the restoration of myelin content in the cortex is incomplete, therefore as expected not equating to normal developmental myelination (Lazzarini, 2004). The limitations of remyelination are obvious in the ultrastructure of myelin, showing reduced myelin sheath thickness and internode length (Perier and Grégoire, 1965; Blakemore, 1974; Merkler *et al.*, 2006).

4.3 Inflammation in repeated targeted cortical EAE lesions

In accordance to a previous report demyelination was accompanied by inflammation which resolved within three weeks after each lesion induction (Merkler *et al.*, 2006). The initial inflammatory response measured by the density of activated macrophages/microglia was markedly stronger compared to the subsequent episodes. Macrophage/microglia activation might be related to myelin content, as the fraction of myelinated axons was also higher before demyelination when compared to remyelination time points. However, this seemed not related to lesion size as the extent of demyelination did not alter after repeated lesions. The relationship between myelin content and inflammation becomes clear when comparing myelin rich white matter lesions, which present with strong inflammation, to grey matter lesions, which present with relatively little myelin and reduced inflammation (Kerschensteiner *et al.*, 2004; Merkler *et al.*, 2006; Peterson *et al.*, 2001; Bo *et al.*, 2003). However, the different local environment of white and grey matter could influence the inflammatory response within a given lesion. Anti-MOG autoantibody titres were consistently high over time and therefore are not the cause for the observed alterations in inflammatory response. Speculatively, excessive blood born monocytes were recruited into the area of inflammation during the initial demyelinating lesion. Why the repeated inflammatory responses were markedly reduced is not clear. One discussed theory is that neurons,

which are abundant in the cerebral cortex could have damped the activation of microglia as proposed by Biber and colleagues (Biber *et al.*, 2007).

The inflammatory process causes tissue damage in EAE and MS. For instance, pro-inflammatory cytokines such as TNF- α , IFN- γ , interleukin-1 β (IL-1 β) and IL-2 have been shown to promote oligodendrocyte death in vitro (Selmaj and Raine, 1988; Vartanian *et al.*, 1995; Curatolo *et al.*, 1997; Hisahara *et al.*, 1997; Jurewicz *et al.*, 2005). Apoptosis-inducing factor-positive oligodendrocyte nuclei were detected around MS plaques, suggesting this pathway may contribute to oligodendrocyte loss and disease progression (Jurewicz *et al.*, 2005). Furthermore, macrophages and microglia are activated by pro-inflammatory cytokines which promote apoptosis of oligodendrocytes through oxidative stress or via activation of transcription factor p53 (Merill and Scolding, 1999; Eizenberg *et al.*, 1995; Ladiwala *et al.*, 1999; Wosik *et al.*, 2003). However, the cytokine concentrations used in our model are not cytotoxic, as no effects were observed in IFA-immunized control animals.

4.4 Preserved axonal integrity after repetitive demyelination

Repetitive lesion induction did not lead to substantial axonal loss. This goes in line with a previous study by Merkler and colleagues (Merkler *et al.*, 2006) which reported preserved axonal integrity and minimal neuronal death in the targeted cortical EAE model. Furthermore, they showed transient accumulation of amyloid precursor protein (APP)-positive spheroids, correlating with inflammation. Acute axonal damage and minimal neuronal loss is also to be assumed in our repetitive lesioning approach, but apparently without any cumulating harming effects, as no axonal loss was detected. The fast resolution of inflammation in targeted cortical EAE lesions possibly prevented further axonal damage. This is supported by several studies suggesting a relationship between the extent of axonal damage and the severity of the inflammatory process in EAE and MS (Mancardi *et al.*, 2001, Shrivel and Dittel, 2006; Rasmussen *et al.*, 2007; Lassmann *et al.*, 2001). However, transected neurites and apoptotic neurons were observed in cortical MS lesions (Peterson *et al.*, 2001). Extensive remyelination observed in the presented study

might have supported axonal preservation as reported by previous studies (Kornek *et al.*, 2000; Irvine and Blakemore, 2008; Trapp and Nave, 2008).

4.5 Oligodendrocyte recruitment in the targeted cortical EAE model

Histological assessment revealed normal olig2-positive cells density within the subpial cerebral cortex which did not decrease even after repeated cycles of demyelination. The cell density even increased at particular time points after lesion induction. This can be explained by the fast proliferative response of oligodendroglial cells observed within demyelinated areas. From this proliferative population the majority were olig2-positive OPCs and only few NogoA-positive cells. This leads to the assumption that the restored oligodendrocyte population in the remyelinated cortex, did not derive from proliferated OPCs. More likely, oligodendrocytes were preferentially recruited from the local pool of abundant OPCs which already persisted before the demyelinating lesion was induced (Dawson *et al.*, 2003, Levine *et al.*, 2001). One can further speculate that the proliferated olig2-positive OPCs might restore the pool of quiescent adult oligodendroglial population to replace those which have differentiated into remyelinating oligodendrocytes. This seems plausible as, differentiation of OPCs offers a repair mechanism which is fast when compared to the longer process required during proliferation and subsequent maturation. Moreover, it allows for oligodendrocyte restoration and extensive remyelination within 21 days. However, both proliferation and differentiation are important mechanisms of oligodendrocyte recruitment and which of both mechanisms finally fail in MS is a controversial issue. Numerous studies reported OPC recruitment in MS lesions (Prineas *et al.*, 1989; Schonrock *et al.*, 1998; Scolding *et al.*, 1998; Chang *et al.*, 2000; Maeda *et al.*, 2001). This is supported by experimental demyelination studies underlining the potential of OPC recruitment (Carrol and Jennings, 1994; Penderis *et al.*, 2003; Fancy *et al.*, 2004; Levine and Reynolds, 1999; Sim *et al.*, 2002). Despite OPC numbers decreasing with disease progression, they remain within the lesion, however are unresponsive, which therefore indicates a differentiation failure of oligodendroglial progenitor cells as the major determinant of remyelination failure in chronic MS (Kuhlmann *et al.*, 2008). The importance of efficient differentiation is obvious in GFP-

PDGF- α transgenic animals, where elevated OPC numbers did not improve remyelination after chemical demyelination (Woodruff *et al.*, 2004). Nevertheless, the likelihood of OPC recruitment failure can not be excluded since OPC depletion may occur after a single demyelinating event (Keirstead *et al.*, 1998). This effect is more obvious after protracted and sustained exposure to a demyelinating stimulus (Linnington *et al.*, 1992; Ludwin, 1980). However, in our experimental setting we could not detect a reduction of OPC in the demyelinated cortex. This can be explained by the fact that MOG EAE is not directed against OPCs since these cells do not express the MOG antigen.

The density of proliferated OPCs appeared higher at day three after lesion induction than after 21 days. A reason for this may be the excessive recruitment of OPCs undergoing apoptosis as reported in a previous study (Calver *et al.*, 1998). In addition, this observed process can be partly explained by the normal turn over of OPCs, as Olig2 and NG2-positive cells are the major cycle related cell population in the CNS (Dawson *et al.*, 2000; Levine *et al.*, 2001; Geha *et al.*, 2009; Dimou *et al.*, 2008; Zhu *et al.*, 2008).

Not all OPCs within the cerebral cortex do differentiate to myelinating/remyelinating oligodendrocytes (Franklin and ffrench-Constant 2008). Several studies present evidence that different OPC subpopulations with different functions such as synaptic transmission may exist (Karadottir *et al.*, 2008; Jacobs *et al.*, 2005). This may be achieved by glutamate and N-methyl D-aspartate (NMDA) receptors which have been shown to be expressed on oligodendroglial membranes (Bergles *et al.*, 2000; Karadottir *et al.*, 2005; Kukley *et al.*, 2007). The putative existence of further OPC subpopulations could explain why a substantial number of quiescent OPC remain in high numbers in the normal cerebral cortex (Dawson *et al.*, 2003, Levine *et al.*, 2001). Another supporting reason is that OPC subpopulations derived from OPCs responded differentially to trophic factors such as PDGF-AA, FGF-2 and IGF-1 (Mason *et al.*, 2002). Furthermore, competing waves of embryonic oligodendrocyte lineages during development support the existence of two different oligodendroglial populations (Kessar *et al.*, 2006). Whether aforementioned cells are also present in the brain of the Lewis rat and whether these cells respond to inflammatory demyelination is unknown.

NogoA is considered a reliable marker for adult mature oligodendrocytes (Kuhlmann *et al.*, 2007). However, during the transition from OPCs to remyelinating oligodendrocytes, some cells may express both olig2 and NogoA. Nevertheless, the proportion of wrong positive cells might be small. In all probability, the restored population of NogoA-positive oligodendrocytes contributed to remyelination. However, the presence of remyelinating oligodendrocytes in the targeted EAE model should be confirmed by PLP in-situ hybridization and electron microscopy in future experiments.

4.6 The origin of proliferated OPCs

The origin of proliferated OPCs reported in this study is unknown. However, our data indicate that OPCs were locally recruited as substantial numbers of proliferated OPCs were already observed within demyelinated areas at day three after lesion induction. Thus, recruitment from remote brain areas unlikely occurred in such a short time frame. Additionally, few OPCs might have migrated from adjacent cortical areas as increased numbers of proliferated OPCs were also detected in unaffected cortical areas located close to the lesion (data not shown). Furthermore, the subventricular zone (SVZ) is discussed in the literature as a potent source for OPCs. The SVZ harbours mitogenic type B cells from which OPCs but also astrocytes and neurons derive from this region (Levison and Goldman, 1997; Carrol *et al.*, 1998; Menn *et al.*, 2006). These cells migrate through the rostral migratory pathway (RMS) to their destination and have been shown to be a potential source of oligodendrocyte recruitment in experimental demyelination studies (Aguirre *et al.*, 2007; Nait-Oumesmar *et al.*, 1999; Picard-Riera *et al.*, 2002). SVZ activation was also described in MS patients (Nait-Oumesmar *et al.*, 2007), although the role of SVZ proliferation and migration might play only a minor role in human disease. Firstly, the contribution of SVZ-derived cells may be relatively small compared to local OPCs, and especially as it occurs in remote places of the brain. Secondly, oligodendroglial precursors may be recruited from areas adjacent to demyelinated lesions. This is supported by increased oligodendroglial cell counts observed at the rim of MS lesions (Raine *et al.*, 1981; Prineas *et al.*, 1989; Robinson *et al.*, 1998).

4.7 Indications of overstressed remyelination capacity

Histological evaluation revealed extensive remyelination after repetitive demyelination. In addition, oligodendrocyte population recovered at least after the first two demyelinating events. However, twenty-one days after the fourth lesion induction NogoA-positive cells counts ranged between the values of the demyelinated and control groups. Therefore, it is hard to state whether the oligodendrocyte population is fully restored or not. Assuming the previous statement, reduced oligodendrocyte number could indicate the start of impaired oligodendrocyte recruitment, which is unclear after the fourth injection. This may have become more apparent if further lesioning was performed. Similarly, exhaustion of the remyelination capacity can be induced after protracted and sustained exposure to a demyelinating stimulus, this does not reflect those conditions of cortical MS lesions (Linington *et al.*, 1992; Ludwin, 1980).

Furthermore, one should keep in mind that MS patients may experience many demyelinating episodes during the usually long disease course, whereby cortical demyelinating lesions can be observed in early disease stages (Okuda *et al.*, 2009; Lebrun *et al.*, 2008). Moreover, signs of previous demyelination were detected in normal appearing grey matter of MS patients (Albert *et al.*, 2007). When considering the number of undetected and obvious lesions that MS patients suffer throughout disease, loss of remyelination capacity due to frequent demyelinating episodes still provides a possible explanation for chronic demyelinated plaques.

4.8 Role of reactive astrocytes on remyelination

Moderate astrogliosis was observed in close proximity to the needle track. In concordance to our results, cortical MS lesions present with moderate astrogliosis compared to white matter lesions (Stadelmann *et al.*, 2008). The role of astrocytes on de- and re-myelination is not fully understood. On the one hand astrocyte-derived hyaluronan seem to inhibit OPC maturation and thereby may contribute to the chronicity of plaques (Back *et al.*, 2005). On the other hand astrocytes may also be beneficial as they secrete the neuroprotective ciliary neurotrophic factor (Albrecht *et al.*, 2007). Furthermore, lack of astrocytes is associated with reduced numbers of OPCs in experimental demyelination,

which indicates an important role of these cells on remyelination (Talbot *et al.*, 2005). However, aforementioned effects may play a minor role in our model, since astrogliosis observed in our study is negligible.

4.9 Hormonal effects on targeted cortical EAE

For induction of targeted EAE lesions female Lewis rats were used. To analyse whether disturbances in estrous cycle may interfere with the outcome of our experiments, the estrous cycle was determined in a subgroup of animals. Preliminary results indicate a transient disturbance of the estrous cycle in the targeted cortical EAE model (Appendix, Figure A). Whether a disturbed estrous cycle might interfere with remyelination and oligodendrocyte recruitment needs to be analysed in more detail. However, sex hormonal alterations play a role in MS, as some patients experience an alleviation of symptoms during the third trimester of pregnancy which may be related to high levels of estrogen (Confavreux *et al.*, 1998). Furthermore, 17- β -estradiol and estriol promoted immunosuppression was confirmed in EAE experiments (Confavreux *et al.*, 1998; Voskuhl, 2002; Kim *et al.*, 1999; Bebo *et al.*, 2001; Ito *et al.* 2001). In contrast, hormonal fluctuations in menstrual cycle or menopause seems to be associated with exacerbations of MS symptoms, however definite conclusions are missing due to technical limitations and conflicting results (Smith and Studd, 1992; Nicot, 2009).

Stress is linked to hormonal changes and may thereby influence the disease course in autoimmune human diseases and animal models (Heesen *et al.*, 2007; Morale *et al.*, 2001; Foster *et al.*, 2003; Kalantaridou *et al.*, 2004; Herzog *et al.*, 2009). Ovariectomies can be performed to reduce sex hormone related interferences in animal experiments, as for instance estrogen promoted neuroprotection (Hoffman *et al.*, 2001; Offner *et al.*, 2006; Morales *et al.*, 2006). However, changes in estrous cycle related hormonal function may possibly occur in our model, although it is likely not do not to have a strong impact on the disease course, as no obvious intraindividual differences were observed in the analysed parameters.

4.10 Conclusions

This work demonstrates the extensive intrinsic regenerative capacity of the rat cerebral cortex after repeated demyelinating insult. Four cycles of cortical demyelinating episodes did not lead to reduction of the cortical remyelinating capacity in our experimental setting. Our results suggest furthermore that oligodendroglial recruitment occurs by differentiation of existing rather than newly generated OPCs within the cerebral cortex. Findings from these studies will contribute to understanding the underlying processes of remyelination with implications for MS.

5 REFERENCES

Adelmann M, Wood J, Benzel I et al. The N-terminal domain of the myelin oligodendrocyte glycoprotein (MOG) induces acute demyelinating experimental autoimmune encephalomyelitis in the Lewis rat. *J Neuroimmunol* 1995; 63: 17-27.

Aguirre A, Gallo V. Reduced EGFR signaling in progenitor cells of the adult subventricular zone attenuates oligodendrogenesis after demyelination. *Neuron Glia Biol* 2007; 3: 209-220.

Albert M, Antel J, Bruck W, Stadelmann C. Extensive cortical remyelination in patients with chronic multiple sclerosis. *Brain Pathol* 2007; 17: 129-138.

Albrecht PJ, Enterline JC, Cromer J, Levison SW. CNTF-activated astrocytes release a soluble trophic activity for oligodendrocyte progenitors. *Neurochem Res* 2007; 32: 263-271.

Back SA, Tuohy TM, Chen H et al. Hyaluronan accumulates in demyelinated lesions and inhibits oligodendrocyte progenitor maturation. *Nat Med* 2005; 11: 966-972.

Bagert BA. Epstein-Barr virus in multiple sclerosis. *Curr Neurol Neurosci Rep* 2009; 9: 405-410.

Bansal R, Pfeiffer SE. Inhibition of protein and lipid sulfation in oligodendrocytes blocks biological responses to FGF-2 and retards cytoarchitectural maturation, but not developmental lineage progression. *Dev Biol* 1994; 162: 511-524.

Barkhof F, Bruck W, De Groot CJ *et al.* Remyelinated lesions in multiple sclerosis: magnetic resonance image appearance. *Arch Neurol* 2003; 60: 1073-1081.

Barres BA, Hart IK, Coles HS *et al.* Cell death and control of cell survival in the oligodendrocyte lineage. *Cell* 1992; 70: 31-46.

Barres BA, Raff MC, Gaese F, Bartke I, Dechant G, Barde YA. A crucial role for neurotrophin-3 in oligodendrocyte development. *Nature* 1994; 367: 371-375.

- Bebo BF, Jr., Fyfe-Johnson A, Adlard K, Beam AG, Vandembark AA, Offner H. Low-dose estrogen therapy ameliorates experimental autoimmune encephalomyelitis in two different inbred mouse strains. *J Immunol* 2001; 166: 2080-2089.
- Beebe GW, Kurtzke JF, Kurland LT, Auth TL, Nagler B. Studies on the natural history of multiple sclerosis. 3. Epidemiologic analysis of the army experience in World War II. *Neurology* 1967; 17: 1-17.
- Ben-Nun A, Wekerle H, Cohen IR. Vaccination against autoimmune encephalomyelitis with T-lymphocyte line cells reactive against myelin basic protein. *Nature* 1981; 292: 60-61.
- Bergles DE, Roberts JD, Somogyi P, Jahr CE. Glutamatergic synapses on oligodendrocyte precursor cells in the hippocampus. *Nature* 2000; 405: 187-191.
- Besnard F, Perraud F, Sensenbrenner M, Labourdette G. Effects of acidic and basic fibroblast growth factors on proliferation and maturation of cultured rat oligodendrocytes. *Int J Dev Neurosci* 1989; 7: 401-409.
- Biber K, Neumann H, Inoue K, Boddeke HW. Neuronal 'On' and 'Off' signals control microglia. *Trends Neurosci* 2007; 30: 596-602.
- Blakemore WF. Ethidium bromide induced demyelination in the spinal cord of the cat. *Neuropathol Appl Neurobiol* 1982; 8: 365-375.
- Blakemore WF. Pattern of remyelination in the CNS. *Nature* 1974; 249: 577-578.
- Blakemore WF. Remyelination of the superior cerebellar peduncle in the mouse following demyelination induced by feeding cuprizone. *J Neurol Sci* 1973; 20: 73-83.
- Bo L, Vedeler CA, Nyland HI, Trapp BD, Mork SJ. Subpial demyelination in the cerebral cortex of multiple sclerosis patients. *J Neuropathol Exp Neurol* 2003; 62: 723-732.
- Bo L. The histopathology of grey matter demyelination in multiple sclerosis. *Acta Neurol Scand Suppl* 2009; 51-57.
- Brownell B, Hughes JT. The distribution of plaques in the cerebrum in multiple sclerosis. *J Neurol Neurosurg Psychiatry* 1962; 25: 315-320.

- Calver AR, Hall AC, Yu WP *et al.* Oligodendrocyte population dynamics and the role of PDGF in vivo. *Neuron* 1998; 20: 869-882.
- Carroll WM, Jennings AR, Ironside LJ. Identification of the adult resting progenitor cell by autoradiographic tracking of oligodendrocyte precursors in experimental CNS demyelination. *Brain* 1998; 121 (Pt 2): 293-302.
- Carroll WM, Jennings AR. Early recruitment of oligodendrocyte precursors in CNS demyelination. *Brain* 1994; 117 (Pt 3): 563-578.
- Chang A, Nishiyama A, Peterson J, Prineas J, Trapp BD. NG2-positive oligodendrocyte progenitor cells in adult human brain and multiple sclerosis lesions. *J Neurosci* 2000; 20: 6404-6412.
- Confavreux C, Hutchinson M, Hours MM, Cortinovis-Tourniaire P, Moreau T. Rate of pregnancy-related relapse in multiple sclerosis. Pregnancy in Multiple Sclerosis Group. *N Engl J Med* 1998; 339: 285-291.
- Curatolo L, Valsasina B, Caccia C, Raimondi GL, Orsini G, Bianchetti A. Recombinant human IL-2 is cytotoxic to oligodendrocytes after in vitro self aggregation. *Cytokine* 1997; 9: 734-739.
- Dawson MR, Levine JM, Reynolds R. NG2-expressing cells in the central nervous system: are they oligodendroglial progenitors? *J Neurosci Res* 2000; 61: 471-479.
- Dawson MR, Polito A, Levine JM, Reynolds R. NG2-expressing glial progenitor cells: an abundant and widespread population of cycling cells in the adult rat CNS. *Mol Cell Neurosci* 2003; 24: 476-488.
- Dimou L, Simon C, Kirchhoff F, Takebayashi H, Gotz M. Progeny of Olig2-expressing progenitors in the gray and white matter of the adult mouse cerebral cortex. *J Neurosci* 2008; 28: 10434-10442.
- Dustin ML, Cooper JA. The immunological synapse and the actin cytoskeleton: molecular hardware for T cell signaling. *Nat Immunol* 2000; 1: 23-29.
- Dutta R, McDonough J, Yin X *et al.* Mitochondrial dysfunction as a cause of axonal degeneration in multiple sclerosis patients. *Ann Neurol* 2006; 59: 478-489.

- Edgar JM, Garbern J. The myelinated axon is dependent on the myelinating cell for support and maintenance: molecules involved. *J Neurosci Res* 2004; 76: 593-598.
- Eizenberg O, Faber-Elman A, Gottlieb E, Oren M, Rotter V, Schwartz M. Direct involvement of p53 in programmed cell death of oligodendrocytes. *EMBO J* 1995; 14: 1136-1144.
- Fancy SP, Zhao C, Franklin RJ. Increased expression of Nkx2.2 and Olig2 identifies reactive oligodendrocyte progenitor cells responding to demyelination in the adult CNS. *Mol Cell Neurosci* 2004; 27: 247-254.
- Filippi M, Yousry T, Horsfield MA *et al.* A high-resolution three-dimensional T1-weighted gradient echo sequence improves the detection of disease activity in multiple sclerosis. *Ann Neurol* 1996; 40: 901-907.
- Foster SC, Daniels C, Bourdette DN, Bebo BF, Jr. Dysregulation of the hypothalamic-pituitary-gonadal axis in experimental autoimmune encephalomyelitis and multiple sclerosis. *J Neuroimmunol* 2003; 140: 78-87.
- Franklin RJ, Ffrench-Constant C. Remyelination in the CNS: from biology to therapy. *Nat Rev Neurosci* 2008; 9: 839-855.
- Franklin RJ, Kotter MR. The biology of CNS remyelination: the key to therapeutic advances. *J Neurol* 2008; 255 Suppl 1: 19-25.
- Franklin RJ. Why does remyelination fail in multiple sclerosis? *Nat Rev Neurosci* 2002; 3: 705-714.
- Fritz RB, Chou CH, McFarlin DE. Relapsing murine experimental allergic encephalomyelitis induced by myelin basic protein. *J Immunol* 1983; 130: 1024-1026.
- Fruttiger M, Karlsson L, Hall AC *et al.* Defective oligodendrocyte development and severe hypomyelination in PDGF-A knockout mice. *Development* 1999; 126: 457-467.
- Geha S, Pallud J, Junier MP *et al.* NG2+/Olig2+ Cells Are the Major Cycle-Related Cell Population of the Adult Human Normal Brain. *Brain Pathol* 2009.
- Genain CP, Nguyen MH, Letvin NL *et al.* Antibody facilitation of multiple sclerosis-like lesions in a nonhuman primate. *J Clin Invest* 1995; 96: 2966-2974.

Geurts JJ, Bo L, Pouwels PJ, Castelijns JA, Polman CH, Barkhof F. Cortical lesions in multiple sclerosis: combined postmortem MR imaging and histopathology. *AJNR Am J Neuroradiol* 2005; 26: 572-577.

Geurts JJ, Stys PK, Minagar A, Amor S, Zivadinov R. Gray matter pathology in (chronic) MS: modern views on an early observation. *J Neurol Sci* 2009; 282: 12-20.

Gilmore CP, Donaldson I, Bo L, Owens T, Lowe J, Evangelou N. Regional variations in the extent and pattern of grey matter demyelination in multiple sclerosis: a comparison between the cerebral cortex, cerebellar cortex, deep grey matter nuclei and the spinal cord. *J Neurol Neurosurg Psychiatry* 2009; 80: 182-187.

Gold R, Linington C, Lassmann H. Understanding pathogenesis and therapy of multiple sclerosis via animal models: 70 years of merits and culprits in experimental autoimmune encephalomyelitis research. *Brain* 2006; 129: 1953-1971.

Goldschmidt T, Antel J, Konig FB, Bruck W, Kuhlmann T. Remyelination capacity of the MS brain decreases with disease chronicity. *Neurology* 2009; 72: 1914-1921.

Griffiths I, Klugmann M, Anderson T *et al.* Axonal swellings and degeneration in mice lacking the major proteolipid of myelin. *Science* 1998; 280: 1610-1613.

Griot C, Vandeveld M, Richard A, Peterhans E, Stocker R. Selective degeneration of oligodendrocytes mediated by reactive oxygen species. *Free Radic Res Commun* 1990; 11: 181-193.

Haase CG, Tinnefeld M, Lienemann M, Ganz RE, Faustmann PM. Depression and cognitive impairment in disability-free early multiple sclerosis. *Behav Neurol* 2003; 14: 39-45.

Haines JL, Terwedow HA, Burgess K *et al.* Linkage of the MHC to familial multiple sclerosis suggests genetic heterogeneity. The Multiple Sclerosis Genetics Group. *Hum Mol Genet* 1998; 7: 1229-1234.

Hall SM. The effect of injections of lysophosphatidyl choline into white matter of the adult mouse spinal cord. *J Cell Sci* 1972; 10: 535-546.

- Hampton DW, Anderson J, Pryce G *et al.* An experimental model of secondary progressive multiple sclerosis that shows regional variation in gliosis, remyelination, axonal and neuronal loss. *J Neuroimmunol* 2008; 201-202: 200-211.
- Heesen C, Gold SM, Huitinga I, Reul JM. Stress and hypothalamic-pituitary-adrenal axis function in experimental autoimmune encephalomyelitis and multiple sclerosis - a review. *Psychoneuroendocrinology* 2007; 32: 604-618.
- Herzog CJ, Czeh B, Corbach S *et al.* Chronic social instability stress in female rats: a potential animal model for female depression. *Neuroscience* 2009; 159: 982-992.
- Hillert J, Olerup O. Multiple sclerosis is associated with genes within or close to the HLA-DR-DQ subregion on a normal DR15,DQ6,Dw2 haplotype. *Neurology* 1993; 43: 163-168.
- Hinks GL, Chari DM, O'Leary MT *et al.* Depletion of endogenous oligodendrocyte progenitors rather than increased availability of survival factors is a likely explanation for enhanced survival of transplanted oligodendrocyte progenitors in X-irradiated compared to normal CNS. *Neuropathol Appl Neurobiol* 2001; 27: 59-67.
- Hisahara S, Shoji S, Okano H, Miura M. ICE/CED-3 family executes oligodendrocyte apoptosis by tumor necrosis factor. *J Neurochem* 1997; 69: 10-20.
- Hoffman GE, Le WW, Murphy AZ, Koski CL. Divergent effects of ovarian steroids on neuronal survival during experimental allergic encephalitis in Lewis rats. *Exp Neurol* 2001; 171: 272-284.
- Hohlfeld R, Wekerle H. Immunological update on multiple sclerosis. *Curr Opin Neurol* 2001; 14: 299-304.
- Ibarrola N, Mayer-Proschel M, Rodriguez-Pena A, Noble M. Evidence for the existence of at least two timing mechanisms that contribute to oligodendrocyte generation in vitro. *Dev Biol* 1996; 180: 1-21.
- Irvine KA, Blakemore WF. Remyelination protects axons from demyelination-associated axon degeneration. *Brain* 2008; 131: 1464-1477.

- Issazadeh S, Mustafa M, Ljungdahl A *et al.* Interferon gamma, interleukin 4 and transforming growth factor beta in experimental autoimmune encephalomyelitis in Lewis rats: dynamics of cellular mRNA expression in the central nervous system and lymphoid cells. *J Neurosci Res* 1995; 40: 579-590.
- Ito A, Bebo BF, Jr., Matejuk A *et al.* Estrogen treatment down-regulates TNF-alpha production and reduces the severity of experimental autoimmune encephalomyelitis in cytokine knockout mice. *J Immunol* 2001; 167: 542-552.
- Itoyama Y, Sternberger NH, Webster HD, Quarles RH, Cohen SR, Richardson EP, Jr. Immunocytochemical observations on the distribution of myelin-associated glycoprotein and myelin basic protein in multiple sclerosis lesions. *Ann Neurol* 1980; 7: 167-177.
- Jabs R, Pivneva T, Huttmann K *et al.* Synaptic transmission onto hippocampal glial cells with hGFAP promoter activity. *J Cell Sci* 2005; 118: 3791-3803.
- Jacobs EC, Pribyl TM, Feng JM *et al.* Region-specific myelin pathology in mice lacking the golli products of the myelin basic protein gene. *J Neurosci* 2005; 25: 7004-7013.
- Jeffery ND, Blakemore WF. Locomotor deficits induced by experimental spinal cord demyelination are abolished by spontaneous remyelination. *Brain* 1997; 120 (Pt 1): 27-37.
- Johnson RT. The virology of demyelinating diseases. *Ann Neurol* 1994; 36 Suppl: S54-S60.
- Jurewicz A, Matysiak M, Tybor K, Kilianek L, Raine CS, Selmaj K. Tumour necrosis factor-induced death of adult human oligodendrocytes is mediated by apoptosis inducing factor. *Brain* 2005; 128: 2675-2688.
- Kabat EA, Wolf A, Bezer AE, Murray JP. Studies on acute disseminated encephalomyelitis produced experimentally in rhesus monkeys. *J Exp Med* 1951; 93: 615-633.
- Kalantaridou SN, Makrigiannakis A, Zoumakis E, Chrousos GP. Stress and the female reproductive system. *J Reprod Immunol* 2004; 62: 61-68.

- Kangarlu A, Bourekas EC, Ray-Chaudhury A, Rammohan KW. Cerebral cortical lesions in multiple sclerosis detected by MR imaging at 8 Tesla. *AJNR Am J Neuroradiol* 2007; 28: 262-266.
- Karadottir R, Cavelier P, Bergersen LH, Attwell D. NMDA receptors are expressed in oligodendrocytes and activated in ischaemia. *Nature* 2005; 438: 1162-1166.
- Karadottir R, Hamilton NB, Bakiri Y, Attwell D. Spiking and nonspiking classes of oligodendrocyte precursor glia in CNS white matter. *Nat Neurosci* 2008; 11: 450-456.
- Keirstead HS, Blakemore WF. Identification of post-mitotic oligodendrocytes incapable of remyelination within the demyelinated adult spinal cord. *J Neuropathol Exp Neurol* 1997; 56: 1191-1201.
- Keirstead HS, Levine JM, Blakemore WF. Response of the oligodendrocyte progenitor cell population (defined by NG2 labelling) to demyelination of the adult spinal cord. *Glia* 1998; 22: 161-170.
- Kerschensteiner M, Stadelmann C, Buddeberg BS *et al.* Targeting experimental autoimmune encephalomyelitis lesions to a predetermined axonal tract system allows for refined behavioral testing in an animal model of multiple sclerosis. *Am J Pathol* 2004; 164: 1455-1469.
- Kessaris N, Fogarty M, Iannarelli P, Grist M, Wegner M, Richardson WD. Competing waves of oligodendrocytes in the forebrain and postnatal elimination of an embryonic lineage. *Nat Neurosci* 2006; 9: 173-179.
- Kidd D, Barkhof F, McConnell R, Algra PR, Allen IV, Revesz T. Cortical lesions in multiple sclerosis. *Brain* 1999; 122 (Pt 1): 17-26.
- Kim S, Liva SM, Dalal MA, Verity MA, Voskuhl RR. Estriol ameliorates autoimmune demyelinating disease: implications for multiple sclerosis. *Neurology* 1999; 52: 1230-1238.
- Kornek B, Storch MK, Weissert R *et al.* Multiple sclerosis and chronic autoimmune encephalomyelitis: a comparative quantitative study of axonal injury in active, inactive, and remyelinated lesions. *Am J Pathol* 2000; 157: 267-276.

- Kuhlmann T, Miron V, Cuo Q, Wegner C, Antel J, Bruck W. Differentiation block of oligodendroglial progenitor cells as a cause for remyelination failure in chronic multiple sclerosis. *Brain* 2008; 131: 1749-1758.
- Kuhlmann T, Remington L, Maruschak B, Owens T, Bruck W. Nogo-A is a reliable oligodendroglial marker in adult human and mouse CNS and in demyelinated lesions. *J Neuropathol Exp Neurol* 2007; 66: 238-246.
- Kukley M, Capetillo-Zarate E, Dietrich D. Vesicular glutamate release from axons in white matter. *Nat Neurosci* 2007; 10: 311-320.
- Kurtzke JF. Rating neurologic impairment in multiple sclerosis: an expanded disability status scale (EDSS). *Neurology* 1983; 33: 1444-1452.
- Kutzelnigg A, Faber-Rod JC, Bauer J *et al.* Widespread demyelination in the cerebellar cortex in multiple sclerosis. *Brain Pathol* 2007; 17: 38-44.
- Kutzelnigg A, Lucchinetti CF, Stadelmann C *et al.* Cortical demyelination and diffuse white matter injury in multiple sclerosis. *Brain* 2005; 128: 2705-2712.
- Ladiwala U, Li H, Antel JP, Nalbantoglu J. p53 induction by tumor necrosis factor-alpha and involvement of p53 in cell death of human oligodendrocytes. *J Neurochem* 1999; 73: 605-611.
- Lappe-Siefke C, Goebbels S, Gravel M *et al.* Disruption of *Cnp1* uncouples oligodendroglial functions in axonal support and myelination. *Nat Genet* 2003; 33: 366-374.
- Lassmann H, Bruck W, Lucchinetti C. Heterogeneity of multiple sclerosis pathogenesis: implications for diagnosis and therapy. *Trends Mol Med* 2001; 7: 115-121.
- Lazzarini, RA. Myelin biology and disorders. San Diego, CA: Elsevier Academic press, 2004.
- Lebrun C, Bensa C, Debouverie M *et al.* Unexpected multiple sclerosis: follow-up of 30 patients with magnetic resonance imaging and clinical conversion profile. *J Neurol Neurosurg Psychiatry* 2008; 79: 195-198.

Levine JM, Reynolds R, Fawcett JW. The oligodendrocyte precursor cell in health and disease. *Trends Neurosci* 2001; 24: 39-47.

Levine JM, Reynolds R. Activation and proliferation of endogenous oligodendrocyte precursor cells during ethidium bromide-induced demyelination. *Exp Neurol* 1999; 160: 333-347.

Levison SW, Goldman JE. Multipotential and lineage restricted precursors coexist in the mammalian perinatal subventricular zone. *J Neurosci Res* 1997; 48: 83-94.

Liebetanz D, Merkler D. Effects of commissural de- and remyelination on motor skill behaviour in the cuprizone mouse model of multiple sclerosis. *Exp Neurol* 2006; 202: 217-224.

Linington C, Bradl M, Lassmann H, Brunner C, Vass K. Augmentation of demyelination in rat acute allergic encephalomyelitis by circulating mouse monoclonal antibodies directed against a myelin/oligodendrocyte glycoprotein. *Am J Pathol* 1988; 130: 443-454.

Linington C, Engelhardt B, Kapocs G, Lassman H. Induction of persistently demyelinated lesions in the rat following the repeated adoptive transfer of encephalitogenic T cells and demyelinating antibody. *J Neuroimmunol* 1992; 40: 219-224.

Lu QR, Sun T, Zhu Z *et al.* Common developmental requirement for Olig function indicates a motor neuron/oligodendrocyte connection. *Cell* 2002; 109: 75-86.

Lublin FD, Reingold SC. Defining the clinical course of multiple sclerosis: results of an international survey. National Multiple Sclerosis Society (USA) Advisory Committee on Clinical Trials of New Agents in Multiple Sclerosis. *Neurology* 1996; 46: 907-911.

Lucchinetti C, Bruck W, Parisi J, Scheithauer B, Rodriguez M, Lassmann H. Heterogeneity of multiple sclerosis lesions: implications for the pathogenesis of demyelination. *Ann Neurol* 2000; 47: 707-717.

Lucchinetti C, Bruck W, Parisi J, Scheithauer B, Rodriguez M, Lassmann H. A quantitative analysis of oligodendrocytes in multiple sclerosis lesions. A study of 113 cases. *Brain* 1999; 122 (Pt 12): 2279-2295.

- Ludwin SK, Maitland M. Long-term remyelination fails to reconstitute normal thickness of central myelin sheaths. *J Neurol Sci* 1984; 64: 193-198.
- Ludwin SK. Chronic demyelination inhibits remyelination in the central nervous system. An analysis of contributing factors. *Lab Invest* 1980; 43: 382-387.
- Maeda Y, Solanky M, Menonna J, Chapin J, Li W, Dowling P. Platelet-derived growth factor-alpha receptor-positive oligodendroglia are frequent in multiple sclerosis lesions. *Ann Neurol* 2001; 49: 776-785.
- Magliozzi R, Howell O, Vora A *et al.* Meningeal B-cell follicles in secondary progressive multiple sclerosis associate with early onset of disease and severe cortical pathology. *Brain* 2007; 130: 1089-1104.
- Mancardi G, Hart B, Roccatagliata L *et al.* Demyelination and axonal damage in a non-human primate model of multiple sclerosis. *J Neurol Sci* 2001; 184: 41-49.
- Martinez-Caceres EM, Espejo C, Brieva L *et al.* Expression of chemokine receptors in the different clinical forms of multiple sclerosis. *Mult Scler* 2002; 8: 390-395.
- Mason JL, Goldman JE. A2B5+ and O4+ Cycling progenitors in the adult forebrain white matter respond differentially to PDGF-AA, FGF-2, and IGF-1. *Mol Cell Neurosci* 2002; 20: 30-42.
- Matsushima GK, Morell P. The neurotoxicant, cuprizone, as a model to study demyelination and remyelination in the central nervous system. *Brain Pathol* 2001; 11: 107-116.
- McKinnon RD, Matsui T, Aranda M, Dubois-Dalcq M. A role for fibroblast growth factor in oligodendrocyte development. *Ann N Y Acad Sci* 1991; 638: 378-386.
- McKinnon RD, Matsui T, Dubois-Dalcq M, Aaronson SA. FGF modulates the PDGF-driven pathway of oligodendrocyte development. *Neuron* 1990; 5: 603-614.
- McMorris FA, Dubois-Dalcq M. Insulin-like growth factor I promotes cell proliferation and oligodendroglial commitment in rat glial progenitor cells developing in vitro. *J Neurosci Res* 1988; 21: 199-209.

- McRae BL, Kennedy MK, Tan LJ, Dal Canto MC, Picha KS, Miller SD. Induction of active and adoptive relapsing experimental autoimmune encephalomyelitis (EAE) using an encephalitogenic epitope of proteolipid protein. *J Neuroimmunol* 1992; 38: 229-240.
- McTigue DM, Horner PJ, Stokes BT, Gage FH. Neurotrophin-3 and brain-derived neurotrophic factor induce oligodendrocyte proliferation and myelination of regenerating axons in the contused adult rat spinal cord. *J Neurosci* 1998; 18: 5354-5365.
- Menn B, Garcia-Verdugo JM, Yaschine C, Gonzalez-Perez O, Rowitch D, varez-Buylla A. Origin of oligodendrocytes in the subventricular zone of the adult brain. *J Neurosci* 2006; 26: 7907-7918.
- Merkler D, Boretius S, Stadelmann C *et al.* Multicontrast MRI of remyelination in the central nervous system. *NMR Biomed* 2005; 18: 395-403.
- Merkler D, Ernsting T, Kerschensteiner M, Bruck W, Stadelmann C. A new focal EAE model of cortical demyelination: multiple sclerosis-like lesions with rapid resolution of inflammation and extensive remyelination. *Brain* 2006; 129: 1972-1983.
- Merkler D, Schmelting B, Czeh B, Fuchs E, Stadelmann C, Bruck W. Myelin oligodendrocyte glycoprotein-induced experimental autoimmune encephalomyelitis in the common marmoset reflects the immunopathology of pattern II multiple sclerosis lesions. *Mult Scler* 2006; 12: 369-374.
- Merrill JE, Scolding NJ. Mechanisms of damage to myelin and oligodendrocytes and their relevance to disease. *Neuropathol Appl Neurobiol* 1999; 25: 435-458.
- Miller RH. Regulation of oligodendrocyte development in the vertebrate CNS. *Prog Neurobiol* 2002; 67: 451-467.
- Morale C, Brouwer J, Testa N *et al.* Stress, glucocorticoids and the susceptibility to develop autoimmune disorders of the central nervous system. *Neurol Sci* 2001; 22: 159-162.
- Morales LB, Loo KK, Liu HB, Peterson C, Tiwari-Woodruff S, Voskuhl RR. Treatment with an estrogen receptor alpha ligand is neuroprotective in experimental autoimmune encephalomyelitis. *J Neurosci* 2006; 26: 6823-6833.

- Munz C, Steinman RM, Fujii S. Dendritic cell maturation by innate lymphocytes: coordinated stimulation of innate and adaptive immunity. *J Exp Med* 2005; 202: 203-207.
- Nait-Oumesmar B, Decker L, Lachapelle F, Vellana-Adalid V, Bachelin C, Van Evercooren AB. Progenitor cells of the adult mouse subventricular zone proliferate, migrate and differentiate into oligodendrocytes after demyelination. *Eur J Neurosci* 1999; 11: 4357-4366.
- Nait-Oumesmar B, Picard-Riera N, Kerninon C *et al.* Activation of the subventricular zone in multiple sclerosis: evidence for early glial progenitors. *Proc Natl Acad Sci U S A* 2007; 104: 4694-4699.
- Nicot A. Gender and sex hormones in multiple sclerosis pathology and therapy. *Front Biosci* 2009; 14: 4477-4515.
- Nishiyama A, Lin XH, Giese N, Heldin CH, Stallcup WB. Co-localization of NG2 proteoglycan and PDGF alpha-receptor on O2A progenitor cells in the developing rat brain. *J Neurosci Res* 1996; 43: 299-314.
- Noble M, Murray K, Stroobant P, Waterfield MD, Riddle P. Platelet-derived growth factor promotes division and motility and inhibits premature differentiation of the oligodendrocyte/type-2 astrocyte progenitor cell. *Nature* 1988; 333: 560-562.
- Offner H, Polanczyk M. A potential role for estrogen in experimental autoimmune encephalomyelitis and multiple sclerosis. *Ann N Y Acad Sci* 2006; 1089: 343-372.
- Oksenberg JR, Baranzini SE, Sawcer S, Hauser SL. The genetics of multiple sclerosis: SNPs to pathways to pathogenesis. *Nat Rev Genet* 2008; 9: 516-526.
- Okuda DT, Mowry EM, Beheshtian A *et al.* Incidental MRI anomalies suggestive of multiple sclerosis: the radiologically isolated syndrome. *Neurology* 2009; 72: 800-805.
- Ono K, Bansal R, Payne J, Rutishauser U, Miller RH. Early development and dispersal of oligodendrocyte precursors in the embryonic chick spinal cord. *Development* 1995; 121: 1743-1754.

- Ono K, Fujisawa H, Hirano S, Norita M, Tsumori T, Yasui Y. Early development of the oligodendrocyte in the embryonic chick metencephalon. *J Neurosci Res* 1997; 48: 212-225.
- Park SK, Miller R, Krane I, Vartanian T. The erbB2 gene is required for the development of terminally differentiated spinal cord oligodendrocytes. *J Cell Biol* 2001; 154: 1245-1258.
- Patani R, Balaratnam M, Vora A, Reynolds R. Remyelination can be extensive in multiple sclerosis despite a long disease course. *Neuropathol Appl Neurobiol* 2007; 33: 277-287.
- Patrikios P, Stadelmann C, Kutzelnigg A *et al.* Remyelination is extensive in a subset of multiple sclerosis patients. *Brain* 2006; 129: 3165-3172.
- Paxinos, G., Watson, C. *The rat brain in stereotaxic coordinates*. Fourth edition. New York: Academic Press, Spiral Bound, 1998.
- Pender MP. Demyelination and neurological signs in experimental allergic encephalomyelitis. *J Neuroimmunol* 1987; 15: 11-24.
- Penderis J, Shields SA, Franklin RJ. Impaired remyelination and depletion of oligodendrocyte progenitors does not occur following repeated episodes of focal demyelination in the rat central nervous system. *Brain* 2003; 126: 1382-1391.
- Perier O, Gregoire A. Electron microscopic features of multiple sclerosis lesions. *Brain* 1965; 88: 937-952.
- Peterson JW, Bo L, Mork S, Chang A, Trapp BD. Transected neurites, apoptotic neurons, and reduced inflammation in cortical multiple sclerosis lesions. *Ann Neurol* 2001; 50: 389-400.
- Pfeiffer SE, Warrington AE, Bansal R. The oligodendrocyte and its many cellular processes. *Trends Cell Biol* 1993; 3: 191-197.
- Picard-Riera N, Decker L, Delarasse C *et al.* Experimental autoimmune encephalomyelitis mobilizes neural progenitors from the subventricular zone to undergo oligodendrogenesis in adult mice. *Proc Natl Acad Sci U S A* 2002; 99: 13211-13216.

- Pomeroy IM, Matthews PM, Frank JA, Jordan EK, Esiri MM. Demyelinated neocortical lesions in marmoset autoimmune encephalomyelitis mimic those in multiple sclerosis. *Brain* 2005; 128: 2713-2721.
- Prineas JW, Kwon EE, Goldenberg PZ *et al.* Multiple sclerosis. Oligodendrocyte proliferation and differentiation in fresh lesions. *Lab Invest* 1989; 61: 489-503.
- Pringle NP, Mudhar HS, Collarini EJ, Richardson WD. PDGF receptors in the rat CNS: during late neurogenesis, PDGF alpha-receptor expression appears to be restricted to glial cells of the oligodendrocyte lineage. *Development* 1992; 115: 535-551.
- Probert L, Eugster HP, Akassoglou K *et al.* TNFR1 signalling is critical for the development of demyelination and the limitation of T-cell responses during immune-mediated CNS disease. *Brain* 2000; 123 (Pt 10): 2005-2019.
- Qian X, Davis AA, Goderie SK, Temple S. FGF2 concentration regulates the generation of neurons and glia from multipotent cortical stem cells. *Neuron* 1997; 18: 81-93.
- Quarles RH. Myelin-associated glycoprotein (MAG): past, present and beyond. *J Neurochem* 2007; 100: 1431-1448.
- Raff MC, Abney ER, Miller RH. Two glial cell lineages diverge prenatally in rat optic nerve. *Dev Biol* 1984; 106: 53-60.
- Raine CS, Scheinberg L, Waltz JM. Multiple sclerosis. Oligodendrocyte survival and proliferation in an active established lesion. *Lab Invest* 1981; 45: 534-546.
- Rasmussen S, Wang Y, Kivisakk P *et al.* Persistent activation of microglia is associated with neuronal dysfunction of callosal projecting pathways and multiple sclerosis-like lesions in relapsing—remitting experimental autoimmune encephalomyelitis. *Brain* 2007; 130: 2816-2829.
- Reynolds R, Hardy R. Oligodendroglial progenitors labeled with the O4 antibody persist in the adult rat cerebral cortex in vivo. *J Neurosci Res* 1997; 47: 455-470.
- Rivers TM, Sprunt DH, Berry GP. Observations on attempts to produce acute disseminated encephalomyelitis in monkeys. *J Exp Med* 1933; 58: 39–53.

- Robinson S, Tani M, Strieter RM, Ransohoff RM, Miller RH. The chemokine growth-regulated oncogene-alpha promotes spinal cord oligodendrocyte precursor proliferation. *J Neurosci* 1998; 18: 10457-10463.
- Sander M. Hirnrindenbefunde bei multipler Sklerose. *Monatsschr. Psych. Neurol.* 1898; IV: 429-436.
- Saneto RP, Low KG, Melner MH, de VJ. Insulin/insulin-like growth factor I and other epigenetic modulators of myelin basic protein expression in isolated oligodendrocyte progenitor cells. *J Neurosci Res* 1988; 21: 210-219.
- Schluesener HJ, Sobel RA, Linington C, Weiner HL. A monoclonal antibody against a myelin oligodendrocyte glycoprotein induces relapses and demyelination in central nervous system autoimmune disease. *J Immunol* 1987; 139: 4016-4021.
- Schonrock LM, Kuhlmann T, Adler S, Bitsch A, Bruck W. Identification of glial cell proliferation in early multiple sclerosis lesions. *Neuropathol Appl Neurobiol* 1998; 24: 320-330.
- Schwab C, McGeer PL. Complement activated C4d immunoreactive oligodendrocytes delineate small cortical plaques in multiple sclerosis. *Exp Neurol* 2002; 174: 81-88.
- Scolding N, Franklin R, Stevens S, Heldin CH, Compston A, Newcombe J. Oligodendrocyte progenitors are present in the normal adult human CNS and in the lesions of multiple sclerosis. *Brain* 1998; 121 (Pt 12): 2221-2228.
- Selmaj KW, Raine CS. Tumor necrosis factor mediates myelin and oligodendrocyte damage in vitro. *Ann Neurol* 1988; 23: 339-346.
- Serafini B, Rosicarelli B, Franciotta D *et al.* Dysregulated Epstein-Barr virus infection in the multiple sclerosis brain. *J Exp Med* 2007; 204: 2899-2912.
- Serafini B, Rosicarelli B, Magliozzi R, Stigliano E, Aloisi F. Detection of ectopic B-cell follicles with germinal centers in the meninges of patients with secondary progressive multiple sclerosis. *Brain Pathol* 2004; 14: 164-174.
- Shen S, Sandoval J, Swiss VA *et al.* Age-dependent epigenetic control of differentiation inhibitors is critical for remyelination efficiency. *Nat Neurosci* 2008; 11: 1024-1034.

Shriver LP, Dittel BN. T-cell-mediated disruption of the neuronal microtubule network: correlation with early reversible axonal dysfunction in acute experimental autoimmune encephalomyelitis. *Am J Pathol* 2006; 169: 999-1011.

Sibley WA, Bamford CR, Clark K. Clinical viral infections and multiple sclerosis. *Lancet* 1985; 1: 1313-1315.

Sim FJ, Zhao C, Penderis J, Franklin RJ. The age-related decrease in CNS remyelination efficiency is attributable to an impairment of both oligodendrocyte progenitor recruitment and differentiation. *J Neurosci* 2002; 22: 2451-2459.

Simpson JE, Newcombe J, Cuzner ML, Woodroffe MN. Expression of monocyte chemoattractant protein-1 and other beta-chemokines by resident glia and inflammatory cells in multiple sclerosis lesions. *J Neuroimmunol* 1998; 84: 238-249.

Skegg K. Multiple sclerosis presenting as a pure psychiatric disorder. *Psychol Med* 1993; 23: 909-914.

Smith EJ, Blakemore WF, McDonald WI. Central remyelination restores secure conduction. *Nature* 1979; 280: 395-396.

Smith R, Studd JW. A pilot study of the effect upon multiple sclerosis of the menopause, hormone replacement therapy and the menstrual cycle. *J R Soc Med* 1992; 85: 612-613.

Sospedra M, Martin R. Immunology of multiple sclerosis. *Annu Rev Immunol* 2005; 23: 683-747.

Stadelmann C, Albert M, Wegner C, Bruck W. Cortical pathology in multiple sclerosis. *Curr Opin Neurol* 2008; 21: 229-234.

Stadelmann C, Bruck W. Interplay between mechanisms of damage and repair in multiple sclerosis. *J Neurol* 2008; 255 Suppl 1: 12-18.

Stangel M, Trebst C. Remyelination strategies: new advancements toward a regenerative treatment in multiple sclerosis. *Curr Neurol Neurosci Rep* 2006; 6: 229-235.

Takeda K, Kaisho T, Akira S. Toll-like receptors. *Annu Rev Immunol* 2003; 21: 335-376.

- Talbott JF, Loy DN, Liu Y *et al.* Endogenous Nkx2.2+/Olig2+ oligodendrocyte precursor cells fail to remyelinate the demyelinated adult rat spinal cord in the absence of astrocytes. *Exp Neurol* 2005; 192: 11-24.
- Taylor EW. Zur pathologischen Anatomie der multiplen Sklerose. *Deutsche Zeitschrift für Nervenheilkunde* 1892; 1-26.
- Trapp BD, Nave KA. Multiple sclerosis: an immune or neurodegenerative disorder? *Annu Rev Neurosci* 2008; 31: 247-269.
- Tsai HH, Frost E, To V *et al.* The chemokine receptor CXCR2 controls positioning of oligodendrocyte precursors in developing spinal cord by arresting their migration. *Cell* 2002; 110: 373-383.
- Vana AC, Lucchinetti CF, Le TQ, Armstrong RC. Myelin transcription factor 1 (Myt1) expression in demyelinated lesions of rodent and human CNS. *Glia* 2007; 55: 687-697.
- Vartanian T, Fischbach G, Miller R. Failure of spinal cord oligodendrocyte development in mice lacking neuregulin. *Proc Natl Acad Sci U S A* 1999; 96: 731-735.
- Vartanian T, Li Y, Zhao M, Stefansson K. Interferon-gamma-induced oligodendrocyte cell death: implications for the pathogenesis of multiple sclerosis. *Mol Med* 1995; 1: 732-743.
- Vercellino M, Merola A, Piacentino C *et al.* Altered glutamate reuptake in relapsing-remitting and secondary progressive multiple sclerosis cortex: correlation with microglia infiltration, demyelination, and neuronal and synaptic damage. *J Neuropathol Exp Neurol* 2007; 66: 732-739.
- Vercellino M, Plano F, Votta B, Mutani R, Giordana MT, Cavalla P. Grey matter pathology in multiple sclerosis. *J Neuropathol Exp Neurol* 2005; 64: 1101-1107.
- von Budingen HC, Hauser SL, Ouallet JC, Tanuma N, Menge T, Genain CP. Frontline: Epitope recognition on the myelin/oligodendrocyte glycoprotein differentially influences disease phenotype and antibody effector functions in autoimmune demyelination. *Eur J Immunol* 2004; 34: 2072-2083.

- Voskuhl RR. Gender issues and multiple sclerosis. *Curr Neurol Neurosci Rep* 2002; 2: 277-286.
- Warrington AE, Pfeiffer SE. Proliferation and differentiation of O4+ oligodendrocytes in postnatal rat cerebellum: analysis in unfixed tissue slices using anti-glycolipid antibodies. *J Neurosci Res* 1992; 33: 338-353.
- Watanabe M, Hadzic T, Nishiyama A. Transient upregulation of Nkx2.2 expression in oligodendrocyte lineage cells during remyelination. *Glia* 2004; 46: 311-322.
- Wegner C, Esiri MM, Chance SA, Palace J, Matthews PM. Neocortical neuronal, synaptic, and glial loss in multiple sclerosis. *Neurology* 2006; 67: 960-967.
- Wolswijk G, Riddle PN, Noble M. Platelet-derived growth factor is mitogenic for O-2Aadult progenitor cells. *Glia* 1991; 4: 495-503.
- Woodruff RH, Franklin RJ. Demyelination and remyelination of the caudal cerebellar peduncle of adult rats following stereotaxic injections of lysolecithin, ethidium bromide, and complement/anti-galactocerebroside: a comparative study. *Glia* 1999; 25: 216-228.
- Woodruff RH, Fruttiger M, Richardson WD, Franklin RJ. Platelet-derived growth factor regulates oligodendrocyte progenitor numbers in adult CNS and their response following CNS demyelination. *Mol Cell Neurosci* 2004; 25: 252-262.
- Wosik K, Antel J, Kuhlmann T, Bruck W, Massie B, Nalbantoglu J. Oligodendrocyte injury in multiple sclerosis: a role for p53. *J Neurochem* 2003; 85: 635-644.
- Wren D, Wolswijk G, Noble M. In vitro analysis of the origin and maintenance of O-2Aadult progenitor cells. *J Cell Biol* 1992; 116: 167-176.
- Yajima K, Suzuki K. Demyelination and remyelination in the rat central nervous system following ethidium bromide injection. *Lab Invest* 1979; 41: 385-392.
- Yeh HJ, Ruit KG, Wang YX, Parks WC, Snider WD, Deuel TF. PDGF A-chain gene is expressed by mammalian neurons during development and in maturity. *Cell* 1991; 64: 209-216.

Yusuf-Makagiansar H, Anderson ME, Yakovleva TV, Murray JS, Siahaan TJ. Inhibition of LFA-1/ICAM-1 and VLA-4/VCAM-1 as a therapeutic approach to inflammation and autoimmune diseases. *Med Res Rev* 2002; 22: 146-167.

Zarei M. Clinical characteristics of cortical multiple sclerosis. *J Neurol Sci* 2006; 245: 53-58.

Zhou Q, Choi G, Anderson DJ. The bHLH transcription factor Olig2 promotes oligodendrocyte differentiation in collaboration with Nkx2.2. *Neuron* 2001; 31: 791-807.

Zhu X, Hill RA, Nishiyama A. NG2 cells generate oligodendrocytes and gray matter astrocytes in the spinal cord. *Neuron Glia Biol* 2008; 4: 19-26.

6 APPENDIX

6.1 Effect of targeted cortical EAE lesion on estrous cycle

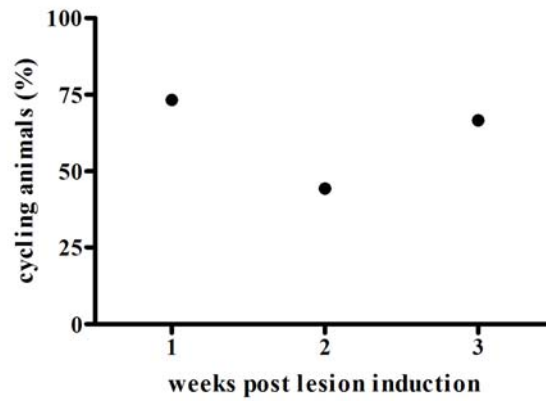


Figure A: Effect of targeted cortical EAE on estrous cycle

The effect of targeted cortical EAE on the estrous cycle was analyzed. Daily vaginal smears were collected and values are given as percentage of rats having regular estrous cycle each week. Two weeks post lesion induction a transient disruption of the estrous cycle was observed in some s.c. MOG immunized animals. The phases of estrous cycle were determined using standard criteria as described by Herzog and colleagues (Herzog *et al.*, 2009). Animals per group: n = 15 (week 1) and n = 9 (weeks 2 and 3).

6.2 Acknowledgements

The present study was completed in the Department of Neuropathology at the University Medical Center Göttingen. I would like to thank Prof. Wolfgang Brück for facilitating and providing the research environment for my work.

I am especially thankful to my supervisors and mentors Prof. Christine Stadelmann and Dr. Doron Merkler for their great support, guidance and helpful discussions over the past three years. Furthermore, I would like to thank Dr. Doron Merkler for teaching me so many valuable techniques.

I wish to thank Mariann Schedensack, Uta Scheidt, Brigitte Maruschak, Angela Detmar and Katja Schulz for their technical assistance.

Thanks to my friends and colleagues at the Department of Neuropathology for the great working atmosphere. Special thanks go to Dr. Pascal Dowling for proofreading my manuscript. I am grateful to Prof. Fuchs for giving me the opportunity and time to complete my project.

I am grateful to my family for the support throughout my life.

Finally, I would like to thank Tina for her endless patience and love.

6.3 Curriculum Vitae

CURRICULUM VITAE

PERSONAL DATA

Name: Enrique Garea Rodriguez
 Date of birth: 23/10/1980
 Place of birth: Minden, Germany
 Nationality: Spanish
 Contact information: German Primate Center
 Clinical Neuroscience Laboratory
 Kellner Weg 4, 37077 Göttingen
 egarea-rodriguez@cnl-dpz.de

EDUCATION AND QUALIFICATIONS

Since 2006	Department of Neuropathology, University Medical Center Göttingen PhD student Research project: “Damage and repair in experimental cortical demyelination” Supervisors: Prof. Christine Stadelmann and Dr. Doron Merkler
2000-2006	University of Bielefeld, Germany Biological studies Degree: Diplom “MIT AUSZEICHNUNG”
2000	Besselgymnasium, Minden Abitur

PROFESSIONAL EXPERIENCE

Since 2009	German Primate Center, Göttingen Scientist
2006-2009	University Medical Center, Göttingen Scientist

PUBLICATIONS

- 2009 Garea-Rodriguez E, Kreutzfeldt M, Brück W, Stadelmann C, Merkler D. Sustained oligodendroglial recruitment after repetitive cortical inflammatory demyelination. Poster presentation 8th Meeting of the Göttingen Neuroscience Society
- 2008 **Garea-Rodriguez E**, Kreutzfeldt M, Stadelmann C, Merkler D. Effect of repeated inflammatory demyelination on intrinsic remyelination in the targeted cortical EAE model. Poster presentation DGNN 2008, Würzburg
- 2007 Lehmann K, **Rodriguez EG**, Kratz O, Moll GH, Dawirs RR, Teuchert-Noodt G. Early preweaning metamphetamine and postweaning rearing conditions interfere with the development of peripheral stress parameters and neural growth factors in gerbils. *Int J Neurosci.* 2007 Nov; 117 (11): 1621-38.
- Garea-Rodriguez E**, Stadelmann C, Merkler D, Brück W. Copaxone in the cuprizone mouse model. Poster presentation ECTRIMS 2007, Prague
- Garea-Rodriguez E**, Merkler D, Brück W, Stadelmann C. Repetitive demyelination in the rat cerebral cortex. Poster presentation 7th Meeting of the Göttingen Neuroscience Society